9-9-2019 10:00 AM

Experimental and Numerical Evaluation of a Novel Piling System for Sound Wall Applications

Daniel Mroz
The University of Western Ontario

Supervisor
Dr. M. Hesham El Naggar
The University of Western Ontario

Follow this and additional works at: https://ir.lib.uwo.ca/etd

Part of the Geotechnical Engineering Commons

Recommended Citation

Abstract

Sound walls are utilized for mitigating ambient noise caused by traffic or industrial and commercial activities. Drilled shafts are conventionally used as foundations for sound walls; however, steel piles can provide faster installation and immediate utilization. A novel pile concept was developed which comprises an H-pile modified to better resist typical load patterns faced by sound wall piles, which may include lateral force and moment from wind and uplift force from adfreeze. The modifications include one or two plates welded to the pile and anti-heave anchors (nodes) welded along the pile flange. The main objective of this research program is to assess the suitability of these modifications for sound wall applications.

A full-scale pile load testing program was performed on fourteen steel piles installed with vibratory driving and two drilled shafts. The testing program included monotonic and cyclic lateral load tests and uplift load tests. A numerical model was developed with the program LPILE which was validated using the experimental results and then used to perform a parametric study considering different plate dimensions and a range of practical soil conditions. A second numerical model was developed using GSNAP to extend the cyclic lateral load analysis to include higher loads and more load cycles.

The results showed that plate modified piles had a 22% increase in lateral load capacity compared to unmodified H-piles. The corresponding parametric study demonstrated that widening the plate is typically more efficient for increasing the pile's lateral capacity than increasing the plate length. The cyclic lateral load tests revealed that the lateral stiffness of the novel piles remains approximately constant within 100 cycles. The GSNAP model simulated that the pile will experience less than 10 mm of ground level deflection at 1000 cycles of the design lateral load. The axial tension load tests concluded that adding nodes decreased the uplift capacity of H-piles. A comparison of the load transfer mechanism between a pile with and without nodes showed that the portion of the pile where nodes exist had a significantly reduced shaft resistance due to disturbance of the clay occurring during installation. It was observed that the installation quality of the piles directly affected their uplift and lateral load capacity.

Keywords

Summary for Lay Audience

Sound walls are utilized for reducing noise caused by traffic or industrial and commercial activities. Drilled shafts are conventionally used as foundations for sound walls; however, steel piles can provide faster installation and immediate utilization. A novel pile concept was developed which comprises an H-pile modified to better resist typical load patterns faced by sound wall piles, which may include lateral force and moment from wind and uplift force occurring in regions where soil experiences seasonal freeze and thaw. The modifications include one or two plates welded to the pile and soil anchors (nodes) welded along the pile flange. The main objective of this project is to assess the suitability of these modifications for sound wall applications.

A full-scale pile load testing program was performed on fourteen steel piles installed with vibratory driving and two drilled shafts. The testing program included static and cyclic lateral load tests and uplift load tests. A numerical model was developed for static laterally loaded piles and validated using the experimental results and then used to simulate the pile with different plate dimensions and installed in a range of practical soil conditions. A second numerical model was developed to extend the cyclic lateral load analysis to include higher loads and more load cycles.

The results showed that plate modified piles had a 22% increase in lateral load capacity compared to unmodified H-piles. The numerical model demonstrated that widening the plate is typically more efficient for increasing the pile's lateral capacity than lengthening it. The cyclic lateral load tests revealed that pile deflection remains approximately constant within 100 cycles. The cyclic model demonstrated that the pile will experience under 10 mm of ground level deflection at 1000 cycles of the design lateral load. The uplift load tests concluded that nodes decreased the uplift capacity of H-piles. Analyzing the load transferred from the pile to the soil showed that the pile section where nodes exist had a reduced shaft resistance due to disturbance of the clay occurring during installation. It was observed that the installation quality of the piles directly affected their uplift and lateral load capacity.

Co-Authorship Statement

This thesis was prepared in accordance with the regulations for a monograph thesis specified by the School of Graduate and Postdoctoral Studies of Western University. All tasks required for the thesis including field testing, numerical modelling, interpretation of results, and thesis writing were carried out by the candidate under the supervision and guidance of Dr. M. Hesham El Naggar.

Acknowledgments

There are many people I would like to thank who provided help throughout my academic career at Western University. It was with their support that I was able to successfully complete my thesis.

First, I would like to express my sincere thanks to my supervisor Dr. M. Hesham El Naggar for giving me the opportunity to work under someone so distinguished in the engineering community. His guidance and encouragement were invaluable. It was my absolute pleasure to be one of his students.

I would like to acknowledge the support of Atlantic Industries Ltd. for providing the testing specimens and partial funding for my research.

I wanted to express my very deep thanks to the Lardner family for generously awarding me the William E. and Ruth Lardner Award. Their financial assistance provided peace of mind and helped me focus on my studies.

Much thanks go to the Western University staff for all their assistance. Special acknowledgements go to the structural laboratory manager, Dr. Aiham Adawi, and the field station manager at the Western Field Station, Peter Duenk, who went above and beyond to help make my project a success.

I am grateful towards all my colleagues at Western University who aided me during my research. Special thanks go to my colleagues Maged Abdlrahem and Osama Drbe for their insightful discussions and valuable guidance and to Mehdi Heidari for his aid during numerical modelling. I would also like to thank the following for their support during my field testing: Mohamed Abdelsalam Mansour, Majid Kh Touqan, Omar El Naggar, Abdelrahman Aly, Abdalla Alhashmi, Mohammed Alwalan, and Safwat Ramadan.

Last but not least, I wish to express gratitude to my wife Jodi for her love, encouragement, and support during my studies.

Table of Contents

List of Tables

List of Figures

List of Appendices

List of Abbreviations and Symbols

AWT   above water table

BH   bore hole

BWT   below water table

CU   consolidated undrained triaxial compression test

F.S.   factor of safety

LI   liquidity index

LL   liquid limit

L/D   pile length over diameter ratio

PI   plasticity index

PL   plastic limit

SPT   standard penetration test

A_p cross-sectional area of pile

B   pile width

C_d borehole diameter correction factor

C_r rod length correction factor

C_s sampler type correction factor

e	eccentricity
ER_r	generalized SPT energy ratio
E_s	Young's modulus of soil
E_p	Young's modulus of pile
f_{ad}	adfreeze bond stress
f_s	unit shaft resistance
H	ultimate lateral capacity of pile
H_o	ultimate lateral capacity of novel pile with original tested dimensions
Δh	distance between tension and compression side strain gauge
I_p	moment of inertia of pile cross-section
k	k soil modulus parameter
k_L	lateral stiffness of pile
k_{LO}	lateral stiffness of pile at first load cycle
K_r	pile flexibility factor
L	length of plate attachment
L_p	length of pile
M	bending moment

N (or N_{field})	uncorrected SPT blow count
N_{60}	SPT blow count corrected for field conditions to an average energy ratio of 60%
$N_{1,60}$	SPT blow count corrected for overburden pressure and energy ratio
P	applied load to pile
P_a	atmospheric pressure (approximately 100 kPa)
P_c	axial compression point load
P_L	lateral point load
P_p	perimeter of pile cross-section
Q_s	ultimate shaft resistance of pile
Q_u	ultimate axial load of pile
S_u (or c_u)	undrained shear strength
W	width of plate attachment
α	adhesion coefficient
ε_a	axial strain
ε_c	axial strain on compression side of pile
ε_t	axial strain on tension side of pile

ε_{50} axial strain at one half of the soils final shear strength

ϕ' drained friction angle

ν Poisson's ratio

γ soil unit weight

γ_{bulk} soil bulk unit weight

γ_{sat} soil saturated unit weight

Chapter 1

1 Introduction

1.1 Background and Overview

Sound walls (also known as noise barriers or acoustical barriers) are utilized for the mitigation of ambient noise due to traffic or industrial and commercial activities. An example of a sound wall preventing traffic noise from entering a nearby residential area is shown in Figure 1-1. Sound wall foundations are typically subject to a complex loading system of a small axial load combined with a large lateral load and bending moment produced by wind. In regions where seasonal frost and thaw occur, adfreeze bond stresses may produce uplift forces which need to additionally be addressed in the design. Sound wall panels are typically very light and therefore only impose a small axial compression load on the piles. A schematic of the typical loading pattern on sound wall piles is shown in Figure 1-2 where P_L is the resultant lateral wind force, P_c is the axial compression force, M is bending moment, e is the eccentricity of the lateral point load applied above the pile head, and f_{ad} is adfreeze bond stress.

Figure 1-1: Example of a sound wall reducing traffic noise from entering residential area.
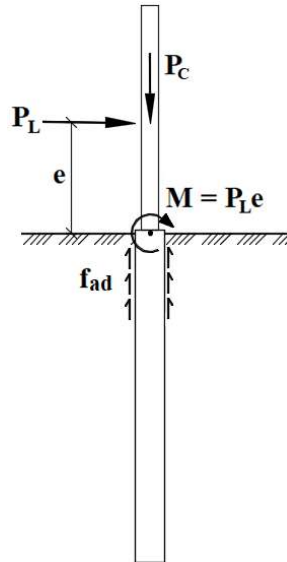
Figure 1-2: Typical loading pattern on piles supporting sound walls.

Short drilled shafts are conventionally utilized to support sound walls due to their high lateral stiffness and high uplift resistance, which counteracts these forces. However, foundation systems that can provide enhanced lateral capacity, cost-savings, and fast installation and utilization are desirable to further reduce cost and construction schedules of sound walls. Standard steel H piles offer efficient installation and immediate use due to forgoing the need to wait for concrete to cure; however, they lack the required lateral stiffness to adequately support sound walls. Furthermore, they may not provide adequate resistance to uplift forces from adfreeze due to their low self-weight.

Modifications have been proposed by Atlantic Industries Ltd. (AIL) to increase both the lateral capacity and uplift capacity of typical steel H-piles. Four preliminary lateral load tests were performed by AIL on early concepts of modified H-piles that were fitted with plates welded along the pile flange just below the ground surface. The same tests were performed on unmodified H-piles. The tests showed that modifying the H-piles reduced the lateral deflection by an average of 59% compared to the unmodified piles at the same low magnitude lateral load. Due to the success of these preliminary tests, a full-scale pile load testing program was planned and executed to study the novel piles and fully investigate their suitability for sound wall applications.

The use of these novel piles has the potential of realizing major cost savings since foundations accounts for a large portion of the total cost of the sound wall. For example, the Ohio Department of Transportation estimates that of the 10-20 million dollars spent on sound walls, drilled shafts account for approximately half of the total cost (Liang, 2002).

1.2 Summary Description of Novel Pile Concept

Two similar concepts of novel piles were tested and compared to standard drilled shafts and plain steel H-piles: single plate piles and double plate piles. Standard structural steel W sections were fitted with steel plates welded to the pile flange for the portion of the pile immediately below the ground surface. Piles with only one plate are designated as single plate piles as shown in Figure 1-3 (a). The double plate piles were fitted with plates on either side of the outside flange of the pile as shown in Figure 1-3 (b) (note that the section of pile above the plate is used to extend the height of the loading point). The purpose of adding the plate is to increase the pile-soil contact area, which in turn increases the area of soil passively resisting the applied load. The failure load of laterally loaded piles is dependent on the limiting pressure above the point of pile rotation (short piles) or above the plastic hinge (long piles) (Fleming et al., 2009). Therefore, the plate was selected to cover only the top portion of the pile. The sizing of the plate was based on the preliminary study performed by AIL. The purpose of the double plate pile is to potentially further enhance the pile's resistive capabilities which is based on the assumption that the second plate will give the pile more flexural rigidity, and the soil confined between the two plates will add additional shear resistance along the edge. Additionally, some of the singe plate piles were equipped with "nodes" which are small pieces of flat bar welded on either side of the pile flange and pointed 45° above the horizontal as shown in Figure 1-3 (c). These nodes are meant to anchor the pile into the soil thus increasing their uplift resistance. The nodes are angled in this manner so that the piles can be driven downwards with relative ease compared to moving the pile upward again. The piles were installed with vibratory driving which has the benefit of faster installation rates compared to traditional impact driving. Dimensions of the pile, plate, and nodes tested in this study are provided in section 3.4 of this document.
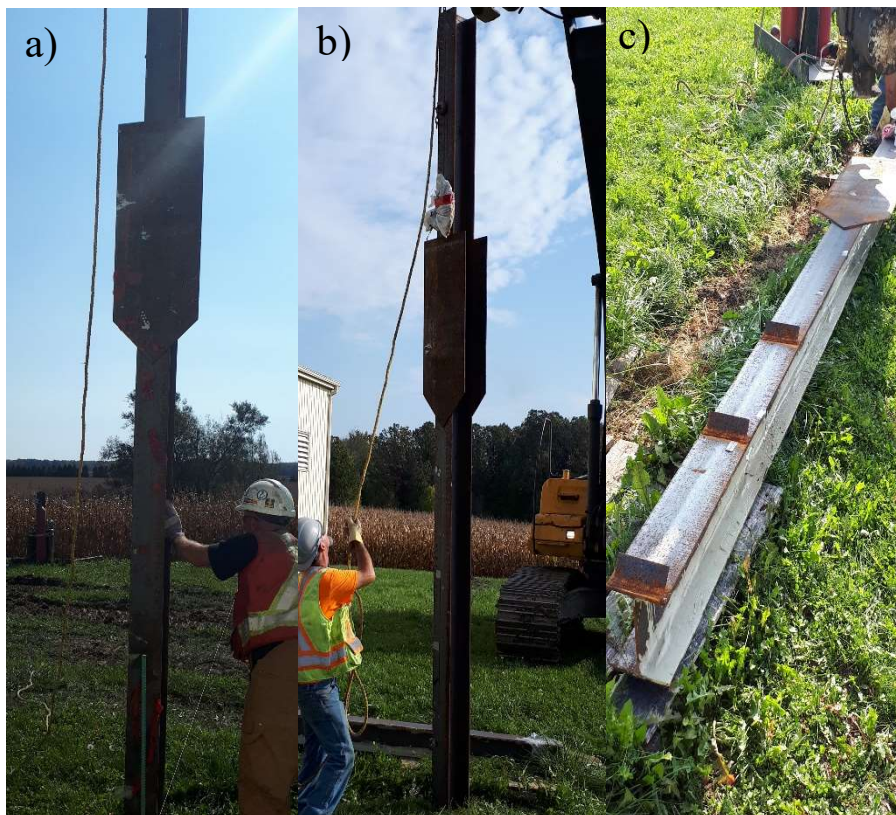
Figure 1-3: Novel piles tested in study: a) single plate piles, b) double plate piles, c) single plate piles with nodes.

1.3 Research Objectives

The main objective of this thesis is to investigate the performance of the proposed novel deep foundation concept and fully characterize its capacity for sound wall applications. The information gathered from this research will be used to determine if the novel pile design can be used as a suitable alternative to drilled shafts and to provide design recommendations.

The specific objectives of this research program are as follows:

1. Monitor the pile driving process to assess their constructability and installation efficiency.

2. Measure the ultimate load capacity of the novel piles when subjected to monotonic lateral loading and uplift loading through full-scale field load testing.

3. Assess the performance of the novel piles when subjected to cyclic lateral loading by measuring the degradation stiffness during repetitive loading and determine whether piles with two plates improve performance over piles with only one plate.

4. Assess the effect of installing nodes on the uplift performance of the piles installed in cohesive soil.

5. Study the load transfer mechanism of the piles when subjected to lateral and uplift forces by utilizing data from the strain gauges attached to the piles.

6. Develop a representative numerical model of a monotonic laterally load novel pile with commercially available software using the data from the load tests to calibrate the model. This model will be used to theoretically assess the performance of piles with different plate dimensions and installed in a range of practical soil conditions.

7. Develop a representative numerical model of a cyclic laterally loaded pile. This model will be used to extend the evaluation of a novel pile subjected to cyclic loads by simulating larger forces and more load cycles.

8. Provide a list of design recommendations when using the novel pile concept.

9. Provide recommendations for a second phase of testing taking into consideration the results of the original tests and observations made prior, during, and after testing.

1.4   Research Methodology

To fulfill the objectives stated in section 1.3, the research was completed in two main phases. The first phase comprised a full-scale pile load testing program on the novel piles, unmodified piles, and drilled shafts. The second phase involved calibrating a numerical model using experimental data from phase one. The field testing program consisted of monotonic and cyclic lateral load tests and uplift load tests to assess the novel piles performance when subjected to wind and adfreeze loads. The results of the novel piles were compared to unmodified steel H-piles which were tested in the same

manner allowing for a full analysis of the impact made by plate modifications. Furthermore, some novel piles were equipped with nodes and likewise compared to those without. The steel piles were equipped with strain gauges so that the load transfer mechanism could be analyzed. Because drilled shafts are commonly used to support sound walls, they were also installed and tested to establish a baseline for comparing the performance of the new proposed pile systems located within the same soil stratigraphy.

After the field testing was completed, engineering software was used to calibrate and validate a numerical model representing the novel pile systems. Once the models were validated, a parametric study was performed on the novel piles with the goal of looking at the impact of plate dimensions on H-piles installed in a range of practical soil conditions with varying strength. The information gathered from the parametric study can provide insight into proper design methods and numerical modelling procedures for future use.

1.5   Thesis Organization

Chapter Two provides a literature review discussing topics related to the concepts that are explored during the research program. Since there is limited literature for piles supporting sound walls specifically, and no research on plate modified H piles (or piles with enlarged diameters near the ground surface), the purpose of this review is to introduce and provide context for the concepts that will be tested. The topics covered in the literature review include: basic theory of piles subjected to lateral loads, cyclic loading and degradation, drilled shaft design recommendations for sound wall purposes, ice adhesion loading, vibratory versus impact driving methods, and the preliminary load tests performed by AIL.

Chapter Three describes the testing site and the results of the geotechnical investigation, which included a survey of existing borehole data, the completion of an additional borehole, and field and laboratory soil tests. The description of the pile specimens tested for this project is also provided. This section also summarizes the strain gauge installation, protection, and interpretation methods. Lastly, the pile installation is described followed by details, observations, and comments made during the installation process.

Chapter Four presents the details of the monotonic and lateral cyclic testing procedures of the piles and the results of the lateral load testing program. A numerical model was developed and calibrated for the novel piles using the experimental data from the monotonic lateral field tests and soil property data from the geotechnical investigation. The calibrated model was used to conduct a parametric study considering a range of plate dimensions over a practical range of soil conditions. A second numerical model was calibrated for cyclic loading which was then used to expand the analysis to include higher loads and more cycles.

Chapter Five presents details of the uplift testing procedures of the piles and the results of the uplift load testing program. This included a study of the axial load transfer mechanism for the novel piles using the strain gauge data. The ultimate uplift capacity measured in the field was compared to the estimated uplift capacity using the alpha method, which is the standard method of calculating a pile's axial load capacity in cohesive soil. This section also presents findings regarding the impact of the nodes on the uplift capacity of the novel piles including a comparison the load transfer mechanism between piles with and without nodes.

Chapter Six provides the summary and conclusions of the research, including key findings and design recommendation when using novel piles. This is followed by recommendations for future testing in the second phase of the overall project.

1.6   Original Contributions

The original contributions presented in this thesis are as follows:

1.   Design and execution of a full-scale pile load testing program on the novel pile concepts. The lateral load testing portion of the program includes a description of the physical test setup which allows for testing the piles under loads that are representative for sound wall applications (namely simultaneous lateral force and moment and cyclic two-way lateral force) without requiring additional reaction piles. The axial tension testing portion of the program includes a description of

the physical test setup which allows for testing the piles under uplift forces without the installation of reaction piles or requiring larger scale equipment.

2. Development of a simple and reliable numerical modelling procedure for the novel piles when subjected to monotonic lateral loads using commercially available software and readily available correlations for input parameters.

3. Development of a simple and reliable numerical modelling procedure for the novel piles when subjected to cyclic lateral loads using software currently in development at The University of Western Ontario.

Chapter 2

2 Literature Review

2.1 Introduction

A very limited number of studies investigated pile design and behaviour with a focus on sound walls foundations. The available literature only studied drilled shafts and did not consider steel piles. Therefore, the literature review provides context for the key information that will be explored during this study. Section 2.1 briefly introduces the behaviour of piles subjected to lateral loads. Section 2.2 summarizes the mechanism of cyclic soil degradation and its effect on the ultimate lateral load capacity and deflection of piles. Section 2.3 discusses recommended design practices for drilled shafts pertaining specifically to sound wall applications. Section 2.4 briefly discusses uplift loading on piles through adfreeze and typical mitigation techniques that have been used in practice. Section 2.5 examines the effect of using vibratory driving over impact driving on the axial and lateral performance of piles. Lastly, section 2.6 summarizes the results of a preliminary pile load test program performed by Atlantic Industries Ltd. on the novel pile concept.

2.2 Basic Theory of Laterally Loaded Piles

Lateral loads acting on deep foundations are primarily supported by passive resistance of the soil in front of the pile and the shear resistance of the soil surrounding it. As horizontal loads are applied to the pile, stresses develop in the soil in front of the pile (Fleming et al., 2009). As the load increases, the stress in front of the pile increases while the stress behind the pile decreases as illustrated in Figure 2-1. The soil experiences either normal stress, shear stress, or some combination thereof depending on its location with reference to the pile (Reese and Van Impe, 2011).

The nature of load distribution along a pile and pile failure mode are dependent on two main attributes: pile head fixity and pile flexural rigidity. There are two broad categories for pile head fixity: free head and fixed head. This is dependent on how the pile is

attached to the supported superstructure. Free head piles are allowed to rotate at the head without restriction, whereas fixed head piles are completely restrained from rotating. These concepts are largely theoretical and in practice piles exhibit traits somewhere between the two conditions (Budhu, 2011).
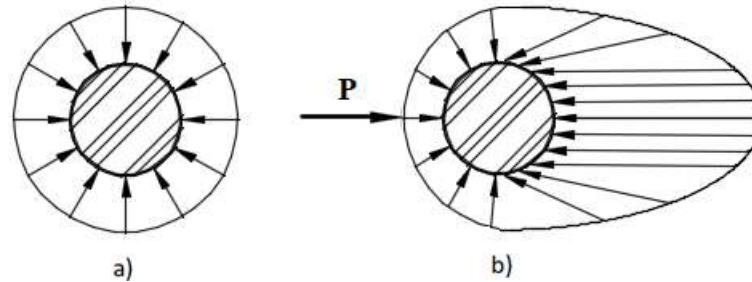
Figure 2-1: Distribution of stress along a pile cross section a) at rest, b) subjected to lateral load, after Reese and Van Impe (2011).

In terms of relative pile rigidity (stiffness), there are two main categories: short (rigid) and long (flexible) piles. The behaviour that develops is dependant mainly on the pile flexural rigidity (stiffness) relative to the soil and its length. Piles that are slender or have relatively low stiffness tend to behave as long (flexible) piles. The length/depth ratio (L/D) of a pile can be an indicator of the failure mode. A general rule of thumb is that piles with L/D of 10 to 12 or more will likely behave as long piles, whereas piles with smaller values will typically behave as short piles (Tomlinson and Woodward, 2008). Pile behavior can also be estimated with the pile-flexibility factor K_r, which is calculated from Equation 2-1:

$$K_r = \frac{E_p I_p}{E_s L_p{}^4} \qquad\qquad (2\text{-}1)$$

where E_p and E_s is the Young's modulus of the pile and soil, I_p is the moment of inertia of the pile cross-section about the axis of bending, and L_p is the length of the pile. Piles with a flexibility factor greater than 10^{-2} tend to behave as short piles whereas much smaller values of K_r indicate long pile behaviour (Poulos and Davis, 1980).

The ultimate capacity of short piles is governed by soil failure. Short piles under free head conditions rotate along a single point at some point along their length as shown in Figure 2-2 (a). Passive resistance develops in the soil in front of the pile above the center of rotation, and behind the pile below the center of rotation. Failure occurs once the sum of forces on the upper portion of the pile exceeds the sum of forces in the lower portion of the pile. Short piles under fixed head conditions are prevented from rotating, and therefore fail by translation, or a horizontal movement as shown in Figure 2-2 (b) (Budhu, 2011).
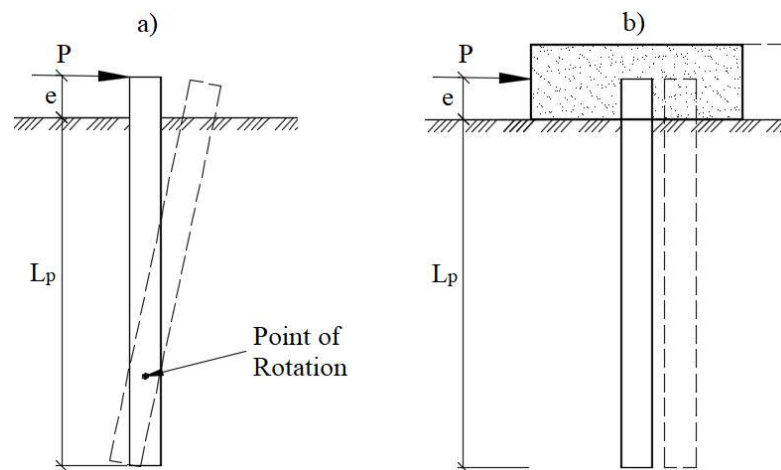
Figure 2-2: Failure mechanism of short piles with a) free head fixity b) fixed head fixity, after Tomlinson and Woodward (2008).

The maximum applied load for long piles is governed by the flexural capacity of the pile itself, and therefore the bending moment will exceed the capacity of the pile before the soil can fail. For both free and fixed head piles, a point of maximum bending moment will occur along the pile length near the ground surface which will form a plastic hinge within the pile. The difference between free head and fixed head long piles is the number of fracture points. For free head piles, the top of the pile is free to rotate and therefore only one fracture point at some distance below the ground surface will occur as shown in Figure 2-3 (a). Fixed head long piles will experience two fracture points, one below the ground surface and one near the connection between the pile and pile cap as shown in Figure 2-3 (b) (Tomlinson and Woodward, 2008). The passive soil resistances prevents the pile from displacing significantly below the yield point. Therefore, only the soil

above this hinge is relevant for calculating the ultimate capacity of long piles (Fleming et al., 2009).
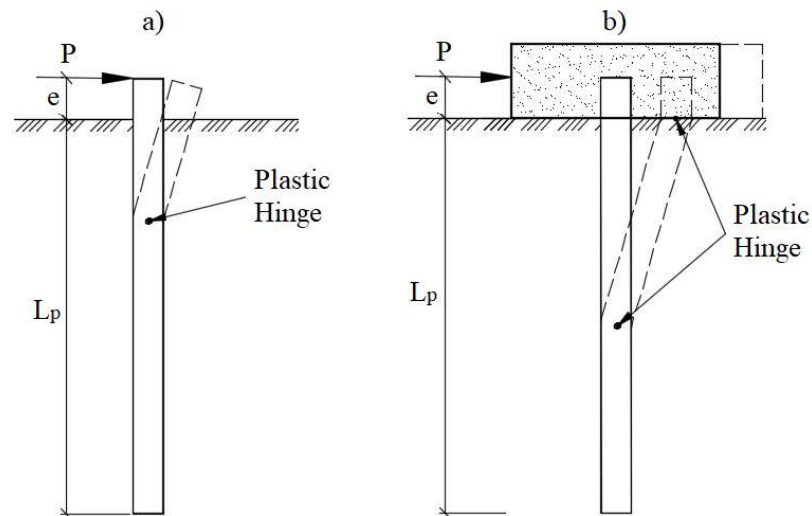
Figure 2-3: Failure mechanism of long piles with a) free head fixity b) fixed head fixity, after Tomlinson and Woodward (2008).

2.3 Cyclic Loading and Soil Degradation

Cyclic lateral loads are often imposed on pile foundations and originate from wind, waves, traffic, earth pressure, and water pressures (Long and Vanneste, 1994). Cyclic lateral loading can potentially cause major and permanent lateral deflections for deep foundations. Cyclic lateral loading also decreases the post-cyclic ultimate capacity of piles (Basack and Nimbalkar, 2018). There are two main mechanisms which cause an increase in lateral displacement and decrease in lateral load capacity of a pile as the number of loading cycles increases. The first is a series of plastic deformations occurring with each cycle that are exacerbated over time. The second mechanism involves a progressive decrease in soil strength and stiffness per load cycle; also known as soil cyclic degradation (Poulos, 1982).

For clay soils, the decrease in strength and stiffness is caused by a rearrangement and reorientation of clay particles and development of excess porewater pressures, which do

not dissipate during loading cycles (Basack and Nimbalkar, 2018). In sand, the particles likewise rearrange during cyclic loading to produce similar effects to the ultimate capacity and deflection behaviour of deep foundations (Basack and Dey, 2011).

There are some differences in the way stiff and soft to medium stiff clays behave when supporting laterally loaded piles. Stiff clays tend to remain compressed for protracted periods of time. Subsequently reapplying load will force water from the soil, which in turn scours the clay leading to a reduction in lateral resistance. Soft to medium stiff clays typically do not maintain a compressed state due to weakness which leads to collapse of the soil, but still exhibits a loss of lateral resistance during cyclic lateral loading (Reese and Van Impe, 2011).

The gapping and collapse mechanism is likewise observed in sandy soil. Upon lateral loading of a pile and a subsequent reversal of load, a portion of sand will collapse back into the gap due to overburden pressure. The caving of soil adjacent to the pile will prevent the pile from returning to its initial position. It was also observed that dense sand tends to loosen during cyclic loading and loose sand conversely will densify (Reese and Van Impe, 2011).

The severity of cyclic loading depends on the type of loading applied to the pile; one-way load (force is applied in the same direction) imposes more cumulative pile displacement than two-way loading (force is applied in both direction per load cycle) (Haiderali et al., 2015). The effect of cyclic lateral loading on piles is also dependent on the number of load cycles, the frequency of applied loading, and the amplitude of loading. Many experiments proving these points are available in literature. Two examples which very clearly demonstrated these facts were presented in Basack (2010) and Basack and Nimbalkar, (2018). These papers considered scale four by four pile groups installed in a pure soft clay soil profile and identical specimens installed in a medium dense sand (up to 33% of the total pile depth within the soil profile) underlain by soft clay. These tests showed that the ultimate lateral capacity decreases as the number of cycles increases. However, the incremental drop in capacity decreased over many cycles until the capacity remained approximately stable after a certain number of cycles. The tests further showed

that a lower frequency of load application resulted in a lower lateral capacity, and the approximate drop in capacity was proportional for all number of load cycles that were analyzed.

Lastly, the lateral capacity of piles decreased with increasing load amplitude, which remained proportional with an increasing number of load cycles. This reduction in capacity showed a more drastic drop under high amplitudes in the pure clay soil, but no definitive pattern could be established from the mixed soil profile.

2.4   Drilled Shaft Design Recommendations for Sound Wall Applications

Colorado Department of Transportation (CDOT) performed lateral pile load tests on drilled shafts sized according to typical design dimensions for piles supporting sound walls. One of the objectives was to establish a pile design procedure that is straightforward and would optimize the pile dimensions. The study included a comprehensive review of design methods currently used to design piles for both ultimate and serviceability requirements, and two fully instrumented lateral load tests on drilled shafts, one of each in a cohesionless and cohesive soil profile. A very detailed soil investigation was conducted for each site to confirm the best methods for estimating soil properties used to predict pile response (Nusairat et al., 2004).

The report concluded that the best method for strength limit design is Brom's method with a safety factor of two (a depth of soil equal to one and a half times the pile diameter from the ground surface should be neglected), and the best method for serviceability limit design is using COMP624P (LPILE). Finite element modelling can also be used to design drilled shafts. However due to the level of expertise required to produce accurate and reliable results, it is recommended to leave this approach for critical projects, atypical foundation dimensions, complex loading conditions, and unique soil types (Nusairat et al., 2004).

The soil strength properties for cohesive soils can be obtained employing the triaxial CU test, direct shear test, the pressuremeter test using the approach dictated by FHWA

(1989), or the SPT test when using correlations provided by the Ohio Department of Transportation (ODOT) (Liang, 2002). For cohesionless soils, the recommended methods of estimating strength characteristics are the SPT test using the ODOT correlations or the pressuremeter test. The correlations compiled by Liang are summarized in Table 2-1 and Table 2-2, which correspond to cohesionless and cohesive soils, respectively.

Table 2-1: Recommended k soil modulus parameter correlations for cohesionless soil, after Liang (2002).

N		2 - 4	4 - 10	10 - 20	20 - 30	30 - 50	50 - 60
φ (°)		25 - 35	20 - 38	33 - 41	35 - 43	37 - 45	39 - 48
k (kN/m³)	AWT	< 6790	6790	24430	24430	61000	67800
	BWT	< 5430	5430	16300	16300	33900	37900
γ_{bulk} (kN/m³)	Min.	16 - 17	17 - 17.5	18 - 19	19 - 19.5	19.5 - 20	20 - 20.5
	Max.	18 - 18.5	19 - 19.5	19 - 20.5	20 - 20.5	20.5 - 23	22 - 23

Table 2-2: Recommended k soil modulus parameter correlations for cohesive soil, after Liang (2002).

$N_{1,60}$	0 - 2	2 - 4	4 - 8	8 - 16	16 - 32	32 - 64
S_u (kPa)	0 - 12	12 - 24	24 - 48	48 - 96	96 - 192	192+
ε_{50}	> 0.02	0.02 - 0.01	0.01 - 0.007	0.007 - 0.005	0.005 - 0.004	0.004 - 0.002
k (kN/m³)	< 8140	8140	27150	136000	271000	543000
γ_{sat} (kN/m³)	15.5 - 19	17 - 20.5	17 - 20.5	19 - 21	20.5 - 23	22 - 23

2.5   Ice Adhesion Loading

Frost heaving is defined as the upward movement of soil due to freezing. The soil can adhere to the pile surface when frozen (also known as adfreeze), and as it moves upwards it pulls the pile along with the soil which emits induces a force that is capable of displacing the pile upwards. This is defined as frost jacking, and the force exhibited is known as adfreeze force. Field tests show that this adfreeze bond stress can range from less than 100 kPa up to as much as 980 kPa. Many factors affect the formation and

magnitude of adfreeze forces, but the most relevant are soil texture, moisture content, and the pile material or surface (Péwé and Paige, 1963). Without proper mitigation measures, frost jacking can cause several inches of uplift a year, and as much as several feet over longer durations. This amount of displacement, especially if differential uplift occurs, can cause serious structural damage. Frost jacking can be a concern in temperate regions as long as seasonal freeze and thaw of soils occurs (Crory and Reed, 1965).

Several methods are currently used to mitigate the effect of adfreeze loading on piles. Some of the more common methods fall into one of the following categories: coating of the pile in the adfreeze zone, manipulating the pile dimensions, changing the composition or properties of the soil surrounding the pile, and anchoring the pile in the ground.

2.5.1   Pile Coating

The magnitude of adfreeze force can be reduced by placing a medium between the soil and the pile within the zone where these forces originate. A portion of the pile may be greased and then wrapped with tar paper, which allows the pile to slide relatively free within the zone where adfreeze occurs. Tar paper could also be substituted with polyethylene for a more durable solution. For long-term applications, a steel sleeve anchored to the ground could be used to cover part of the pile, preventing adfreeze forces from contacting the pile itself (Péwé and Paige, 1963).

2.5.2   Adjusting Pile Dimensions

The dimensions of the pile can be adjusted to either reduce the upward force or increase the downward force. The weight of the pile can be increased by enlarging its dimensions, which will counteract the upward adfreeze force. Increasing the pile dimensions will also provide more surface area for soil to be in contact with the pile thus increasing the shaft resistance. Alternatively, the pile cross-section can be reduced in the adfreeze zone to reduce the surface area in contact with frozen soil (Péwé and Paige, 1963).

2.5.3   Soil Composition and Properties

Adfreeze forces on piles can be reduced without modifying the piles. There are methods to change the properties of the surrounding soil. Since frost heave is dependent on

moisture, it can be reduced by lowering the water table below the adfreeze zone. The soil surrounding the pile may be replaced with a coarse-grained material, which is less susceptible to frost heaving. This method however is not practical for long piles (Péwé and Paige, 1963). The natural soil around the pile can also be chemical treated to alter ice formation behaviour and therefore reduce frost jacking. Different chemicals such as spent sulphite liquor or polyvinyl alcohol have been used successfully in reducing adfreeze loads. The chemicals can be introduced as a slurry into predrilled holes or injected into soil under high pressures (Hardy, 1953; Lyazgin et al., 2003).

2.5.4   Anti-Heave Anchoring

Some concepts of anti-heave anchors have been developed to increase the uplift capacity of piles. The concept can be likened to that of helical piles or drilled shafts with belled ends in that they allow additional soil to support the pile in the vertical direction. For piles in saturated clay, the added resistance is a function of the undrained shear strength of the clay which is dependent on the depth and width of the foundation, and the weight of soil directly above the element protruding from the pile. For piles in sand, the added resistance is derived from both the frictional resistance of sand along the failure zone and weight of soil within this failure zone. For circular foundations, the failure zone develops at an angle from the horizontal starting at the top of the foundation with extended area (Das, 1999). Figure 2-4 shows some concepts of anchors have been considered but not necessarily tested.
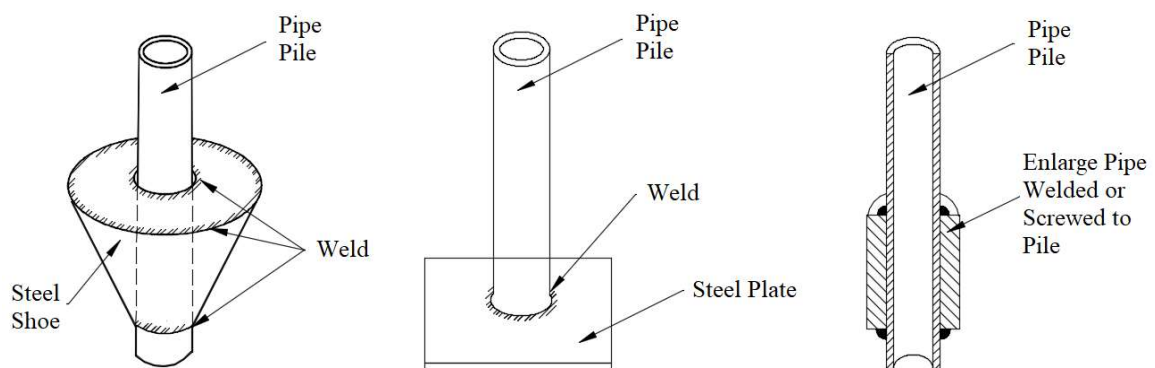
Figure 2-4: Concept sketches for anti-heave anchors to increase uplift capacity of steel pipe piles, after Pihlainen (1951).

The magnitude and distribution of axial force along H-piles and pipe piles were measured in piles installed in Fairbanks Alaska with the goal of characterizing the force and stress along the piles when subjected to cycles of freeze and thaw. The pipe pile was equipped with several concentric plate rings near the bottom of the pile and the H-pile was equipped with several plates welded between the flanges with the aim of increasing uplift capacity. The soil profile was comprised of Fairbanks silt with a surface ice layer and gravel layer on top. The plate rings in conjunction with thermal syphons were reported to provide high stability against uplift for the tested piles (Johnson and Buska, 1988). However, the impact of the rings on the piles uplift capacity was not individually assessed and quantified, but rather the entire system was analyzed together.

2.6 Vibratory versus Impact Driving Methods

Several studies have been performed to compare the effects of impact driving and vibratory driving on pile capacity and behaviour. Vibratory driving provides several benefits over traditional impact driving including faster installation rates (typically three to four times faster than impact driving), reduction in noise and vibration levels, and easier adjustments in case of misplacements or misalignments during installation, all of which makes vibratory driving an economical solution. Furthermore, vibratory driving has no limitations on pile size (I.R., 2015).

2.6.1 Effect on Axial Performance of Piles

Several studies involving different driving methods were compiled and analyzed to evaluate the effect of vibratory driving on a pile's axial capacity (I.R., 2015). These studies encompassed different types and configurations of piles installed in a wide variety of soil profiles (Borel et al., 2006; Briaud et al., 1988; Jeyapolan, 1983; Lammertz, 2008; Mazurkiewicz, 1975; Mosher, 1987; Rocher-Lacoste et al., 2004). The studies showed that vibratory driven piles on average have an 18% lower axial capacity (with a 32% coefficient of variance) than equivalent piles installed with impact driving. The ultimate capacity of vibratory driven piles can be increased by impact driving the piles near the end of the final installation depth. However, this may greatly affect the overall efficiency

of the pile installation process, which is one of the key advantages of using vibratory driving in the first place. An analysis of strain gauge data from these tests indicate that this lower capacity is observed in both skin friction and toe resistance. However, the toe resistance is affected to a larger degree (particularly in pipe piles) indicating that the impact is less severe for piles subject to tension loading. A major contributing factor to this is that impact driving leads to soil plugging (especially in pipe piles). This plugging causes greater displacement at the pile toe leading to more densification of the soil. Piles installed with vibratory driving, however, allow soil to pass through the pile and no plugging occurs. It was also observed that installing piles with low frequencies and velocities is better for pile performance but may cause premature pile refusal.

2.6.2   Effect on Lateral Performance of Piles

A series of lateral load tests were performed on H-piles installed with impact and vibratory driving by Markus Schönit of the Karlsruhe Technical University in 2009. The results of these tests are not yet available publicly; however, they have been briefly discussed in the report sponsored by Deep Foundation Institute (DFI) (I.R., 2015). The test results indicated that both driving methods resulted in similar lateral capacities of the piles and therefore the difference between impact and vibratory driving is negligible for laterally loaded piles. The available data is very limited on this topic and therefore further exploration into the effect of vibratory driving on the lateral capacity of piles is required to reach a definitive conclusion (I.R., 2015).

2.7   Preliminary Pile Load Tests on Novel Pile Concept

A preliminary testing program was performed by AIL on a prototype concept of a "paddle pile", or a pile with a plate welded to the flange near the ground surface. The pile was constructed with a W150x30 steel section with a 950 x 420 x 12 mm plate. The piles were embedded 2.8 meters into sandy soil, which was not compacted to the design specifications. Plain posts with the same length and cross-section were also tested as a comparison to measure the relative improvement of lateral capacity caused by the plate. The pile was installed with 1.275 m of stickup so that the pile could be loaded with

eccentricity to apply moment simultaneously with horizontal force. The piles were installed using vibratory driving.

The method of testing is illustrated in Figure 2-5. A lateral load was applied to the pile at a height of 1.25 m and measured with a dynamometer. Dial gauges were placed at the top and bottom of the above ground section of the pile to measure the lateral deflection and pile rotation. Loads were applied to the pile in increments of 0.89 kN (200 lb) to a final load of 13.34 kN (3000 lb). The results of all four tests are summarized in Table 2-3; the original load-deflection graphs are shown in Appendix A. The average ground level deflection at 3000 lb of lateral force was 17.64 mm for plain piles and 7.262 mm for paddle piles indicating significant improvement in the lateral performance of the modified piles. The piles were exhumed after testing and it was observed that no yielding or damage occurred in the pile or plate. These tests provided a basis for additional testing as applying these simple modifications to the piles greatly enhanced their performance. The results of these tests were shared through personal communication with AIL and are not published in the literature.
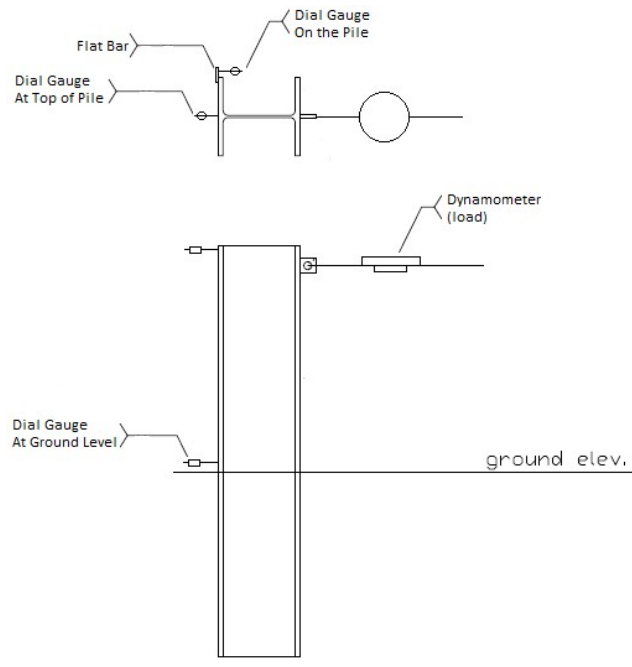
Figure 2-5: Setup for preliminary pile load tests on plain and paddle piles.

Table 2-3: Summary results of preliminary pile load test program.

Test #	Pile Type	Max. Applied Load (kN)	Max. Deflection at Ground Level (mm)
1	Plain Pile 1	13.34	16.23
4	Plain Pile 2	13.34	19.05
2	Paddle Pile 3	13.34	6.65
3	Paddle Pile 4	13.34	7.874

Chapter 3

3   Field Testing Setup and Pile Installation

3.1   Introduction

This chapter summarizes the testing site and the results of the geotechnical investigation performed prior to field testing. A description of the test piles is provided detailing the selected pile dimensions for the H-piles, modified H-piles, and drilled shafts. The chapter also covers the strain gauge instrumentation scheme and methods of interpreting the data to provide the axial load and bending moment distribution along the pile during loading. Lastly, observations and comments of the overall installation process are discussed along with an assessment of the pile installation quality and the efficiency of using the novel piles over drilled shafts.

3.2   Site Location and Description

The field load testing program was conducted at the Environmental Sciences Western Field Station located at 22312 Wonderland Road North, by the intersection at Middlesex County Rd. # 56 and Ten Mile Road. Figure 3-1 shows the testing area with respect to the property. Several studies were conducted previously in the general area of the site and hence there is an accumulation of information of its soil stratigraphy.

3.3   Site Investigation Program

A subsurface site investigation program was performed at the testing location prior to pile installation. This program included a review of previous field and laboratory testing results and the drilling of an additional borehole within the bounds of the testing area to confirm the previous investigations. The field testing was followed by laboratory testing performed on undisturbed and disturbed samples retrieved from the site.

3.3.1   Previously Available Information

Several different subsurface investigations were performed at the Western Environmental Sciences Field Station in the past. The subsurface investigations involved several

boreholes and associated laboratory tests and the results were reported by Khan (2005), Livneh (2006), and Abdelghany, (2008). These boreholes were relatively far from the testing location of this study compared to more recent boreholes that were drilled closer to the test area.
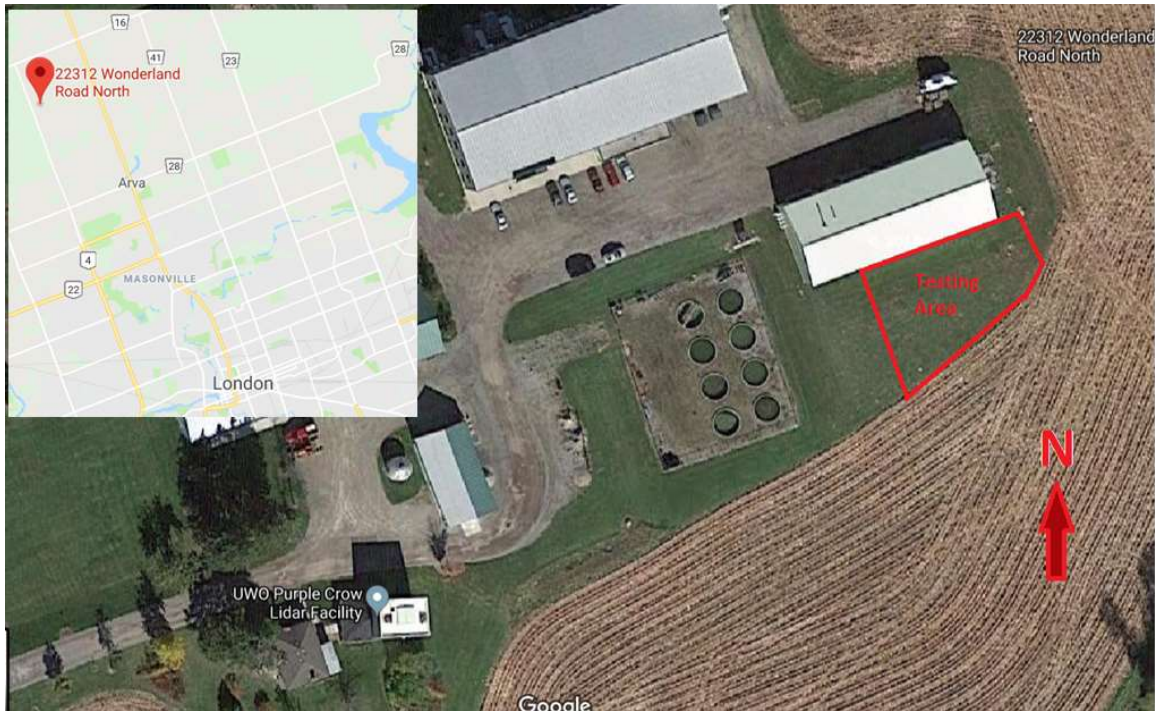
Figure 3-1: Location of testing area at 22312 Wonderland Road N. (Google, n.d.).

More recently, nine shallow boreholes were drilled in 2008 by Atkinson Davies Inc. prior to the construction of various structures on the property (Drbe, 2013). Two of the boreholes, BH 3 and BH 4, were near the test location at an approximate distance of 35 m West-northwest and 20 meters North-northeast from the borehole that was conducted as part of the current study. The boreholes showed that the soil profile comprised 150 to 200 mm of topsoil followed by very stiff to hard brown clayey silt till. Borehole BH 3 indicated a colour change from brown to grey at 2.8 m. The moisture content varied randomly from 9% to 14% within the first 4 meters of the soil and then increased to 29% at 4.4 m. The SPT blow count (N) typically varied from 16 to 46, with the most common values being between 30 to 35. A single SPT test showed a blow count of 98 at 2.8 m in BH 4. The original borehole logs are presented in Appendix B.

Two additional boreholes were drilled in 2012 by Aardvark Drilling Inc. (Drbe, 2013). The boreholes, originally labelled BH-I and BH-II, were located approximately 18 m Northeast and 25 m North-northeast from the current test area. The boreholes showed 200 – 300 mm of topsoil underlain by a stiff to very stiff brown lean clay with sand and trace gravel to a depth of 4.0 m. The SPT blow count ranged from 9 to 18, which corresponds to an undrained shear strength of 58 to 117 kPa. This layer was underlain by 2.5 – 2.75 m of firm to stiff grey lean clay/silt with fine sand and trace gravel. The SPT blow count ranged from 13 to 4 moving downwards, corresponding to an undrained shear strength of 85 to 26. The final layer encountered in BH-I and BH-II was a very stiff lean clay with seams of fine sand. The SPT blow count ranged from 20 to 50 as depth increased. Both boreholes terminated at 8.75 m on hard grey clay. The original borehole logs are shown in Appendix B. A monitoring well was installed in BH-II which established the groundwater level at a depth of 6.41 m. The locations of BH-I, BH-II, BH 3 and BH 4 are shown with reference to the test piles in Figure 3-2.

3.3.2   Field Tests and Sampling

An additional borehole was drilled within the testing area during this study. The data obtained from this borehole was sought to confirm that the previous boreholes were representative of the exact location of testing, in which case the measured soil properties from previous testing can be used in conjunction with the most current data in the analysis of the pile load test program. The borehole was drilled to a depth of 5.5 m, approximately 2.0 m deeper than the bottom of the test piles. The drilling was completed by Aardvark Drilling Inc. using a CME-45 track mounted drill rig. A mixture of split spoon, grab, and Shelby tube samples were taken along the soil profile. The boring showed 0.15 m of topsoil followed by 0.75 m of stiff brown lean clay with sand. The color changed to grey with a lower stiffness from 0.9 m to 2.0 m. Beyond that depth, the soil color was brown again and the soil stiffness increased. The thick lean clay layer was underlain by light grey sandy lean clay at 4.7 m. Cobbles were not encountered during the drilling phase; however, several cobbles were encountered below two meters during the installation of the steel piles and drilled shafts. The groundwater table was not encountered during drilling.
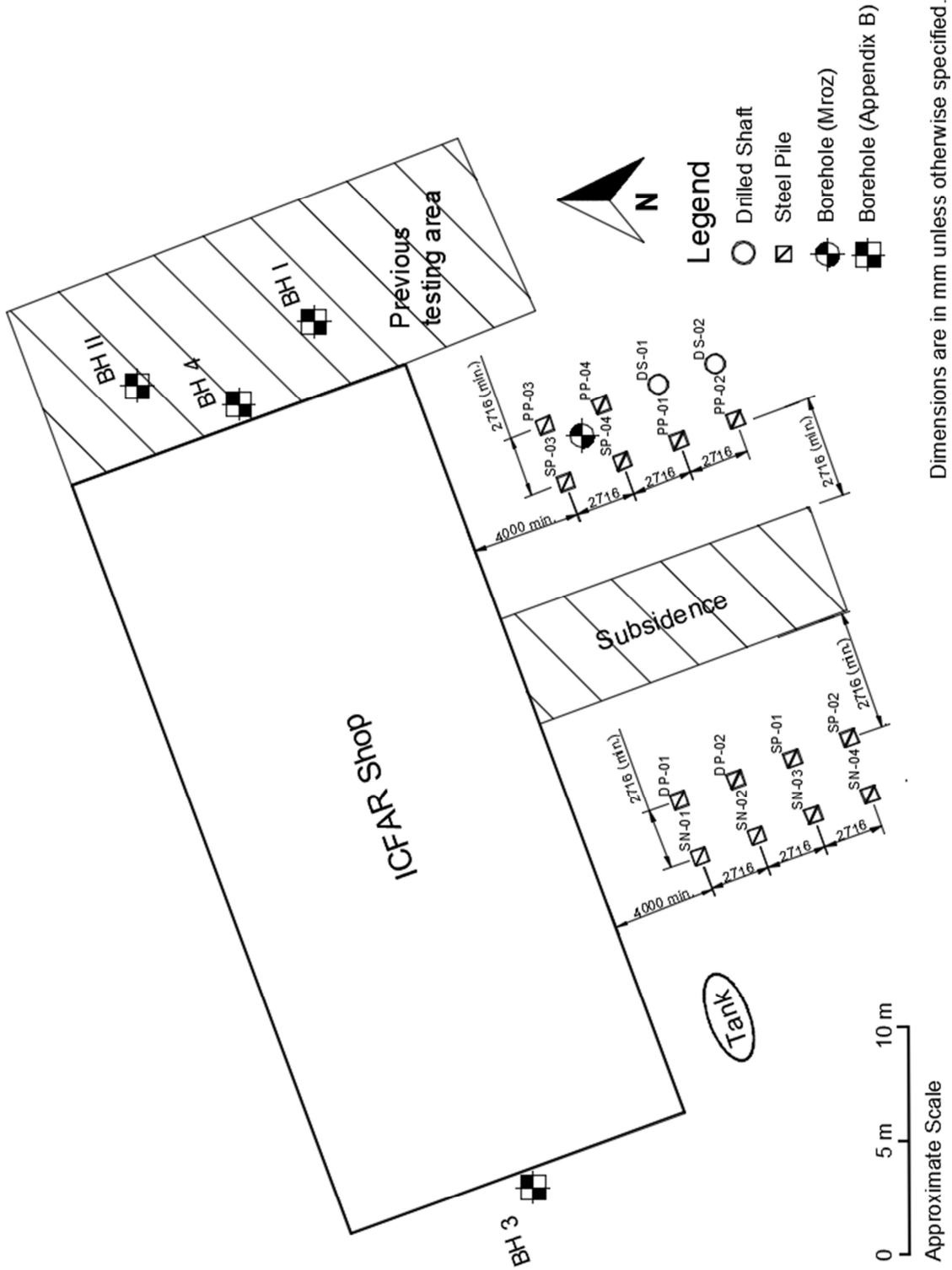
Figure 3-2 - Borehole and Test Pile Locations.

The SPT blow count (N) was recorded for each split spoon sample. A 63.5 kg hammer was dropped 76 cm until the sampler could be driven 450 mm. The spoon was driven in intervals of 150 mm and the blow count was recorded for each interval. The SPT blow count for each test was taken as the summation of the last two intervals. An attempt was made to measure undrained shear strength with a torvane, but the soil was too stiff to get a proper reading. The torvane was designed to take readings below 100 kPa, which was exceeded throughout most of the soil profile.

3.3.3   Laboratory Testing

Moisture content tests were conducted immediately after sampling on all grab and split spoon samples. The moisture content ranged from 12 to 24% within the first five meters of the soil profile. The Atterberg limits and grain size distribution (hydrometer and mechanical sieve) were determined for select soil samples to properly classify the soil profile. A summary of the laboratory testing results is shown in Table 3-1. The soil was classified according to both USCS and AASHTO soil classification systems. All soil tests were performed according to the appropriate ASTM standards. The Atterberg limits and grain size distribution matched laboratory tests from earlier investigations.

Table 3-1: Summary of laboratory testing results on key soil samples.

Sample #	Depth (m)	% Gravel	% Sand	% Silt	% Clay	WC (%)	LL (%)	PI (%)	LI	USCS Soil Classification	AASHTO Soil Classification
SS-02	0.7 - 0.9	1.6	17.8	63.7	16.9	18.7	32	13	-0.02	CL - Lean Clay with	A-6 Clayey Soils
T-03	0.9 - 1.2	0.8	11.7	64.7	22.8	24.4	35	17	0.38	CL - Lean Clay	A-6 Clayey Soils
T-06	2.2 - 2.6	9.1	11.4	48.5	31	13.1	26	12	-0.08	CL - Lean Clay with	A-6 Clayey Soils
SS-09	4.6 - 5.2	0.0	45.1*	-	-	15.3	21	7	0.19	CL - Sandy Lean Clay	A-4 Silty Soils

* Sieve performed only on portion retained on No. 200 sieve.

Two Shelby tubes were taken during drilling and transported back to the laboratory. However, due to the stiffness of the soil, the Shelby tubes provided poor sample recovery. When extracting sample T-03, most of what was recovered experienced substantial disturbance during pushing and therefore was treated as a disturbed sample not fit for advanced testing. Sample T-06 produced enough undisturbed sample for an

unconfined compression test, however a large rock (> 25 mm diam.) was discovered while trimming the sample for the test. The rock comprised a considerable portion of the sample's cross-section and therefore was not used for further testing. The unit weight of select samples was established by measuring the dimensions of small portions of split spoon and Shelby tube samples and weighing them. The calculated unit weights were consistent with earlier investigations, which ranged from 19.8 to 22.3 kN/m³ (Drbe, 2013).

3.3.4   Undrained Shear Strength

The field and laboratory tests confirmed that the substrata at the testing site is predominantly cohesive soils, and therefore it is appropriate to characterize the soil strength according to its undrained shear strength (S_u). Many correlations exist between the SPT blow count of a soil and its undrained shear strength.

3.3.4.1   SPT Corrections

Certain correlations between N and S_u require that the blow count N be normalized to an energy level of 60 %. Skempton, (1986) recommended applying additional corrections for rod length, sampler liners, and borehole diameter. The corrected blow count to energy level, rod length, sample liner and borehole diameter can the by performed according to Equation 3-1 (Sivrikaya and Toğrol, 2006):

$$N_{60} = N \frac{ER_r}{60} C_r C_s C_d \qquad \textbf{(3-1)}$$

where ER_r is the generalized SPT energy ratio, and C_r, C_s, and C_d are the rod length, sampler liner, and borehole diameter correction factors presented in Table 3-2. Overburden corrections are not required for clay soils (Peck et al., 1974).

3.3.4.2   SPT – S_u Correlations

A list of some relevant correlations between SPT blow count and undrained shear strength is shown in Table 3-3. The SPT blow count measured on site were applied to these relationships to estimate the undrained shear strength of the soil profile; the results

are summarized in Table 3-4. The borehole log with all data measured on site and in the laboratory is shown in Figure 3-3. The undrained shear strength of the soil measured from previous investigations was included in the log, which were also estimated from SPT tests.

Table 3-2: SPT corrections for rod length, sampler liner, and borehole diameter, after Skempton (1986).

Correction	Symbol	Description	Correction Factor
Rod Length	C_r	Rod Length (below anvil):	
		≥ 10 m	1.00
		6 - 10 m	0.95
		4 - 6 m	0.85
		3 - 4 m	0.70
Sampler Liner	C_s	Standard Sample US	1.00
		Sampler without liners	1.20
Borehole Diameter	C_d	Borehole Diameter:	
		65 - 115 mm	1.00
		150 mm	1.05
		200 mm	1.15

Table 3-3: S_u - N relationships for fine grained soils.

Su Correlation (kPa)	Soil Description	Source	Source#
6.25 N	Fine-grained soil	Terzaghi and Peck (1967)	1
6.18 N60	Fine-grained soil	Sivrikaya and Toğrol (2002)	2
6-7 N	PI < 20	Stroud (1974)	3

Table 3-4: Estimated undrained shear strength from SPT.

Depth (m)	N	N60	Su (kPa) Source 1	Source 2	Source 3	Average Su (kPa)
0.3 - 0.9	17	14	106	88	111	102
1.5 - 2.1	11	9	69	57	72	66
2.6 - 3.3	22	18	138	114	143	132
4.6 - 5.2	15	15	94	95	98	95

Borehole BH-01

Borehole Log

Western Engineering

Location:	22312 Wonderland Road N (Western field station)	Drilling Method: Hollow stem rotary drilling
Contractor:	Aardvark Drilling Inc.	Ground Elevation: TBD
Drill Rig:	CME-45 Track Rig	Date: May 28, 2018

Sample Type: ▼ Grab ⊞ Split Spoon ▮ Shelby Tube

Soil Type: ▤ Clay ▨ Silt ▦ Sand Gravel

Material Description

Top Soil - silty, some sand, trace gravel (< 25 mm diam.), trace organics
- light brown, firm to stiff, dry to moist, medium plasticity — G-01

Lean CLAY - some sand (f, m, c), trace gravel (< 20 mm diam.)
- brown, very stiff
- moist, medium plasticity — SS-02, SPT 17

Lean CLAY - some sand (mainly fine, tr. m,c), trace gravel (<10 mm diam.)
- grey, varies firm to stiff
- moist, medium plasticity — T-03

SS-04, SPT 11

Lean CLAY - some sand (fine), silty, trace gravel (< 20 mm diam.)
- brown, varies stiff to hard
- moist, medium plasticity — G-05

T-06

SS-07, SPT 22

Rock in spoon, reading not valid, no sample recovery — SS-08, SPT 29?

Lean Clay - sandy (fine), silty
- grey, firm to stiff
- moist to wet, low plasticity — SS-09, SPT 15

25 mm thick sand seam at 4.85 m
- trace silt, trace clay
- compact, wet, well graded

G-10

Bulk Unit Weight (kN/m³): 18 19 20 21 22 23
% fines (passing no. 200): 20 40 60 80 100
PL MC LL: 20 40 60 80 100

Undrained Shear Strength (kPa): 50 100 150 200
Current Tests
Previous Tests

END OF HOLE AT 5.5 m
Notes:
1) No seepage or sloughing observed.
2) Borehole backfilled with bentonite for 0.3 m and augur cuttings for the remainder.
3) Borehole located 8.6 m West and 6.6 m South of Southeast corner of yellow storage garage.
4) Torvane readings discard as the vane size was unsuitable for the stiffness of the soil which led to unrealistic values.

Page 1 of 1

Figure 3-3: Latest borehole log for field testing site.

3.3.4.3   Idealized Soil Profile

Table 3-5 presents the idealized soil profile established from the borehole log, which will be used in interpretation of the test data and in the numerical modelling. The soil profile was subdivided into distinguishable layers and its soil properties were appropriately averaged to a singular value. A range of S_u values was also provided considering all measurements acquired from previous investigation programs, which represents a plausible range of soil strength for calibrating the numerical model. The empirical correlations used are generally rough estimates and therefore setting a reasonable range for soil strength to work with for numerical modelling is appropriate.

Table 3-5: Idealized soil profile at testing site.

Depth (m)	Unit Wt. (kN/m³)	S_u (kPa)	S_u Range (kPa)
0 - 0.9	19	110	90 - 115
0.9 - 2.0	21	60	60 - 70
2.0 - 4.7	21.5	125	100 - 140
4.7 - 7.0	20	95	95 - 100

3.4   Test Specimen Dimensions

The H-pile section selected for this study was W200 x 36 (W8 x 24 imperial designation). The piles were sized according to a preliminary analysis performed by AIL, which considered the maximum bending moment experienced by the pile due to the maximum expected wind force. The total length of the piles was 4850 mm, which allowed for 3500 mm of embedment into the ground and 1350 mm of stickup. A series of holes were drilled into the head of the pile to allow for attachments, which connected the pile to the loading system. The purpose of the stickup was to facilitate applying lateral load to the pile above the ground surface thus generating both lateral load and bending moment at the ground surface in order to simulate the loading pattern of piles supporting sound walls. With the lateral attachment in place, the pile was loaded at 1.25 m above the ground surface. This height is based on the maximum sound wall height of 5.0 meters where the resultant wind force would act at 2.5 m above the ground surface. The height

for the tests was selected at one-half this distance because piles with a higher stickup would be very difficult to test.

The plate dimensions were 950 x 420 x 9 mm (length, width, thickness) with a "stinger" extending 210 mm from the bottom of the plate to facilitate pile installation. Figure 3-4 displays the plate configuration and provides its dimensions. The plates were welded to the pile flange so that the top of the plate was located at ground level. The plates were sized according to the preliminary pile load tests performed by AIL prior to this study.
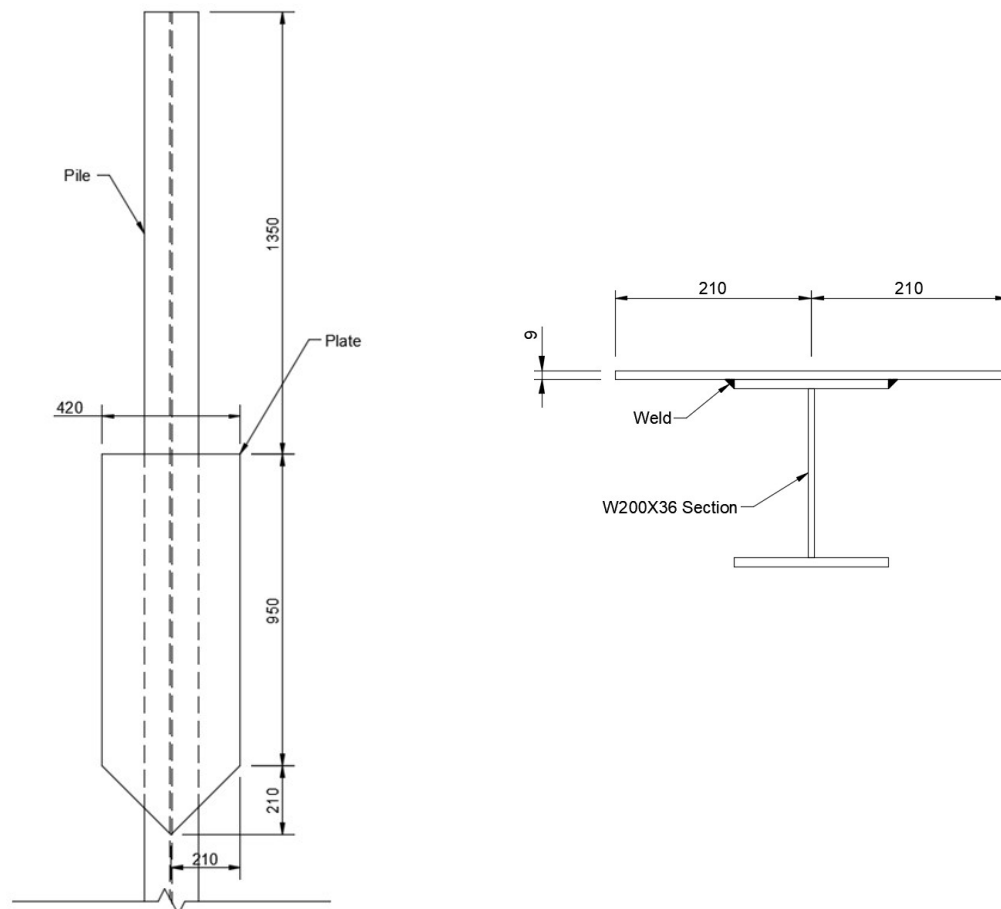
Figure 3-4: Plate dimensions and location on test specimens (dimensions in mm).

The nodes, which were attached to half of the single plate piles, were comprised of 140 x 50 x 9 thick flat bar plates angled 45° upwards from the horizontal. A total of six nodes were placed on a pile, three on either side of the outside pile flange, starting 10 mm from the bottom of the pile and spaced 600 mm as shown in Figure 3-5. The nodes were angled

to facilitate installation while simultaneously increasing the difficulty of upward displacement.
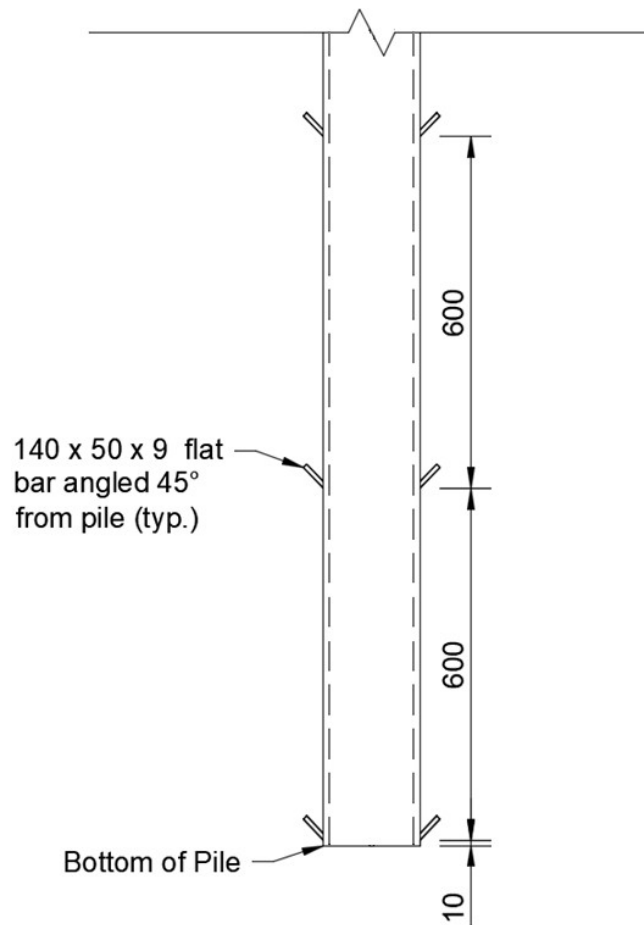
Figure 3-5: Location, dimension, and orientation of nodes on pile (dimensions in mm).

The drilled shafts were 711.2 mm (28") in diameter and were reinforced with a W200 x 36 section set in the center. The drilled shafts were sized according to the typical length and diameter used in construction of sound wall foundations. The concrete portion of the pile ended at the ground surface and the remaining stick-up was comprised only of the steel reinforcing beam. The concrete used for these piles had a minimum specified strength of 27.5 MPa. Five concrete cylinders were cast at the time of pouring and tested in the UWO structural laboratory. The measured 28-day strength of the concrete ranged from 28 to 44 MPa with an average value of 37 MPa.

3.5 Test Pile Instrumentation

The piles were instrumented with foil strain gauges to measure the axial load and bending moment distribution along the pile profile during loading. A total of 210 strain gauges were distributed on the shafts of 13 test piles. All single plate, single plate with nodes, and double plate piles were instrumented at nine levels along their length as shown in Figure 3-6. One of the plain posts was instrumented at levels 1, 2, 3, 4, 7, and 9. Two of the plain posts were instrumented at levels 1 to 4. The remaining plain post and reinforcing posts for the drilled shafts were not instrumented. The purpose of the top strain gauges was to act as a reference to calibrate the strain gauges located below the ground surface, since they are unaffected by soil resistance. The strain gauges were placed in pairs on opposite ends of the pile cross section at each level, located on the inside of the pile flange as close as possible to the web.

C2A-06-250LW-120 foil strain gauges were supplied with wires already attached. Where the length was inadequate to reach the data acquisition system from the strain gauge location, additional wire was spliced. Each strain gauge was tested with a voltmeter after installation and again after wires were spliced to ensure they were functioning. A large number of gauges were also connected to the data acquisition system prior to installation to ensure there was no problems with the instrumentation.

The strain gauges and wires were provided with three levels of protection to ensure the survival of as many strain gauges as possible. After installation, the gauges were first covered with RTV 3145 sealant as shown in Figure 3-7 (a), which is flexible but durable, and adheres very well to the pile surface. Part of the lead wire leading up the gauge was also covered to ensure the gauges were entirely watertight. The gauges and wires were then covered in layers of construction grade sheathing tape as shown in Figure 3-7 (b). This tape was selected because of its strong adhesive properties and durability. The final layer of protective was a coating of ceramic epoxy as shown in Figure 3-7 (c), which entirely covered the surface where the strain gauges were installed. Ceramic epoxy was used for its superior adhesion to surfaces and protection against abrasion. The space where wires ran down the pile was also filled with silicon to prevent water from seeping through, thus making the instrumentation entirely waterproof.
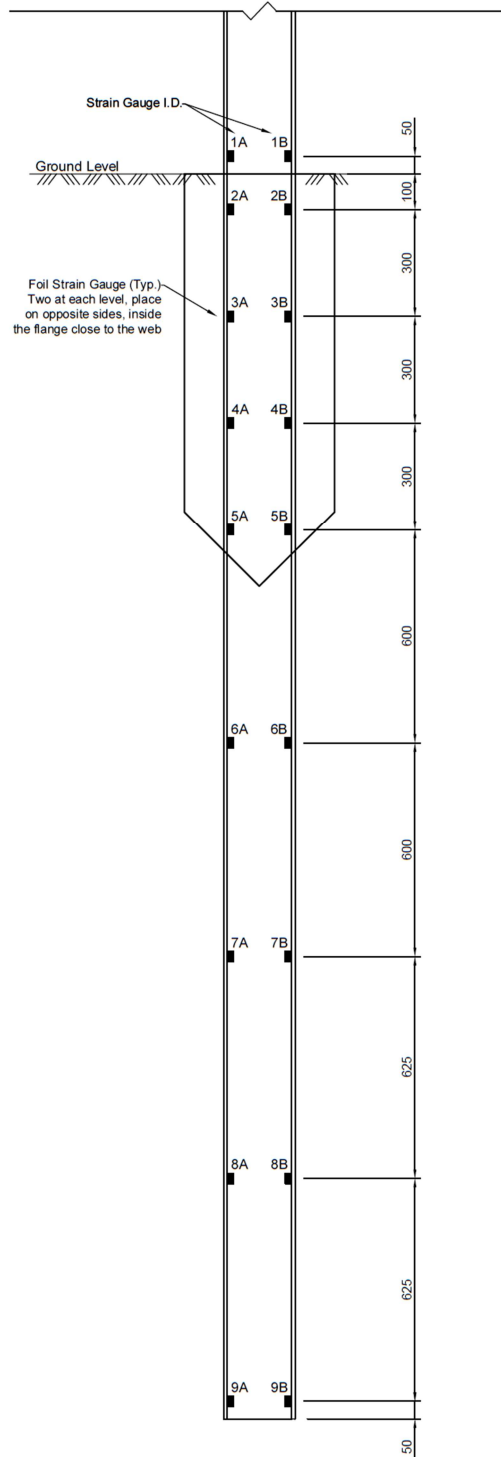
Figure 3-6: Location and identification schematic of strain gauges.

Figure 3-7: Application of a) sealant, b) construction grade sheathing tape and c) ceramic epoxy for strain gauge protection.

3.5.1   Interpretation of Strain Gauge Data

The load transfer mechanism of a loaded pile is calculated by measuring the axial load experienced in the pile and comparing it to the total axial load applied to the pile. The difference between the two values is the load transferred from the pile to the soil. The axial load in the pile can be calculated from the strain reading using Equation 3-2 (Fellenius, 2001):

$$P = A_p E_p \varepsilon_a \tag{3-2}$$

where A_p is the cross-sectional area of the pile, E_p is Young's modulus of the pile, and ε_a is the axial strain. The axial stiffness (E_pA_p) of a steel pile is easy to estimate since the Young's modulus of steel is consistently 200 ± 5 GPa and the cross-sectional area of steel is known for fabricated H-sections. However, the accuracy of converting strain to load can be increased by back calculating the stiffness and each level of strain using the first level reference strain gauges. A method was proposed by Fellenius (2015) to back calculate the combined stiffness of a steel/concrete composite pile, since the actual Young's modulus of concrete is difficult to estimate and is a function of imposed strain and using a singular value may result in significant errors. The secant stiffness of a pile can be estimated with Equation 3-3 (Fellenius, 2015):

$$E_p A_p = \frac{P}{\varepsilon_a} \qquad \text{(3-3)}$$

where P is the applied axial load. Knowing the applied load from a calibrated load cell and strain reading from the reference gauges, E_pA_p can be estimated at each level of load during the test.

For piles subject to lateral loading, it is insightful to measure the bending moment distribution along a pile. The strain measurements can be converted to moment using engineering beam theory according to Equation 3-4 (Bicocchi, 2011):

$$M = \frac{E_p I_p (\varepsilon_t - \varepsilon_c)}{\Delta h} \qquad \text{(3-4)}$$

where E_p is Young's modulus of the pile, I_p is the moment of inertia of the pile cross-section, ε_T is the strain gauge reading on the tension side, ε_C is the strain gauge reading on the compression side, and Δh is the distance between the two gauges.

3.6   Pile Installation Details

This section examines the efficiency and quality of the pile installation. The time required to drive the piles, the position displacement during driving, and quality of the installation are summarized.

3.6.1　Pile Layout Plan

The piles location plan is shown in Figure 3-2. The pile labelling scheme is as follows:

- SP-0#: Single plate piles

- SN-0#: Single plate piles with nodes

- DP-0#: Double plate piles

- PP-0#: Unmodified H-piles (plain piles)

- DS-0#: Drilled shafts

The piles were separated into two groups of eight to provide adequate space for the forklift which was used to move the testing equipment to and from the piles. The piles were situated in areas that were not affected by previous field testing programs.

3.6.2　Installation Procedure

The piles were installed with vibratory driving by means of an excavator mounted 320 vibro hammer. The vibratory system was mounted to the arm of a John Deere mid-size excavator as shown in Figure 3-8. To facilitate securing the pile to the vibratory head, the pile was first secured to the excavator arm by means of a chain. The chain was connected to a 25 mm hole in the pile flange which was made on site with a cutting torch. The excavator arm could then lift the pile vertically and manipulate it into place in the vibratory attachment. The attachment gripped the pile at the web. Due to the relatively small size of the H-section, some deformation of the pile web at the point of attachment was observed. The verticality of the piles was measured using a construction level. Vibratory driving is a suitable method of installing sound wall piles since and lateral capacity is not affected and axial tension capacity is only slightly affected (I.R., 2015).

Figure 3-8: Vibratory driving of the steel piles.

3.6.3   Installation Quality

The initial analysis of the results of the pile load tests (presented in Chapters 4 and 5) revealed that the quality of installation had a significant impact on the performance of the piles. The observed quality of installation based on the judgement of the author was documented for each pile, which included an overall assessment of the entire installation process. To quantify the observed quality of the installation, which will provide a simple method for comparing test results, each pile was given a rating from 1 to 3. A rating of 3 indicates the installation was ideal with little to no issues during driving, a rating of 2 indicates there were some minor issues during installation which may affect the performance of the pile, and a rating of 1 indicates an overall poor installation which will significantly affect the performance of the pile. The installation rating for each pile is summarized in Table 3-6.

The driving position displacement, which refers to how much the pile moves laterally at the end of driving relative to its position when driving started, was recorded for 7 piles. This was done to ensure the installation method did not cause the piles to deviate significantly from their intended location, which could cause issues in the installation of the sound wall panels between adjacent piles. The recorded displacements are listed in Table 3-6, where the Y direction indicates the movement perpendicular to the pile flange (or plate if relevant) whereas the X direction indicates the movement parallel to the pile flange/plate. The placement of the piles was typically off by less than one inch in either direction from their intended location, which is would not cause any issues when installing the sound wall panels.

Table 3-6: Summary of installation quality of each pile.

Pile I.D.	Driving Displacement		Installation Quality Rating (1-3)	Comments
	Δ X (cm)	Δ Y (cm)		
Plain Post 1	2	1	3	
Plain Post 2	3	1	3	
Plain Post 3	0	1	3	
Plain Post 4	NM	NM	3	
Single Plate 1	1	0.5	3	
Single Plate 2	NM	NM	3	Note 1
Single Plate 3	2	1	3	
Single Plate 4	1	2	3	
Node/Plate 1	NM	NM	1	Note 2
Node/Plate 2	NM	NM	1	Note 3
Node/Plate 3	0	2	3	Best node pile install
Node/Plate 4	NM	NM	2	Note 4
Double Plate 1	NM	NM	2	Note 5
Double Plate 2	NM	NM	1	Note 6
Drilled Shaft 1	NA	NA	3	
Drilled Shaft 2	NA	NA	1	Note 7

NM – Not measured.

NA – Not Applicable

Note 1 – Part of the way during installation, the pile was moved up approximately one foot and re-driven to correct alignment. This was not expected to affect capacity significantly.

Note 2 – Difficulty driving the pile near the end was observed, likely due to a cobble. The pile was lifted partly and re-driven twice until installation was complete. Pile capacity was expected to be affected.

Note 3 – The pile was repeatedly lifted and re-driven due to pile moving out of position during driving several times. This was most likely caused by cobbles. Pile capacity was expected to be greatly affected.

Note 4 – Relatively decent installation observed. Some compression of the soil due to the tilting of the pile from the machine during straightening was observed. This was expected to affect pile capacity to some degree.

Note 5 – Relatively decent installation was observed. Some compression of the soil due to the tilting of the pile from the machine during straightening was observed. This was expected to affect pile capacity to some degree.

Note 6 – The pile was partially lifted and re-driven. During the straightening of the pile, the soil adjacent to one side of the plates was compressed by several inches. Pile capacity was expected to be greatly affected.

Note 7 – The steel reinforcing pile was placed approximately 150 mm offset from the center of the drilled shaft (see Figure 3-9).

Figure 3-9: Misaligned reinforcement for DS-02.

3.6.4   Driving Time

The driving time for the novel piles, unmodified H-piles, and drilled shafts are recorded in Table 3-7. The comparison between driving times for the steel piles and drilled shafts was of main importance to quantify the efficiency of installing the novel piles. The times that are recorded for the steel piles include the start of driving to the end of driving, and do not include securing the chain to the piling rig or moving the pile to the installation location. The installation time for the drilled shafts only includes the time required to perform drilling, pouring of concrete, and placing the steel reinforcement into position. The average driving time of the steel piles was approximately 4 minutes and 40 seconds; the installation time for drilled shafts averaged at about 14 minutes, which is approximately 3.0 times longer. Ignoring the two piles which encountered cobbles during driving, the average is reduced to 3 minutes and 12 seconds which is about 4.4 times faster than installing the drilled shafts.

Table 3-7: Installation time of each pile.

Pile I.D.	Time (min)	Notes
Plain Post 1	3	
Plain Post 2	3	
Plain Post 3	4	
Plain Post 4	5	
Single Plate 1	2	
Single Plate 2	4	
Single Plate 3	NM	
Single Plate 4	NM	
Node/Plate 1	13	Difficulty driving near the end due to cobble
Node/Plate 2	NM	
Node/Plate 3	2.25	
Node/Plate 4	3	
Double Plate 1	2.5	
Double Plate 2	10	Pile installed slanted, correction was required
Drilled Shaft 1	11	
Drilled Shaft 2	17	

NM - Not measured

3.6.5   Material Waste

Using steel piles instead of drilled shafts foregoes the requirement for collecting and disposing of waste soil and concrete material. A large volume of soil waste was generated

during the installation of just two drilled shafts as shown in Figure 3-10. The amount of waste material would be significant for large projects requiring many piles, which directly translates to additional costs and time for its removal.

3.6.6   Comments from Installers and Bystanders

The workers from the pile installers (Powell Foundations Inc.) mentioned that they prefer installing drilled shafts rather than steel H piles because it was easier to keep the drilled shafts in the correct position and plumb. However, these issues would be likely be abated when driving in more favorable soil conditions.

Employees from the adjacent building (ICFAR) mentioned that they could clearly hear the steel pile driving from their building. The front doors of their offices are approximately 75 m from the center of the testing grounds.

Figure 3-10: Soil and concrete waste from drilled shaft installation.

3.7 Summary

The piles were installed with vibratory driving. The driving times were measured for each pile to assess the improved installation efficiency of steel-only piles over drilled shafts. The quality of installation for each pile was also documented, which would be used later to explain certain behaviours of the piles during testing. The main observations and conclusions from the installation process are summarized accordingly:

- Vibratory driving is suitable for installing steel piles in cohesive soil profiles. Problems may occur during driving if cobbles or boulders are present in the soil. This can be mitigated by pre-auguring the location of the pile using an auger with a diameter less than the diameter of the pile. However, this method may reduce the overall efficiency of this installation method.

- Installing novel piles with vibratory driving proved to be 3.0 – 4.4 times faster than installing drilled shafts (not counting curing time for concrete). This can lead to significant time and cost savings, especially for large projects requiring many piles.

- Using steel piles does not produce the soil and concrete waste that is associated with the installation of drilled shafts. This waste would have to be collected and disposed which leads to additional costs.

- Using vibratory driving is preferable if restriction on noise levels is a requirement. While this method of driving still produces noticeable disturbance to nearby areas, construction companies use this method over impact driving if reducing noise is mandatory (I.R., 2015).

Chapter 4

4   Performance of Novel Pile Subject to Lateral Loading

4.1   Introduction

Lateral forces from wind are the primary forces sound wall foundations are designed to resist. A lateral load testing program was performed on the novel pile system to assess its performance under such wind forces. The testing program included testing unmodified steel piles to comparatively evaluate the influence of adding plates to H-piles. Two drilled shafts with dimensions commonly designed for sound wall applications were also tested as a baseline to compare current practice against the proposed system. Winds loads are repetitive in nature and therefore several piles were also evaluated under cyclic lateral loading patterns to assess stiffness degradation.

A numerical model was developed using the program LPILE and was calibrated and validated using results from the monotonic load tests. The calibrated model was then used to perform a parametric study on the novel pile configuration considering different plate dimensions and a range of practical soil conditions. The results of the field tests and parametric study was used to provide design recommendations for the plate modified piles. A second numerical model was developed using GSNAP (Geo-Structural Nonlinear Analysis Program)(El Naggar and Heidari, 2018) and was calibrated with the cyclic lateral load test data from the novel piles. The GSNAP model was then used to extend the cyclic analysis to include more cycles and larger forces.

4.2   Testing Setup and Procedure

The piles were tested under monotonic and cyclic lateral load conditions according to ASTM D3966 / D3966M - 07 (2013) method 6.4: Load Applied by Hydraulic Jack(s) Acting Between Two Test Piles or Test Pile Groups. This method of testing was ideal because testing two piles simultaneously is more efficient and does not require the installation of reaction piles, thereby saving additional time and cost of materials. Figure 4-1 shows the test setup used in this study. The load was applied with a model RRH 1006

Enerpac double acting hydraulic jack which has a 1100 kN load capacity and 150 mm stroke, which was connected to a Enerpac ZE3 class hydraulic electric pump. A model 1244 CLX-270K-B Interface load cell and the hydraulic jack were fastened together as a rigid unit and extended with 76 mm hollow core steel bars to connect the entire apparatus to the piles. The connections between the loading device and piles were designed as a pin so that the connection would be free to rotate vertically and so that the load can be applied in both directions. The lateral deflection of each pile was measured with three HLP 190 linear potentiometers secured to a frame that was supported independently of the pile and loading system. The potentiometers were placed at three levels along the pile shaft above ground: one near the ground surface, one placed 850 – 1150 mm above the ground surface, and the third between the two. The potentiometers have a 100 mm stroke and an accuracy of 0.1 mm. All instrumentation was connected to a 7000 series Sciemetric data acquisition system to record all instruments simultaneously. The data acquisition system collected readings every 5 sec for monotonic tests and every 1 sec for cyclic tests.

Figure 4-1: Lateral load test setup for two piles tested simultaneously.

4.2.1   Monotonic Testing Procedure

ASTM D3966 standard does not specify a test procedure for quick maintained load tests for laterally loaded piles. However, it does provide a provision that allows engineers to adjust the specified test methods. A quick maintained load test procedure was employed with load applied in increments of 5% of the anticipated failure load and maintained for four minutes at each increment. The load was advanced until excessive deflection in the pile occurred or until the load could not be maintained. In some cases, the test was terminated due to the hydraulic jack reaching its maximum stroke (the load is applied 1.25 m above the ground surface, and the deflection at the point of loading is greater than the deflection at ground surface). However, a sufficient portion of the load-displacement curve was measured to make an appropriate analysis of the pile's behaviour for all tests.

4.2.2   Cyclic Load Testing Procedure

The cyclic load testing procedure in ASTM D3966 was modified to suit the application of the piles. Cyclic two-way loading was originally planned to be applied at 33%, 67%, and 100% of the approximate maximum failure load of the piles determined from the static tests. In all cases, the tests were terminated prematurely due to reaching the stroke limit of the hydraulic jack. The ideal number of load cycles for wind applications typically ranges into the thousands, but the number of cycles per load increment was limited to 100 cycles for practical reasons when there was no further increase in pile displacement after 100 cycles. The frequency of the load cycles varied according the minimum and maximum displacement experienced at a load cycle. The highest frequency of the first load cycle ranged from 0.022 to 0.025 Hz and decreased as the number of load cycles increased.

4.3   Monotonic Lateral Load Test Results

Monotonic lateral load tests were performed on eight piles: two single plate piles (SP-0#), two single plate piles with nodes (SN-0#), two drilled shafts (DS-0#), and two unmodified (plain) piles (PP-0#). The load-displacement curves for single plate piles SP-03, SP-04, SN-03, and SN-04 are shown in Figure 4-2. The curves were extrapolated to estimate the force at 25 mm of ground level deflection using a combination of: 1)

following the pattern for rate of change in the curve; 2) using numerical modelling to predict the general shape of the curve; and 3) engineering judgement by the author. Note that this was done for all pile load tests where the pile displacement at the ground surface did not reach 25 mm. The average load at 25 mm of deflection for single plate piles was approximately 59.1 kN. The initial portion of the curve for all piles was very similar for the first 3-4 mm of deflection, but SP-03 and SN-03 began to deviate as the load increased. Possible explanations for this include variability in the installation quality, natural variability in the soil, or the effect of uplift testing that was performed prior to lateral testing. The latter explanation most likely suits pile SP-03. The load cell malfunctioned during the test, which led to incorrect readings of the actual load. It was observed that the pile was jacked upwards by at least 25 mm before identifying the issue. This excess uplift displacement likely negatively affected the lateral load capacity of the pile, which was tested less than two weeks later.
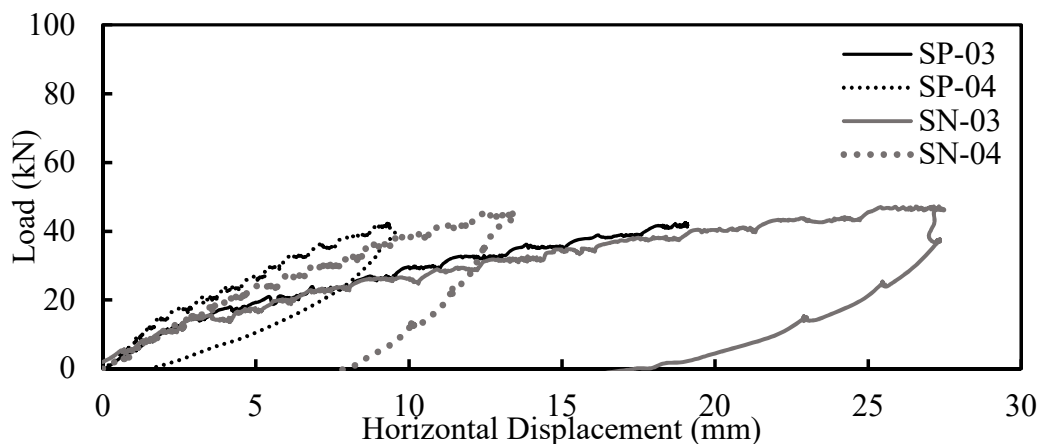
Figure 4-2: Lateral load-displacement curve for single plate piles (SP-03,04, SN-03,04).

The load-displacement curves for drilled shafts DS-01 and DS-02 are presented in Figure 4-3. The load at 25 mm of ground level deflection for DS-01 and DS-02 were approximately 145 kN and 103 kN, respectively. It was observed that at low load levels (P < 28 kN), the displacement was too small to be detected by the linear potentiometers. DS-02 experienced significantly more displacement than DS-01 at the same load levels due to the misplacement of the reinforcing steel. This resulted in a divergence in the load-

displacement curve from DS-01 after approximately 7 mm of displacement, at which point cracks initiated in the concrete and a gap opened at the interface with the steel section at a rapid rate as shown in Figure 4-4.
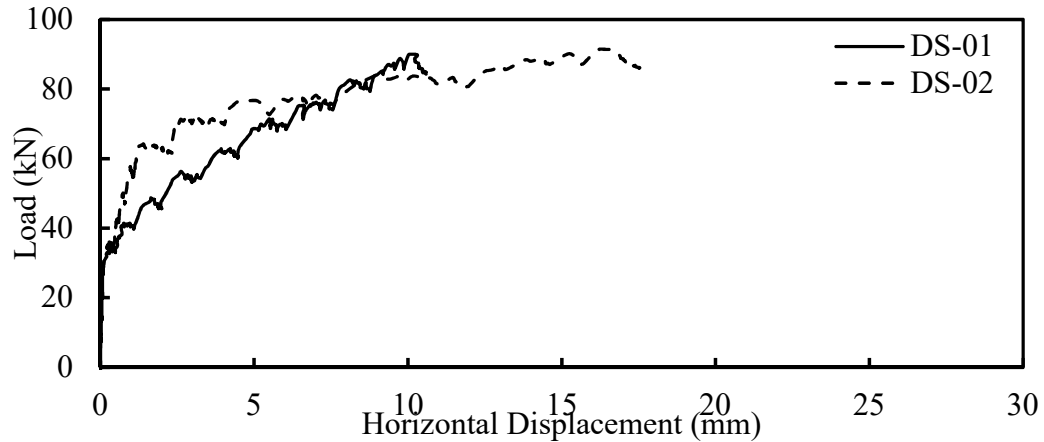
Figure 4-3: Lateral load-displacement curve for drilled shafts (DS-01,02).

Figure 4-4: Crack in DS-02 during lateral load test.

The load-displacement curves for the unmodified H-piles are presented in Figure 4-5. The horizontal displacement at 25 mm of displacement was 45 and 51 kN for PP-01 and PP-02, respectively. Similarly, PP-01 exhibited a lower uplift capacity compared to PP-02 (as will be discussed in Chapter 5). This may be attributed to the difference in pile installation quality and variability in soil conditions.
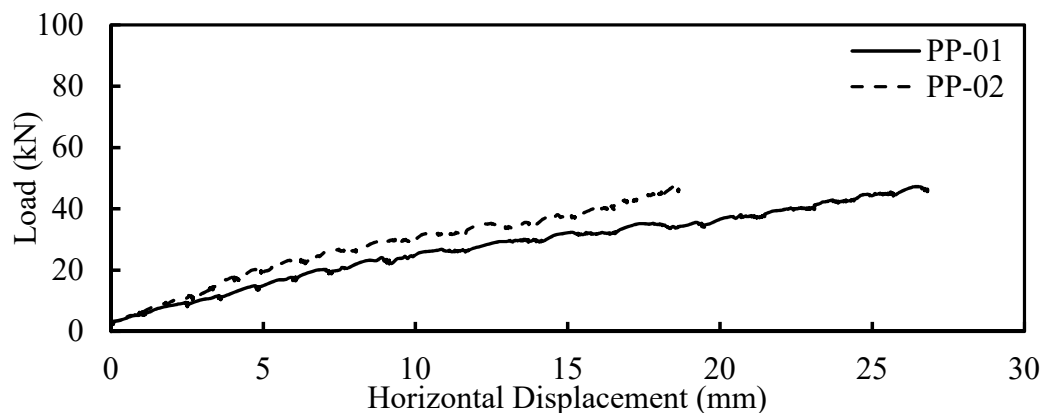
Figure 4-5: Lateral load-displacement curve for plain piles (PP-01,02).

The lateral capacity of the tested piles was compared to their design lateral load (i.e. wind load) in Table 4-1. The total lateral load demand is 26.68 kN, which considers a wall height of 5.0 m, a pile spacing of 3.07 m, and wind pressure with a 25-year return period. The pile spacing is based on the deflection limits of the sound wall and the wind pressure is selected according to the Canadian High Bridge Design Code (CHBDC) in A3.1.1 (CSA Group, 2014). The average lateral capacity of single plate piles was 59.1 kN (F.S. = 2.2), which is approximately 22% higher than the average lateral capacity of 48 kN (F.S. = 1.8) for unmodified H-piles. The single plate piles without nodes had generally higher capacities than those with nodes. This difference in capacity is attributed to installation quality rather than any effect from the nodes. The drilled shafts had significantly higher capacity compared to the steel piles, which was expected due to their much larger cross-section.

Table 4-1: Comparison of tested piles to design wind load.

Pile I.D.	Lateral Load Capacity (kN)	F.S.	Average F.S. Per Pile Type
PP-01	45	1.7	1.8
PP-02	51	1.9	
SP-03	53	2.0	2.4
SP-04	75	2.8	
SN-03	46.5	1.7	2.0
SN-04	62	2.3	
DS-01	145	5.4	4.6
DS-02	103	3.9	

4.4 Monotonic Lateral Numerical Modelling and Parametric Study

The monotonic pile load tests were modelled using LPILE (Ensoft Inc., 2019), which is commercial software widely used to estimate the behaviour of single piles subject to lateral loads. LPILE uses the p-y method, which incorporates a series of non-linear springs distributed along the pile shaft to simulate the relationship between soil pressure per pile length and pile deflection (Ensoft Inc., 2019). LPILE was selected for the parametric study because it is a simple yet reliable tool that is commonly used in industry for designing laterally loaded piles.

4.4.1 Plate Pile Model Calibration and Validation

The LPILE model was first calibrated using data from the static lateral load tests on single plate piles. The calibrated model would require a satisfactory match with the field data for the load-displacement curve and bending moment distribution along the pile. This match is achieved by slightly varying some of the soil properties within its expected/measured range. Once the model was calibrated, it was validated by predicting the behaviour of the unmodified piles tested by the author and the preliminary piles tested by AIL. A successful match with the field data indicates the model is expected to produce reliable results for parameters outside the scope of the field testing that was performed.

4.4.1.1 Soil and Pile Properties and Models

The model selected in LPILE to represent the soil was "modified stiff clay without free water". This model was selected because of the type of soil on site and that the pile shaft was above the water table. Three methods of selecting the soil modulus, k, were tested: 1) the k value is internally selected by LPILE based on the specified undrained shear strength of soil, 2) correlating k with S_u from Liang (2002), or 3) k is estimated by Equation 4-1 (Salgado, 2008):

$$k = \frac{9S_u}{5\varepsilon_{50}B}$$

(4-1)

where S_u is the undrained shear strength of the soil layer, ε_{50} is the axial strain at one half of the soil's final shear strength, and B is the pile width. Note that the original equation was normalized by B to make it a function of pile width in the appropriate units. ε_{50} was estimated using correlations with S_u which are provided by Liang (2002). Equation 4-1 resulted in the best match between the predicted load-displacement curve and field test results for single plate piles. The other two methods slightly over-estimated the response but could be considered satisfactory. S_u for each soil layer was selected using representative values established from field and laboratory testing. The soil properties obtained for the calibrated LPILE model are presented in Table 4-2.

Table 4-2: Soil properties after the calibration of single plate pile LPILE model.

Depth (m)	Unit Wt. (kN/m³)	Su (kPa)	k (kN/m³)	ε_{50}
0 - 0.9	19	110	100000	0.005
0.9 - 2.0	21	60	95000	0.007
2.0+	21.5	125	271000	0.005

The pile properties inputted to LPILE are summarized in Table 4-3. The properties for the unmodified section were taken directly from the handbook of steel construction. The properties for the plate section were calculated manually considering the addition of the plate to the H-pile. The plate section of the pile was modelled as a rectangle with user defined inputs. This rectangle was defined to have the same area, moment of inertia, and width perpendicular to loading as the actual section tested in the field. The non-plate sections of the pile were modelled as H-piles bending about the strong axis. The entire pile was modelled as linear elastic since the load is relatively small compared to the capacity of the pile cross-section and therefore no yielding of steel occurred.

Table 4-3: Pile properties inputted into calibrated LPILE model.

Section of Pile	Length (m)	E (kPa)	I_x (m⁴)	Area (m²)	Width (m)	Model Type
Stickup	1.25	2E+08	3.44E-05	0.00457	0.165	H-pile (Strong axis)
Plated Section	0.95	2E+08	5.72E-05	0.00835	0.42	Pure Elastic Rectangle
Plain Pile	2.55	2E+08	3.44E-05	0.00457	0.165	H-pile (Strong axis)

4.4.1.2 Calibrated Model Load-Displacement Curve and Bending Moment Distribution

The load was applied at 1.25 m above the ground surface at equal increments. LPILE can only provide load-displacement curves for the top of the pile. In this case the load is applied well above the ground surface, which is the desired point of analysis for the load-displacement curve. Therefore, LPILE would normally terminate the analysis well before 25 mm of deflection at the ground level due to excessive deflection at the top. To overcome this issue, the convergence tolerance and number of iterations was increased so that LPILE would not encounter convergence issues at very high displacements. The comparison of the results obtained from the calibrated model with experimental data is shown in Figure 4-6, which shows an excellent match. Only SP4 and SN4 were used in the analysis because SP3 and SN3 experienced lower capacities for reasons explained in subsection 4.3. The estimated moment distribution was also compared to the field test data as shown in Figure 4-7. The bending moment along the pile shaft for all static lateral tests are presented on the same figure since each pile had only a few functioning strain gauges. The bending moment was compared at a horizontal load of 51 kN, which was the highest magnitude shared by all four piles. The model compared very well with the field data, which further confirms that the model was well calibrated and the selected soil parameters are expected to be representative of the field conditions.
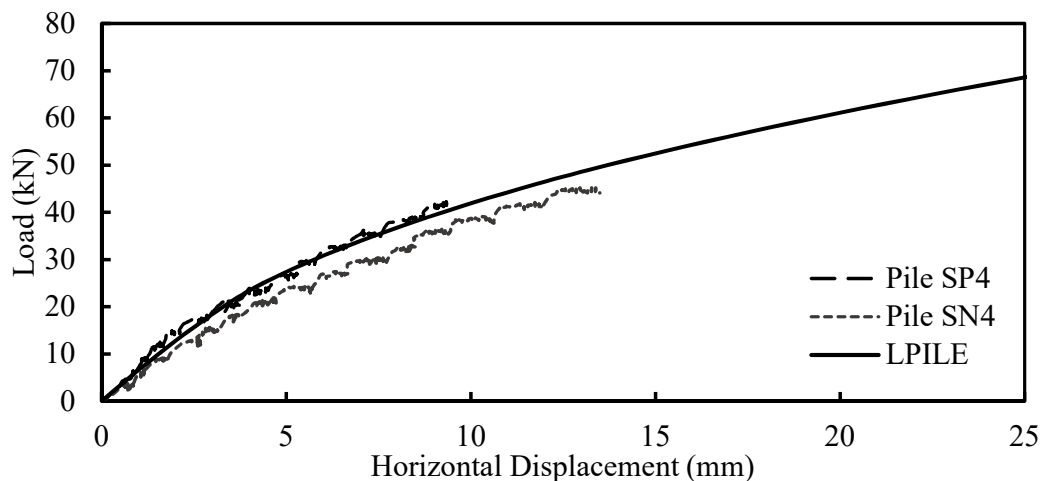
Figure 4-6: Comparison between calibrated LPILE model and experimental data.
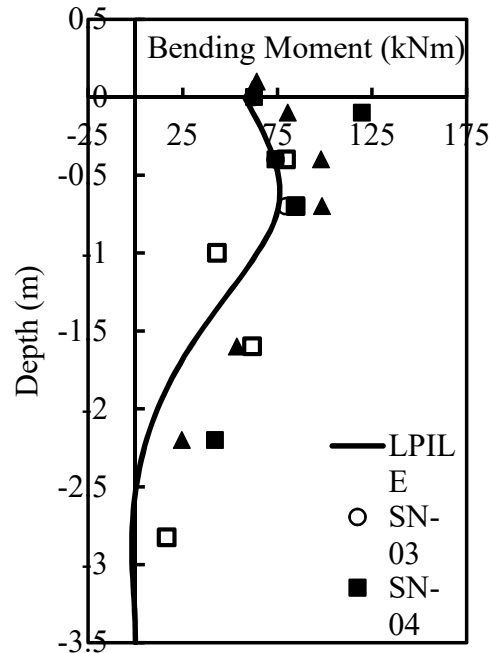
Figure 4-7: Comparison of bending moment distribution along shaft of single plate piles at a horizontal load of 51 kN.

4.4.1.3   LPILE Model Validation

The calibrated model was first validated by modelling the unmodified H piles that were tested in the exact same manner as the single plate piles. The results of the analysis were then compared to the load-displacement curves measured in the field as shown in Figure 4-8. A second validation was performed by modelling the response of single plate piles tested by AIL in the preliminary testing phase. The only details given about the soil profile is that it was comprised of medium dense sandy soil. It was assumed that the sand had a friction angle of 35° and unit weight of 19 kN/m³, which can be considered a median value for medium dense sand (Budhu, 2011). The value for k was inputted as 24430 kN/m³ which was correlated from Liang (2002). The Reese sand model was selected to represent the soil. The comparison between the calculated and measured responses is shown in Figure 4-9. The second model considered a different soil profile than what the novel piles were tested in and therefore cannot be considered a validation of the main numerical model. However, the remainder of the input parameters were

consistent with the first model and therefore a successful match with field data does validate LPILE to be a proper tool for modelling the novel pile design.

The results obtained by LPILE are in excellent agreement with the actual load-displacement curve for both cases. This excellent agreement between calculated and measured responses for clay and sandy soil indicates that LPILE along with the proposed method for modeling the modified pile configuration is suitable for modeling the lateral response of the novel pile and therefore is expected to provide realistic results for the parametric study.
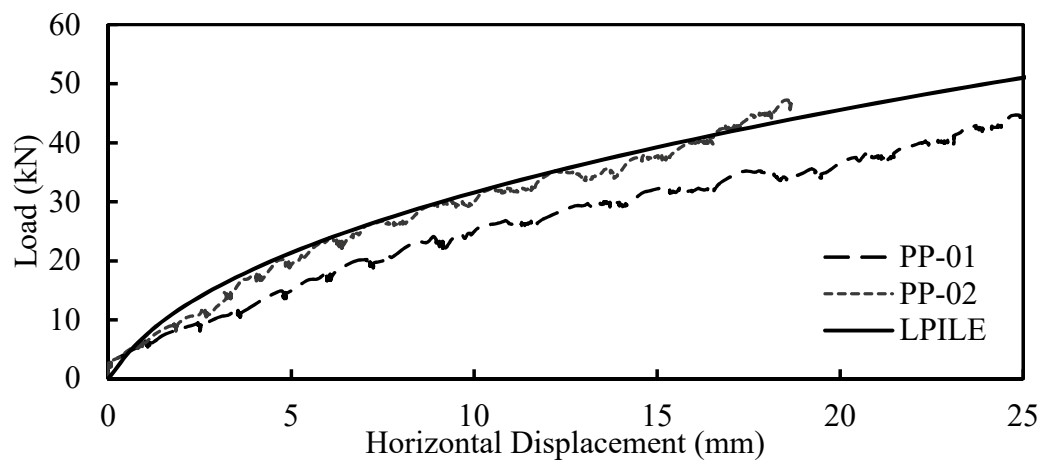
Figure 4-8: Comparison of LPILE model with unmodified H-pile results.
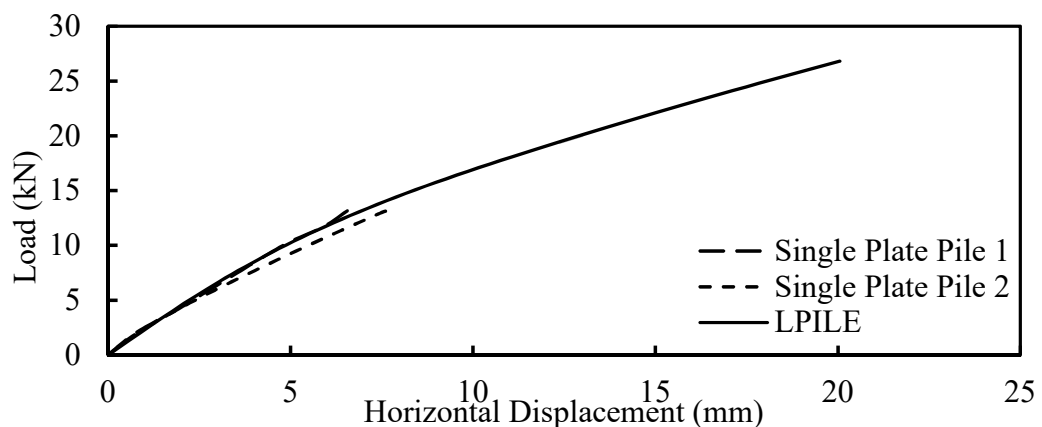
Figure 4-9: Comparison of LPILE model with plate piles from the AIL preliminary tests.

4.4.1.4   Load and Deflection Distribution of Single Plate Piles

The calibrated LPILE model was used to estimate the shear force, bending moment, and horizontal deflection profiles along the shaft of a single plate pile for increasing load increments. The results of the analysis are shown in Figure 4-10. It is observed that only the top 2.0 m of the pile below ground surface experiences deflection while the remaining 1.5 m experiences little or no deflection. This indicates that the pile exhibits flexible behaviour and that the top 2.0 m of the pile, which corresponds 12B or 4.75W of the pile, primarily contributes to the lateral load resistance of the pile, where B is equals the width of the pile flange and W equals the width of the plate.
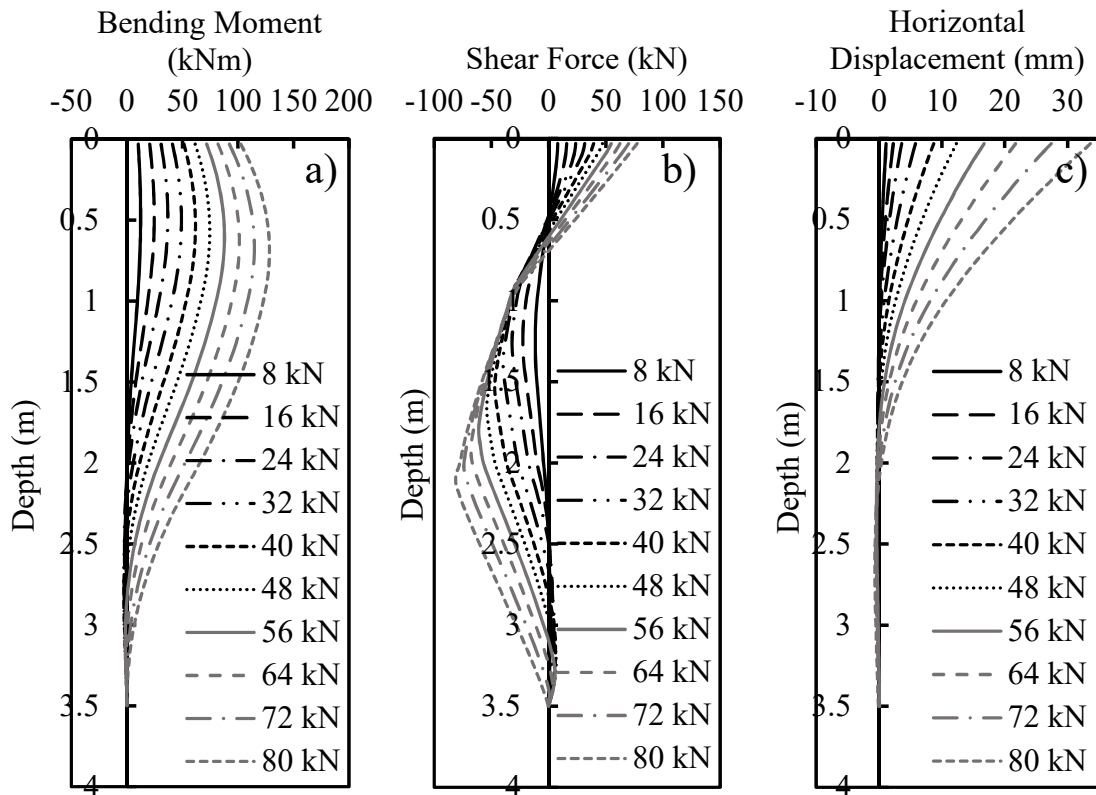
Figure 4-10: a) Shear force, b) bending moment, c) and horizontal deflection distribution along a single plate pile under various loads.

4.4.2   LPILE Parametric Study

The parametric study was conducted to evaluate the effects of the geometrical properties of the plate (plate length and width) of the proposed pile configuration on the lateral capacity of the pile. The plate widths selected for the analysis were 315 mm, 525 mm, and 630 mm (-25%, +25% and +50% of the original width), all at a constant plate length of 950 mm. The plate lengths selected for the analysis were 712.5 mm, 1188 mm, and 1425 mm (-25%, +25% and +50% of the original length), all at a constant plate width of 420 mm. A 25% change in length or width results in the same percentage increase in steel weight, which facilitates the optimization of the pile geometry based on the comparative results. The parametric study considered three different soil profiles: a soil profile similar to that at the test site, a soil profile comprised of clay layers with different levels of strength, and a soil profile comprising sand layers with different levels of strength. Note that all comparisons are made in terms of the lateral force required to induce a 25 mm deflection of the pile at ground level. The total pile length below ground remained at 3.5 m for all cases considered in the parametric study.

4.4.2.1   Single Plate Pile in Test Soil Profile

The variation in pile performance due to plate width and length changes are shown in Figures 4-11 (a) and 4-11 (b), respectively. The applied lateral load that induces 25 mm of deflection at the ground surface for each case is summarized in Table 4-4. For the purpose of comparison, the lateral load for the original pile configuration is also shown in Table 4-4. The analysis shows that increasing the plate width had a greater effect on the pile's stiffness and capacity. This is expected because the plate was situated within the upper stiff clay layer (950 mm long plate vs. 900 mm depth of stiff soil). The soil below the plate had a lower stiffness. Therefore, increasing the plate width increased the area in contact with the stiffer soil, whereas increasing the plate length increased the area of contact with softer soil.
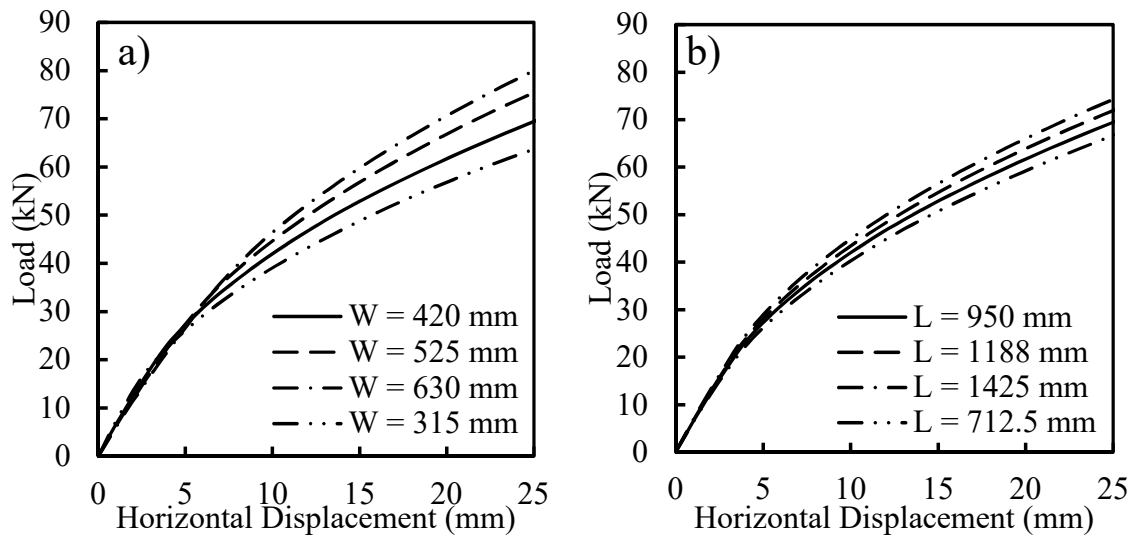
Figure 4-11: Effect of a) plate width and b) plate length on single plate pile behaviour in original soil profile.

Table 4-4: Summary of parametric study for pile in original soil profile.

Plate Length (mm)	Plate Width (mm)	H @ 25 mm (kN)	%H$_o$	Comments
950	420	69	-	Original Dimensions
950	525	75	8.7	Plate 25% Wider
950	630	80	15.9	Plate 50% Wider
950	315	64	-7.2	Plate 25% Narrower
1188	420	72	4.3	Plate 25% Longer
1425	420	74	7.2	Plate 50% Longer
712.5	420	66	-4.3	Plate 25% Shorter

4.4.2.2   Single Plate Pile in Homogenous Clay Soil Profile

A homogenous clay soil profile was considered with three different undrained shear strengths: 25 kPa, 50 kPa, and 100 kPa, which correspond to soft, firm, and stiff clay, respectively. The soil properties used in the LPILE models are summarized in Table 4-5. The unit weights were selected according to some general estimates based on soil type

and strength (Budhu, 2011). The soil modulus parameter, k, was estimated using Equation 4-1 (Salgado, 2008). Because k is dependent on pile width, the lower k value represents the soil at the plated section and the higher k value represents soil below the plate. The soil model selected for generating the p-y curves was the modified stiff clay without free water model, since the water table was assumed to be below the pile toe. The load-displacement curve for a single plate pile with the original dimensions in clay soil with 25 kPa, 50 kPa, and 100 kPa undrained shear strength is shown in Figure 4-12 and the effect of varying plate width and length for each level of clay strength is shown in Figures 4-13 to 4-15. The applied lateral load at 25 mm of deflection at the ground surface for each case is summarized in Table 4-6 and compared to a pile with the original dimensions.

Table 4-5: Selected properties for clay soil profile parametric study.

Su (kPa)	Unit Wt. (kN/m³)	k (kN/m³)	ε_{50}
25	16	11000/27000	0.01
50	18	31000/78000	0.007
100	20	85000/220000	0.005
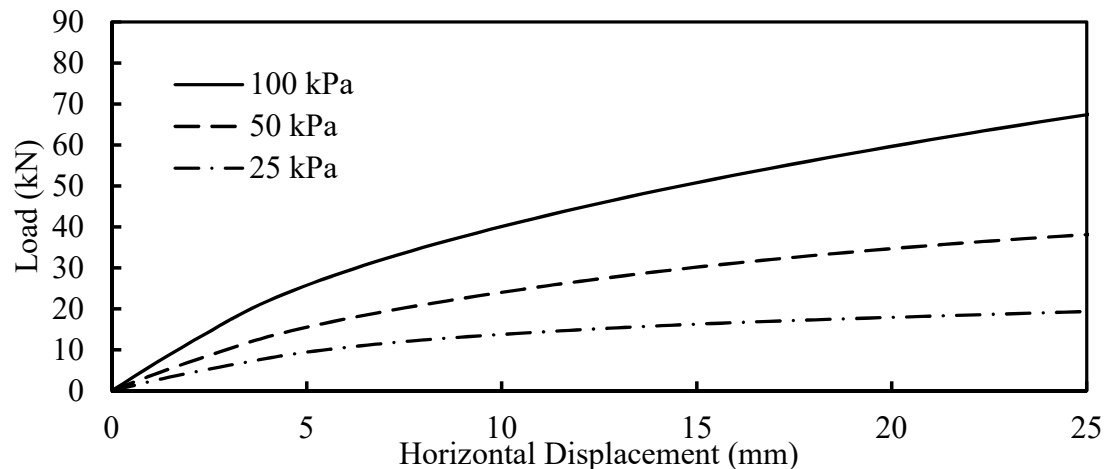
Figure 4-12: LPILE model results of single plate pile in soft, firm, and stiff clay.
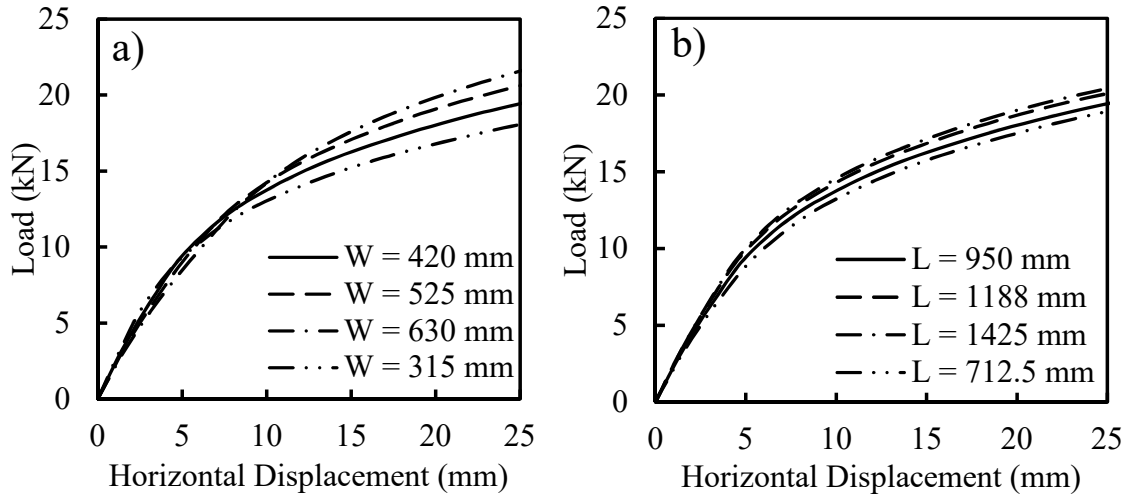
Figure 4-13: Effect of a) plate width and b) plate length on single plate pile behavior in 25 kPa clay.
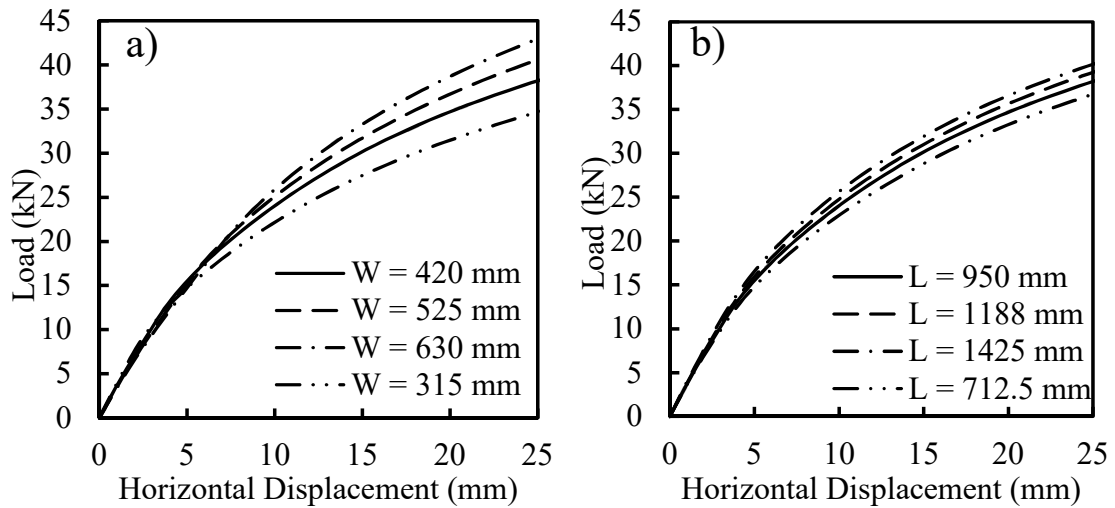
Figure 4-14: Effect of a) plate width and b) plate length on single plate pile behavior in 50 kPa clay.
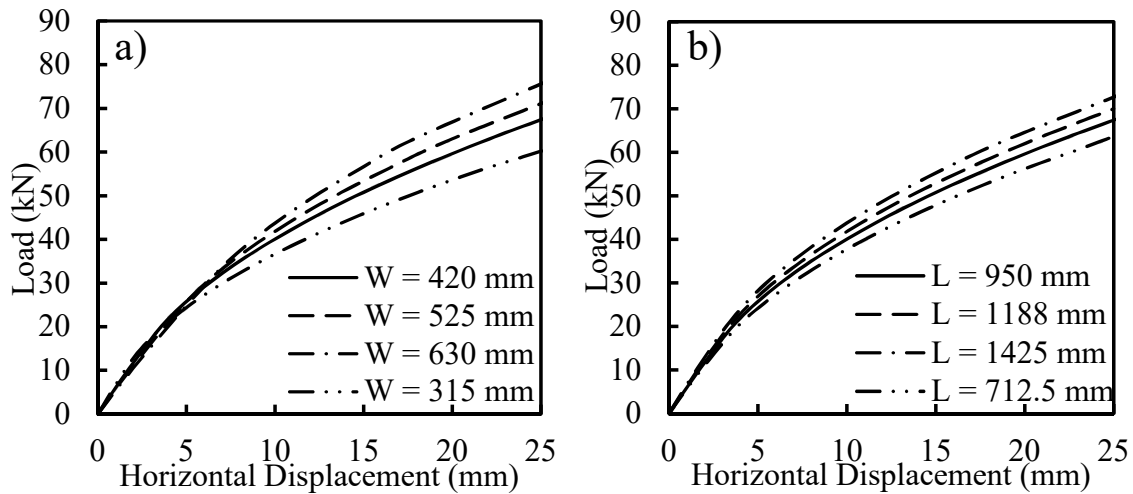
Figure 4-15: Effect of a) plate width and b) plate length on single plate pile behaviour in 100 kPa clay.

Table 4-6: Summary of clay soil profile parametric study.

Su (kPa)	Plate Length (mm)	Plate Width (mm)	H @ 25 mm (kN)	%Ho	Comments
	950	420	19.5	-	Original Dimensions
	950	525	20.75	6.4	Plate 25% Wider
	950	630	21.5	10.3	Plate 50% Wider
25	950	315	18	-7.7	Plate 25% Narrower
	1188	420	20	2.6	Plate 25% Longer
	1425	420	20.5	5.1	Plate 50% Longer
	712.5	420	19	-2.6	Plate 25% Shorter
	950	420	38	-	Original Dimensions
	950	525	40.5	6.6	Plate 25% Wider
	950	630	43	13.2	Plate 50% Wider
50	950	315	34.5	-9.2	Plate 25% Narrower
	1188	420	39	2.6	Plate 25% Longer
	1425	420	40	5.3	Plate 50% Longer
	712.5	420	36.75	-3.3	Plate 25% Shorter
	950	420	67	-	Original Dimensions
	950	525	71	6.0	Plate 25% Wider
	950	630	75.5	12.7	Plate 50% Wider
100	950	315	60	-10.4	Plate 25% Narrower
	1188	420	70	4.5	Plate 25% Longer
	1425	420	73	9.0	Plate 50% Longer
	712.5	420	63.5	-5.2	Plate 25% Shorter

The results of the parametric study in clay soils show that increasing the plate width is more effective than increasing plate length for increasing the lateral capacity of plated piles. This is expected since the lateral capacity of piles is typically governed by the portion of the pile near the ground surface.

4.4.2.3   Single Plate Pile in Sandy Soil Profile

A sandy soil profile was considered at three different friction angles: 30°, 35°, and 40° which corresponds to loose, compact, and dense sand, respectively. The soil properties used in the LPILE model to represent the soil are presented in Table 4-7. The sand unit weight was selected according to some general estimates based on soil type and strength (Budhu, 2011). The k soil modulus parameter was estimated using values for loose, compact, and dense sand above the water table from Liang (2002). The p-y curve soil model used was the Reese sand model.

Table 4-7: Inputted properties for sandy soil profile parametric study.

ϕ' (°)	Unit Wt. (kN/m³)	k (kN/m³)
30	18.5	6790
35	20.5	24430
40	22.5	61000

The load-displacement curve for a single plate pile with the original tested dimensions in 30°, 35°, and 40° sand is shown in Figure 4-16 and the effect of varying plate width and length for each level of sand strength is shown in Figures 4-17 to 4-19. The applied lateral loads that resulted in 25 mm of deflection at the ground surface for each case are summarized in Table 4-8 and are compared to the loads for the original pile configuration.

The results of the parametric study in sand show that increasing the pile width is more effective than increasing plate length for increasing the lateral capacity of a plated pile, however the difference is smaller compared to clay. It was also observed that as the strength of the sand increases, the difference between increasing plate width and plate

length becomes smaller. At $\phi = 40°$, changing the plate width and length by the same percentages yields a similar change in capacity.
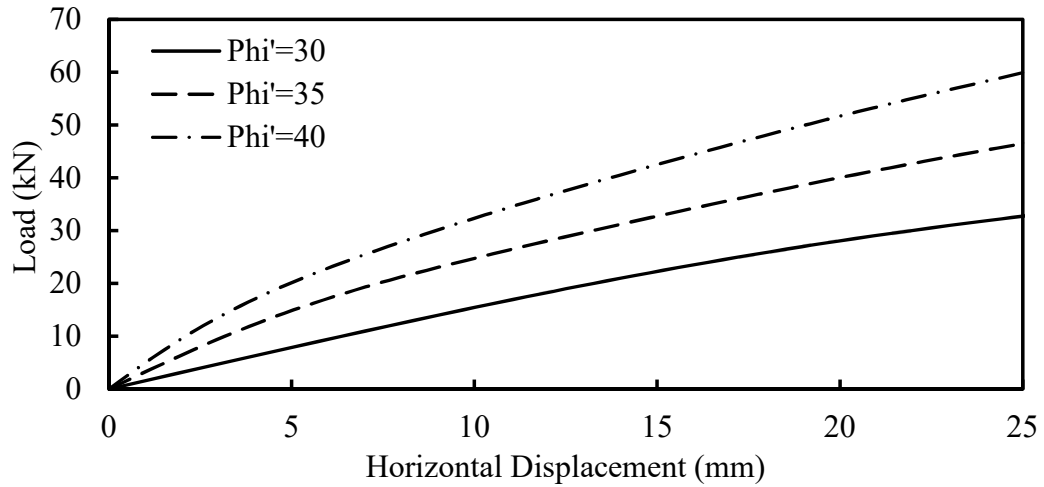
Figure 4-16: LPILE model results of single plate pile in loose, compact, and dense sand.
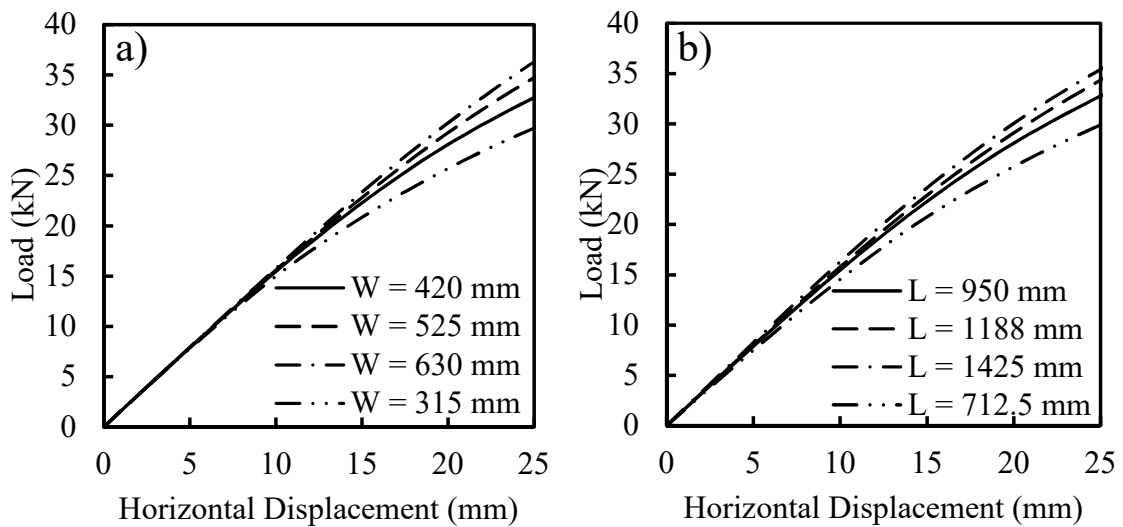
Figure 4-17: Effect of a) plate width and b) plate length on single plate pile behavior in $\phi' = 30°$ sand.
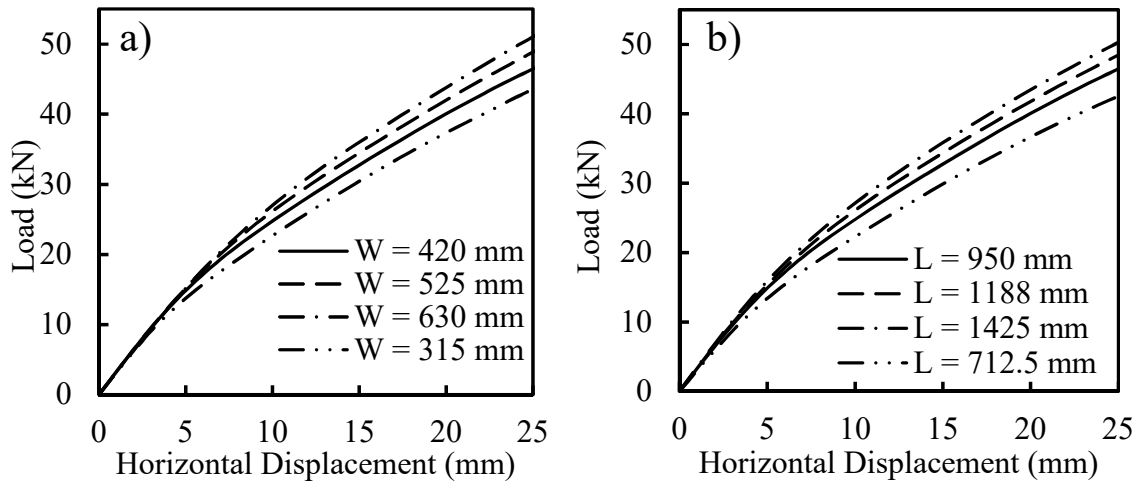
Figure 4-18: Effect of a) plate width and b) plate length on single plate pile behavior in φ' = 35° sand.
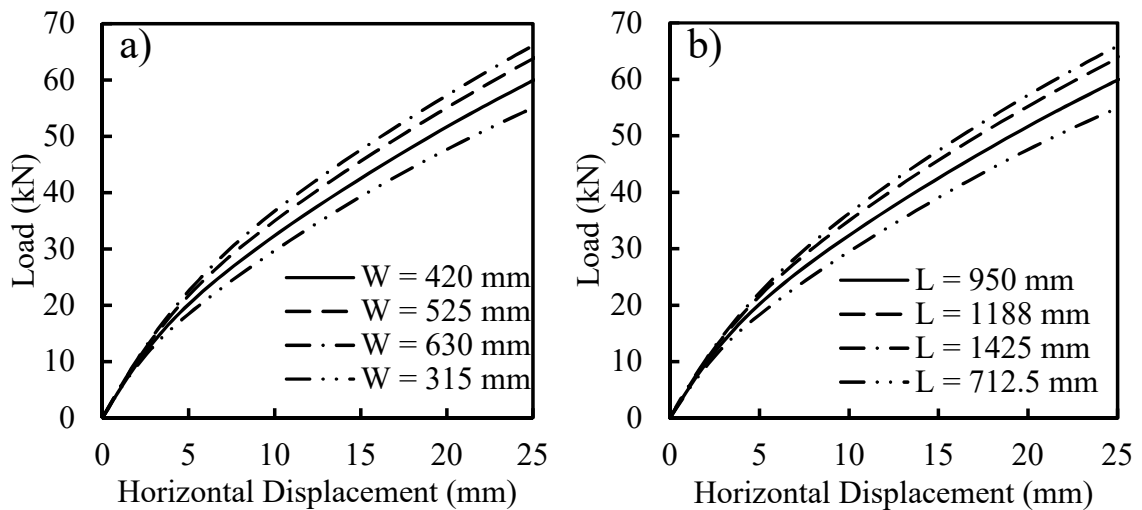
Figure 4-19: Effect of a) plate width and b) plate length on single plate pile behavior in φ' = 40° sand.

Table 4-8: Summary of pure sand soil profile parametric study.

φ' (°)	Plate Length (mm)	Plate Width	H @ 25 mm (kN)	%Ho	Comments
	950	420	33	-	Original Dimensions
	950	525	34.75	5.3	Plate 25% Wider
	950	630	36	9.1	Plate 50% Wider
30	950	315	29.5	-10.6	Plate 25% Narrower
	1188	420	34.25	3.8	Plate 25% Longer
	1425	420	35.5	7.6	Plate 50% Longer
	712.5	420	29.75	-9.8	Plate 25% Shorter
	950	420	46.5	-	Original Dimensions
	950	525	49	5.4	Plate 25% Wider
	950	630	51	9.7	Plate 50% Wider
35	950	315	43.5	-6.5	Plate 25% Narrower
	1188	420	48.5	4.3	Plate 25% Longer
	1425	420	50.25	8.1	Plate 50% Longer
	712.5	420	42.5	-8.6	Plate 25% Shorter
	950	420	60	-	Original Dimensions
	950	525	64	6.7	Plate 25% Wider
	950	630	66	10.0	Plate 50% Wider
40	950	315	55	-8.3	Plate 25% Narrower
	1188	420	63.5	5.8	Plate 25% Longer
	1425	420	66	10.0	Plate 50% Longer
	712.5	420	54.75	-8.8	Plate 25% Shorter

4.4.2.4 Comparison of Lateral Capacity of Novel Pile with Equivalent H Pile

The proposed pile configuration can be beneficial in cases where lateral resistance governs the design of the foundation. The addition of the plate may allow utilizing an H-pile with a smaller cross-section which would still provide adequate axial capacity. The potential cost-savings of the proposed pile configuration was explored by comparing the weight (calculated from a reduction in volume) of steel required for equivalent capacity unmodified H-piles. The lateral capacities were compared at 25 mm of deflection. The smallest comparable W-section was W460x52, which has the smallest cross-sectional area for the same load-resisting capabilities at 25 mm of deflection. Both piles were modelled with a length of 3.5 m below the ground surface, loaded at 1.25 m above the ground surface, and placed in the same soil profile as the testing site. The load-displacement curves are shown in Figure 4-20. Considering only the steel below ground,

the proposed pile configuration only requires 154 kg of steel compared to a W460x52 pile which requires 182 kg of steel. This is an approximate reduction of 15%.
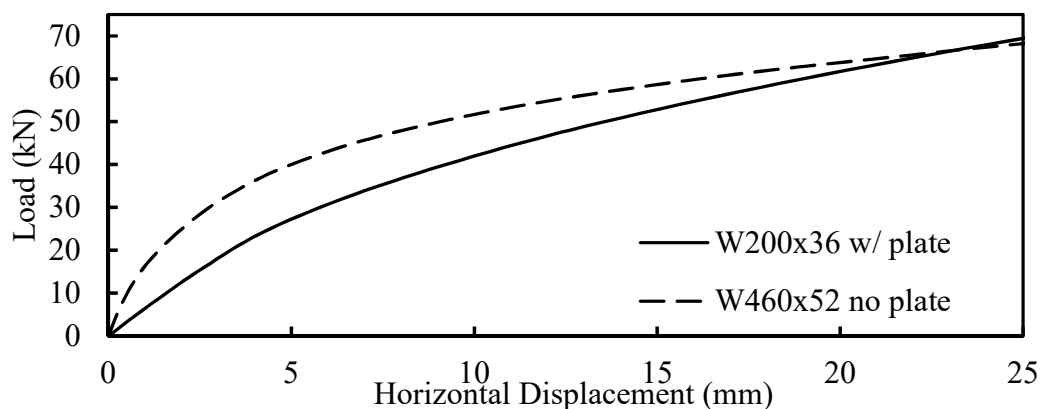
Figure 4-20: Comparison of a W200x36 section with a single plate to an unmodified W460x52 pile.

4.5 Cyclic Lateral Load Test Results

Cyclic lateral load testing was performed on the eight piles that were not tested in monotonic loading: PP-03, PP-04, SP-01, SP-02, SN-01, SN-02, DP-01, and DP-02. The double plate piles were subjected to cyclic loading to evaluate whether the addition of the second plate leads to better performance under cyclic loads by reducing the degradation of soil strength or gapping at the pile-soil interface. The double plate piles were not tested under monotonic load since their lateral capacity is expected to be similar to single plate piles. It was anticipated that the second plate provides the pile more flexural rigidity, and the soil confined between the two plates will add additional shear resistance along the edge. The load-displacement curves for PP-03 and PP-04 are shown in Figure 4-21. Note that the data was reduced for all figures to show only every 10th cycle. These piles were subjected to 100 cycles of two-way loading at 15 kN. A second set of cycles could not be performed due to exceeding the stoke capacity of the hydraulic jack. The curves remained in the elastic region for approximately the first 5 kN. As the load increased, they exhibited non-linear behaviour. The amount of displacement gradually increased at the maximum load as the number of cycles increased. The difference in displacement between the first and last loading cycle is summarized for each pile in Table 4-9, which

may aid in assessing and comparing the reduction in lateral stiffness with the repeated loading of each pile. The single plate piles, SP-01 and SP-02, had similar load-displacement curves to the plain piles as shown in Figure 4-22, both in terms of stiffness and change in horizontal displacement over 100 cycles. This indicates that adding the plate had little effect on the performance of H-piles subject to small cyclic lateral loads. The single plate piles were also subjected to 70 cycles of loading at 24 kN of force immediately after the first 100 cycles. The full 100 cycles could not be achieved due to reaching the stroke limit of the jack. The load displacement curve showed a similar parabolic shape at 24 kN compared to the curve at 15 kN.
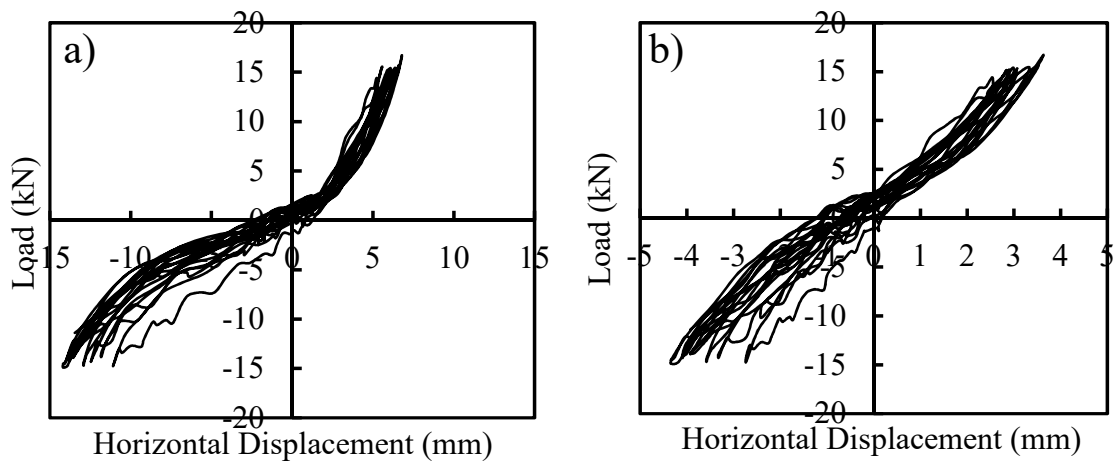
Figure 4-21: Cyclic lateral load test results for a) PP-03 and b) PP-04.
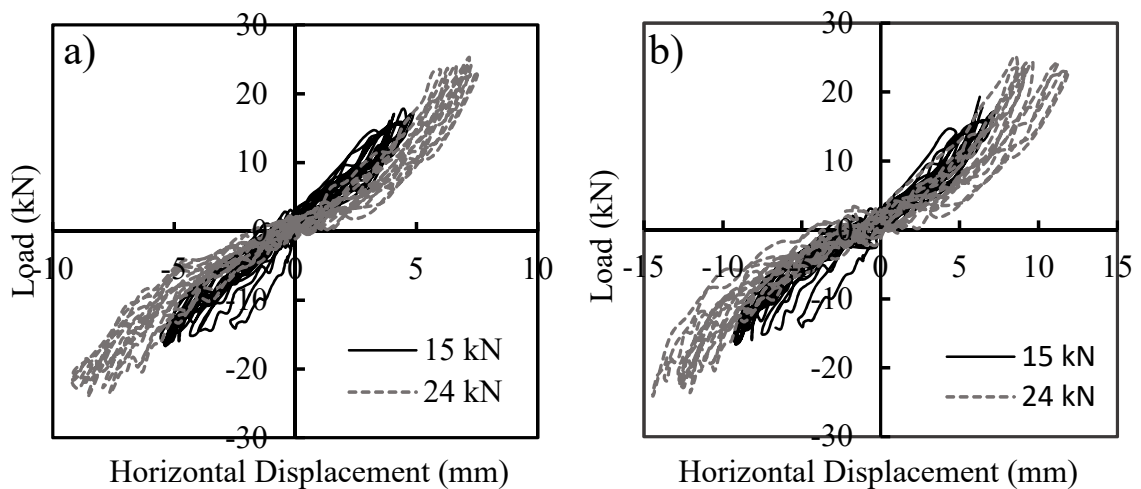
Figure 4-22: Cyclic lateral load test results for a) SP-01 and b) SP-02.

The load-displacement curves for SN-01 and SN-02 are shown in Figure 4-23. The curves exhibit identical behaviour to the single plate piles without nodes in the positive loading direction (push). The change in displacement over 100 cycles was significantly higher in the negative (pull) direction for both piles. This has been observed in other cyclic lateral load tests and is caused by the creation of a gap behind the pile on the opposite direction of loading. When reversing the load in the opposite direction, this gap must first be closed before the soil provides resistance, thus leading to higher displacements in one direction (Abd Elaziz, 2012; El Sharnouby, 2012).
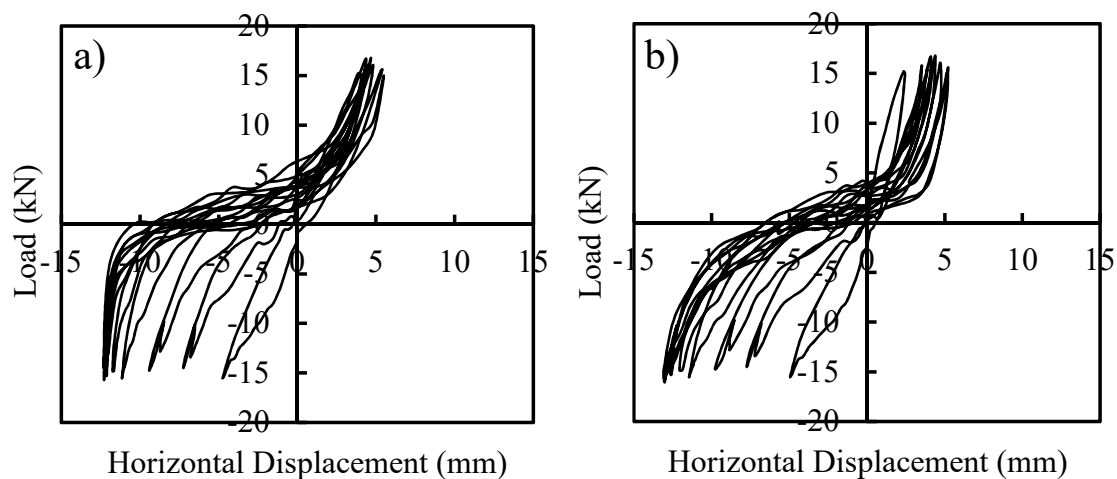
Figure 4-23: Cyclic lateral load test results for a) SN-01 and b) SN-02.

The applied loads were reduced for piles DP-01 and DP-02 to prevent exceeding the stroke limit of the hydraulic jack. Large gaps were identified between the pile and the soil which were created during installation. These gaps would have to be closed during loading before the pile could provide lateral resistance; thus, larger displacements were expected even at low loads. An attempt was made to close the gaps by filling them with drill cuttings from the drilled shaft installation. However, the soil could not be compacted very well manually and therefore did little to remediate the effect of the gap left from the installation. The load-displacement curves are presented Figure 4-24. The load cell reading displayed large fluctuations (+/- 2kN) during the test. The source of the noise could not be established, and the test was carried out under the current conditions. Despite the fluctuation in the curve, the behaviour of the pile is clearly established in the

Figure 4-24. The second set of load cycles were performed at 15 kN for 50 cycles, at which point the stroke limit was exceeded. Due to the poor installation of some of these piles which affected the results, the expected advantage of adding a second plate could not be established. However, the general shape of the curve was similar to that of the single plate piles. The curve was linear up to approximately 5 kN, at which point the response became nonlinear as the load increased.
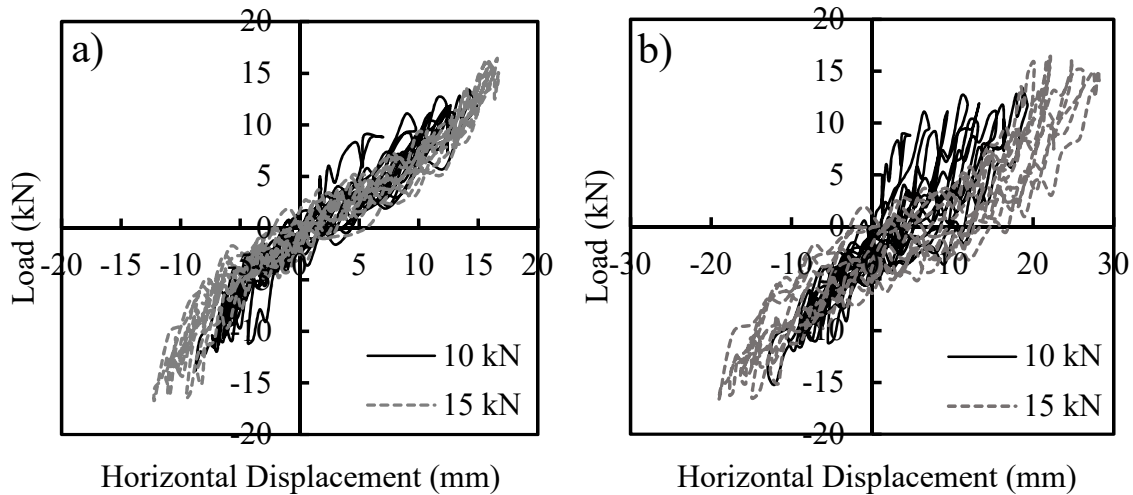
Figure 4-24: Cyclic lateral load test results for a) DP-01 and b) DP-02.

Table 4-9: Change in pile displacement from first to last cycle.

Pile I.D.	Load	Number of Cycles	Δ Displacement (mm) (+) Direction	(-) Direction	Comments
PP-03	15	100	1.5	-3.0	
PP-04	15	100	1.1	-1.6	
SP-01	15	100	1.3	-2.7	
	24	70	1.9	-2.7	
SP-02	15	100	2.2	-4.0	
	24	70	3.2	-2.1	
SN-01	15	100	1.7	-7.5	Gap b/w pile and soil on (-) side
SN-02	15	100	3.0	-8.0	Gap b/w pile and soil on (-) side
DP-01	10	100	7.9	-4.0	Gap from installation b/w pile and soil on (-) side
	15	50	1.7	-3.0	
DP-02	10	100	14.5	-5.4	Gap b/w pile and soil on both sides of pile from installation
	15	50	7.8	-4.2	

The effect of cyclic lateral loading on the piles was evaluated in terms of its lateral stiffness, which can be calculated using Equation 4-2:

$$k_L = \frac{P_{max} - P_{min}}{y_{max} - y_{min}} \qquad\qquad\text{(4-2)}$$

where P_{max} and P_{min} are the maximum and minimum applied load at the specific cycle, and y_{max} and y_{min} are the corresponding deflections to the maximum and minimum applied loads at the specific cycle. To represent the effect of cyclic loading on the tested piles, the ratio of the stiffness (k_L) at increasing cycles to the stiffness of the initial cycle (k_{LO}) is shown for each pile in Figures 4-25 to 4-28. The ratio of k_L/k_{LO} tends to stabilize at a consistent value within 100 cycles of lateral load for all piles. The plain piles experienced the least amount of degradation, with a k_L/k_{LO} ratio levelling off at 0.86 and 0.70 for PP-01 and PP-02, respectively. The ratio was lower for single plate piles SP-01 and SP-02 with value at 0.68 and 0.74, which is approximately 9% lower than plain piles. The ratio at 100 cycles was significantly lower for the remaining four piles, with values of 0.47, 0.40, 0.64, and 0.41 for SN-01, SN-02, DP-01, and DP-02, respectively. The initial stiffness for these four piles is lower than the plain pile and single plate piles as well. These results clearly demonstrate the need for careful installation of piles, as less than ideal installation leads to a severely reduced pile performance. For the second set of cyclic lateral loading on piles SP-01, SP-02, DP-01, and DP-02, it was observed that the stiffness degradation follows a very similar trend to that of the lower load cycles. The reduction in stiffness between the first cycle of the first load increment and the first cycle of the second load increment is 28% and 18% for SP-01 and SP-02, and 31% and 54% for DP-01 and DP-02, respectively. The reduction in stiffness between load cycles is larger for double plate piles, which is attributed to the installation quality. Because an equivalent assessment could not be performed between single and double plate piles, the effectiveness of adding the second plate could not be properly evaluated and is therefore inconclusive.
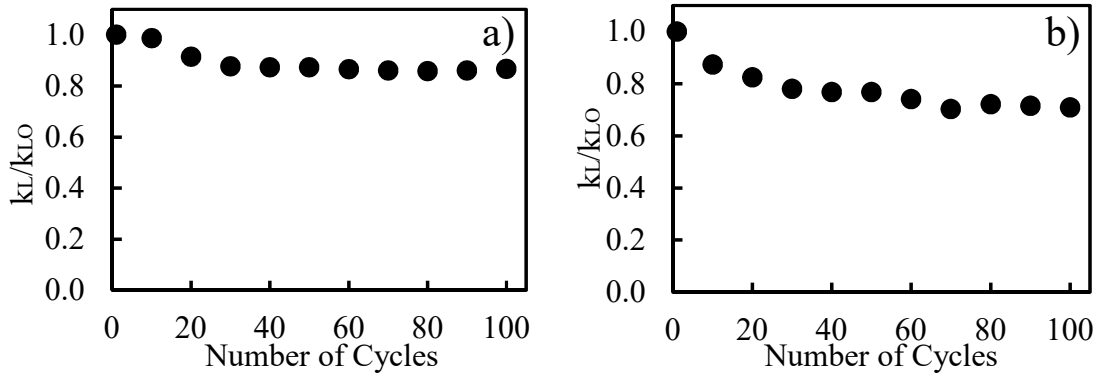
Figure 4-25: Degradation of stiffness of a) PP-03 and b) PP-04 subject to cyclic lateral loads.
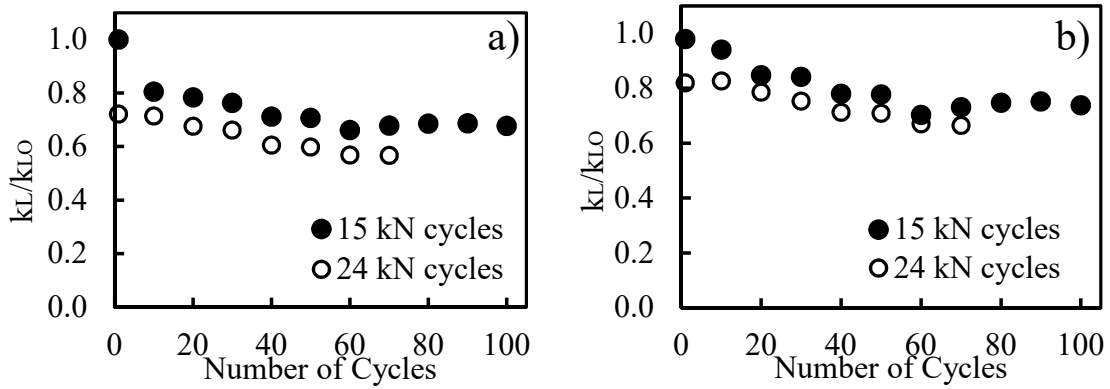
Figure 4-26: Degradation of stiffness of a) SP-01 and b) SP-02 subject to cyclic lateral loads.
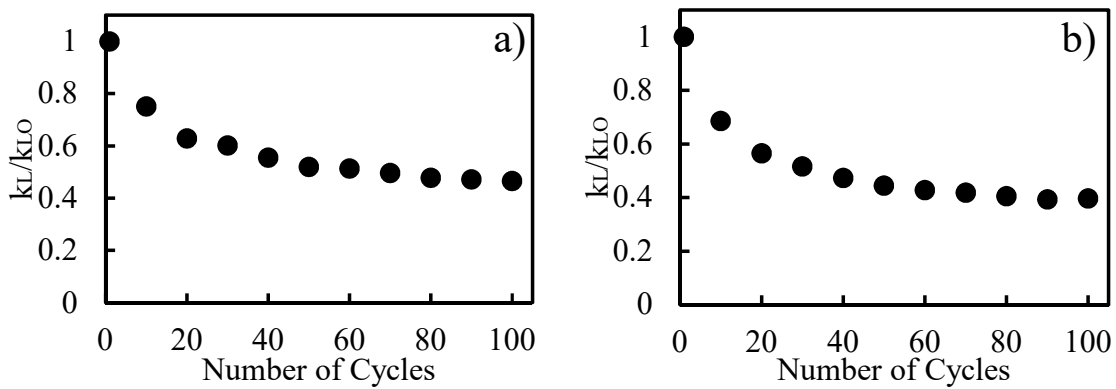
Figure 4-27: Degradation of stiffness of a) SN-01 and b) SN-02 subject to cyclic lateral loads.
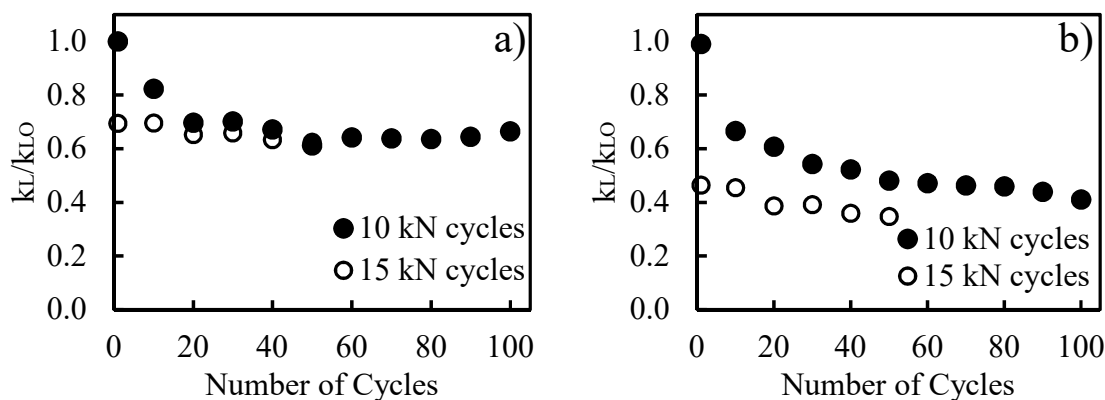
Figure 4-28: Degradation of stiffness of a) DP-01 and b) DP-02 subject to cyclic lateral loads.

4.6 GSNAP Modelling of Cyclically Loaded Novel Piles

The cyclic lateral load tests for single plate piles was terminated prematurely due to reaching the stroke limit of the hydraulic jack. The results of these tests were extended by calibrating a numerical model with the existing data; GSNAP (Geo-Structural Nonlinear Analysis Program) was selected for this purpose. GSNAP incorporates a generalized dynamic beam on nonlinear Winkler foundation (BNWF) soil model and considers key aspects of soil-structure interaction: (El Naggar and Heidari, 2018). GSNAP can simulate the behaviour of piles subjected to a large number of lateral loading cycles. Once the model was calibrated with the field results, a limited parametric study was performed with the model considering higher loads and a large number of load cycles to better characterize the novel pile's performance against repeated loading.

4.6.1 GSNAP Model Calibration

The values of soil undrained shear strength, c_u, soil modulus, k, and ε50 used in the GSNAP analysis was the same as those used in the LPILE analysis. GSNAP requires five additional inputs which dictate the pile's response when subject to cyclic lateral loading: stiffness degradation factor, stiffness curve shape parameter, strength curve shape parameter, strength degradation factor, and the gap parameter. The range of typical values for clay soils along with the selected inputs for the calibrated model are presented in Table 4-10. The stiffness and strength degradation factors were selected as greater than

one since the stiffness degradation decreased as the number of load cycles increased. The selected gapping parameter was 0.14 which was based on the observation that the soil remained mostly compressed after reversing the load on the pile. The meaning of these parameters is further discussed in Allotey and El Naggar (2008)and Heidari et al. (2014).

Table 4-10: Typical range of values for GSNAP input parameters and calibrated model selection.

Parameter	Range	Selected Value from Calibration
Stiffness Degradation Factor	> 1 hardening < 1 degradation	1.45
Strength Degradation Factor	> 1 hardening < 1 degradation	1.45
Stiffness Curve Shape Parameter	1.5 - 2.5	1.5
Strength Curve Shape Parameter	0.75 - 0.95	0.75
Gap Parameter	0 (pure gap) - 1 (entirely confined)	0.14

The cyclic loading pattern applied to the pile was 100 cycles of 15 kN load follow by 70 cycles of 24 kN load. The model output is compared to the field data in Figure 4-29. In general, the model predicted the pile's response to cyclic lateral loading well. The displacements at the second load cycles match, and the shape of the hysteretic loop are captured in the model. However, there exist some discrepancies between the prediction and the field load testing results. The model predicts a stiffer response for the first set of cycles, which is more evident in the positive loading direction. The model also predicts a stiffer response for the second set of cycles in the negative loading direction. However, it is not possible to get a perfect match in both directions due to an uneven stiffness in the tested pile.

4.6.2   Lateral Cyclic Loading Parametric Study

After calibration, the model was analyzed simulating a load of 26.68 kN and 53.36 kN (one and two times the design wind load) for 100 cycles each in succession. The results

of the simulation are shown in Figure 4-30. The single plate pile experiences 9 mm of deflection at the end of the first set of cycles. The pile deflects less than 25 mm for the first three cycles at 53.36 kN but exhibits excessive deflection for subsequent load cycles. This indicates the pile can successfully resist the design load but may experience excessive deflection if significantly higher forces are applied in succession.
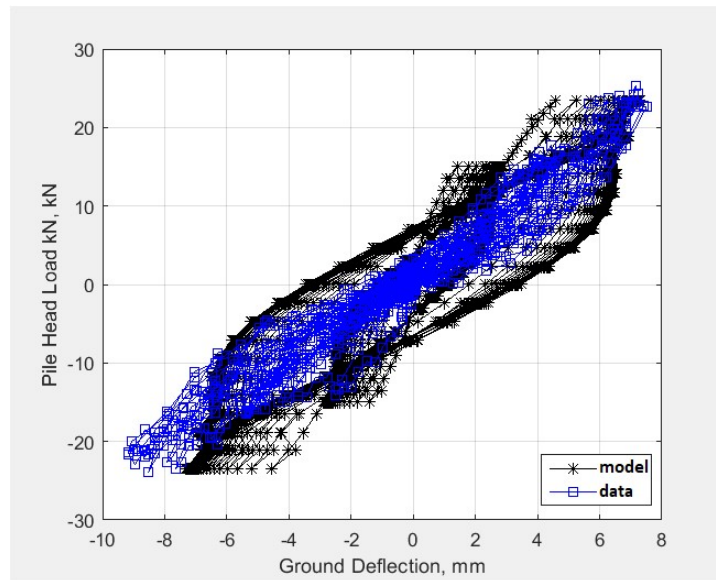
Figure 4-29: Calibrated model of a single plate pile subject to cyclic lateral loading.
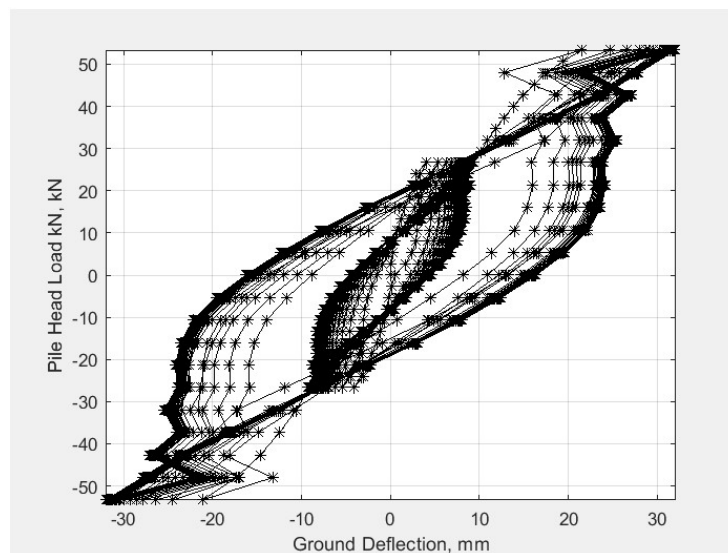
Figure 4-30: Simulated single plate pile at 100 cycles of one and two times the design wind load.

A third analysis was performed considering the effect of the unfactored wind load applied for many cycles to better analyze the pile's performance at the design load. The same model was run with a load of 26.68 kN applied to the pile for 1000 cycles and the results are shown in Figure 4-31. After 1000 cycles, the maximum deflection of the pile was estimated to be less than 10 mm. This indicates that the pile performs well under the design load and the stiffness does not degrade excessively after repeated loading for long periods of time.
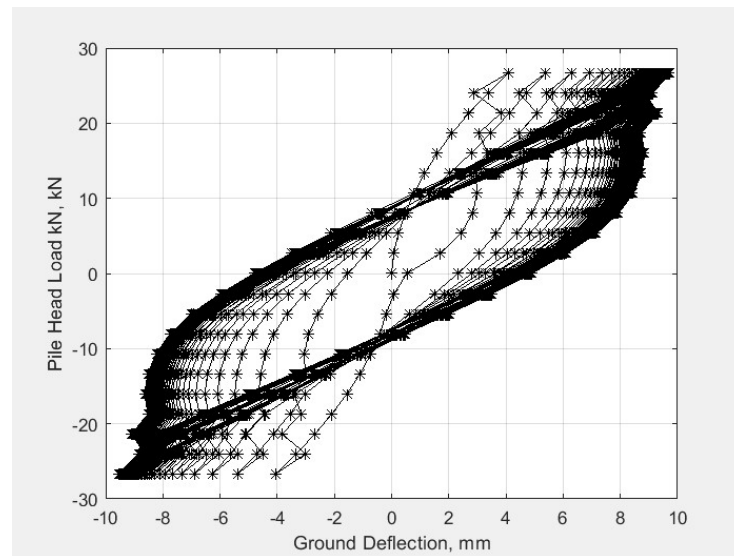
Figure 4-31: Simulated single plate pile at 1000 cycles of the design wind load.

4.7   Summary

A total of 16 piles were subjected to lateral load tests, eight piles were subjected to monotonic loading and the remaining eight piles were subjected to cyclic loading. The results of the monotonic field testing were used to calibrate and validate a numerical model using the program LPILE. The results showed that LPILE is able to simulate the behaviour of single plate piles. The model was used to conduct a parametric study to analyze the effect of different plate dimensions on the pile response in a practical range of soil conditions. The cyclic load test data was analyzed using the program GSNAP, which simulates the pile's behaviour when subjected to repeated loadings. A limited parametric study was conducted considering increased loads and a higher number of cycles. The main findings from the field testing and numerical modelling are as follows:

- The average load capacity of unmodified H-piles and single plate piles was 48.0 kN and 59.1 kN, respectively. This indicates that the addition of the plate increased the lateral capacity of the pile by approximately 22% in this particular soil profile. The capacity of the single plate pile was approximately half of the drilled shaft's lateral capacity.

- The average factor of safety of the single plate piles was 2.2 for a design wind force of 26.68 kN which considers a sound wall height of 5.0 m, a pile spacing of 3.07 m, and a wind pressure with a 25-year return period.

- The horizontal deflection along a single plate pile indicates the pile behaves as flexible. The top 12B or 4.75W of the pile primarily contributes to the lateral load resistance of the pile, where B is equals the width of the pile flange and W equals the width of the plate. The pile experiences negligible movement below this point.

- The installation quality of the pile had a direct effect on its performance when subjected to monotonic and cyclic lateral loads. Piles with an unideal installation typically suffered from reduced lateral capacities and a higher degree of shakedown.

- LPILE proved to be a suitable tool for estimating the performance of single plate piles subject to lateral loading. It is recommended to use the relationship from Salgado (2008) for estimating the k soil modulus parameter and the relationships from Liang (2002) for estimating ε_{50}.

- The plated section of the novel pile can be modelled as a purely elastic rectangular section in LPILE with user inputted area, moment of inertia, and width equivalent to the pile.

- In general, the plate width has greater influence on a pile's lateral capacity compared to plate length, especially in cohesive soils. For cohesionless soils, the different in increase/decrease between plate width and length equalizes as the soil density increases.

- Modified H-piles with plates may be utilized in cases where lateral loads govern the selection of pile dimensions. A smaller pile section may be selected and fitted with a plate to satisfy lateral force requirements. In the case of a 3.5 m pile in stiff to very stiff clay (same soil profile as the field tests), the novel pile requires approximately 15% less steel than an unmodified H-pile with an equivalent lateral capacity at 25 mm of deflection.

- The lateral stiffness degradation stabilizes at approximately 100 or less cycles at low-level loads. The lateral stiffness dropped to approximately 78% of its first cycle value for unmodified H-piles and 71% for single plate piles, which is approximately 9% lower. This indicates that single plate piles experience a minor increase in degradation compared to unmodified piles.

- The benefit of adding a second plate to a pile for improving cyclic performance was not conclusively observed due to installation problems of the double plate piles which directly affected the results.

- The calibrated GSNAP model was used to simulate a single plate pile subjected to cyclic lateral loads. The model was analyzed assuming one and two times the design wind load applied to the pile in succession for 100 cycles each. The model was also analyzed simulating the design wind load applied for 1000 cycles. The maximum deflection did not exceed 10 mm regardless of how many cycles of the design load was applied to the pile. However, the pile was estimated to have excessive deflection after only a few cycles at two times the design load indicating the foundation may exceed response tolerances when subjected to extreme loads.

Chapter 5

5 Performance of Novel Piles Subject to Uplift Loading

5.1 Introduction

Piles supporting sound walls sustain very low axial compression loads due to the low weight of the supported wall. However, in certain regions, these piles may experience significant uplift forces due to adfreeze bond stresses caused by the soil's seasonal freeze and thaw. Due to the low axial compression forces, the uplift forces may well exceed the net uplift capacity of the piles resulting in frost jacking. Therefore, piles supporting sound walls in these regions must be designed to sustain adfreeze forces.

In order to evaluate the performance of the proposed novel pile configurations, a total of 16 instrumented piles were subjected to full scale axial tension load tests. The pile load test data, including strain readings from strain gauges, will provide information to evaluate the load transfer mechanism along the pile and its ultimate uplift capacity. Some of the novel piles were modified with nodes (small anchors) to explore the potential increase in their uplift capacity when installed in cohesive soil.

5.2 Testing Setup and Procedure

The piles were tested under uplift loading employing the test setup according to ASTM D3689 (2013) method 3 as shown in Figures 5-1 and 5-2. The load was applied using a model RRH 1006 Enerpac hydraulic jack reacting against a reaction beam, which was supported on cribbing placed on either end of the test pile. The hydraulic jack was connected to an Enerpac ZE3 class hydraulic electric pump. The reaction beam was composed of a back-to-back channel section welded together with a series of plates (stiffeners) to form a singular relatively rigid beam. A 76 mm solid bar threaded on both ends was passed through the reaction beam and hydraulic jack and was threaded with a hex nut at the top. The bar was connected to a model 1244 CLX-270K-B Interface high capacity load cell on the other end, which was connected to the top of the pile by means of a connection designed to bolt onto the pile web. The uplift displacement of each pile

was measured employing four HLP 190 linear potentiometers and secured to a reference frame that was independent of the pile and loading system. The potentiometers had a 100 mm stroke and measure displacement to an accuracy of 0.1 mm. All instrumentation was connected to a 7000 series Sciemetric data acquisition system to record all instruments simultaneously. The data acquisition system collected readings every 5 sec for all tests.
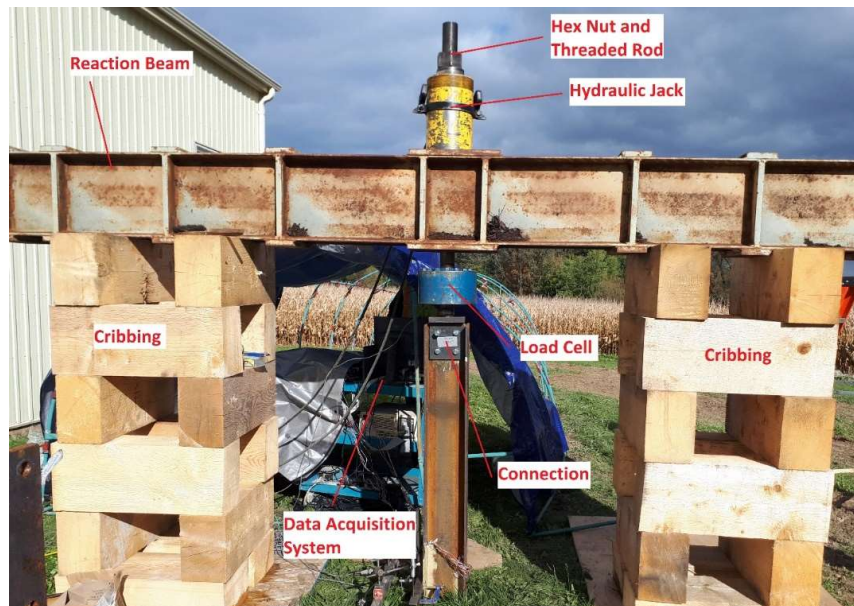
Figure 5-1: Uplift load test setup.
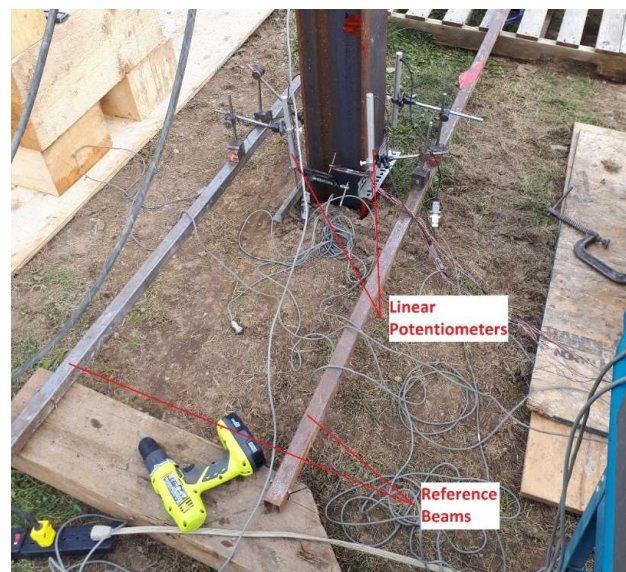
Figure 5-2: Linear potentiometer and reference beam setup for uplift tests.

A quick maintained load test procedure was employed according to ASTM D3689 (2013). The load was applied in increasing increments of 5% of the anticipated failure load which was estimated by calculating the pile's uplift capacity with the alpha method. Each load increment was maintained for four minutes. The load was advanced until excessive displacement occurred, or the load could not be maintained.

5.3   Uplift Load Test Results

The results of the uplift load tests are discussed in this section. All piles were tested in uplift before lateral load testing except for the drilled shafts, which were tested eight days after lateral testing. The load displacement curves are grouped into similar types of piles: plain piles, single plate piles, single plate piles with nodes, double plate piles, and drilled shafts. The failure criterion used to establish the uplift capacity from the load-displacement curves was the load corresponding to 10 mm of displacement at the pile head. The plain piles were tested 8 days after installation, which was deemed as a sufficient waiting period for porewater pressure dissipation due to the relatively high silt and sand content. The load-displacement curves for plain pile uplift tests are presented in Figure 5-3. All four plain piles exhibited similar behaviour except for PP-01, which had a lower stiffness (initial slope of the curve) and uplift capacity. This may be attributed to the variability in the soil strength and the difference in installation quality that was observed during installation. The average uplift resistance of the plain piles was 96.5 kN. The test for PP-04 was terminated at approximately 4 mm because the cribbing had become unbalanced and it was deemed unsafe to continue the test.

The single plate piles were tested 10 days after installation. The load-displacement curves for SP-01, 02, and 04 are shown in Figure 5-4. The results for SP-03 are not available due to a malfunction in the load cell during testing. The actual load was not recorded by the data acquisition system, and the pile was displaced over an inch before recognizing there was an issue. Additionally, the malfunctioning load cell interfered with the other instruments causing them to produce nonsensical readings and therefore the load could not be back calculated from the strain gauge data. The pile could not be re-tested within the available time of the testing period. The average uplift resistance of the single plate

piles was 128 kN, which is about 32% higher than the plain piles. This increase in resistance can be attributed to the increased pile surface area in contact with the soil.
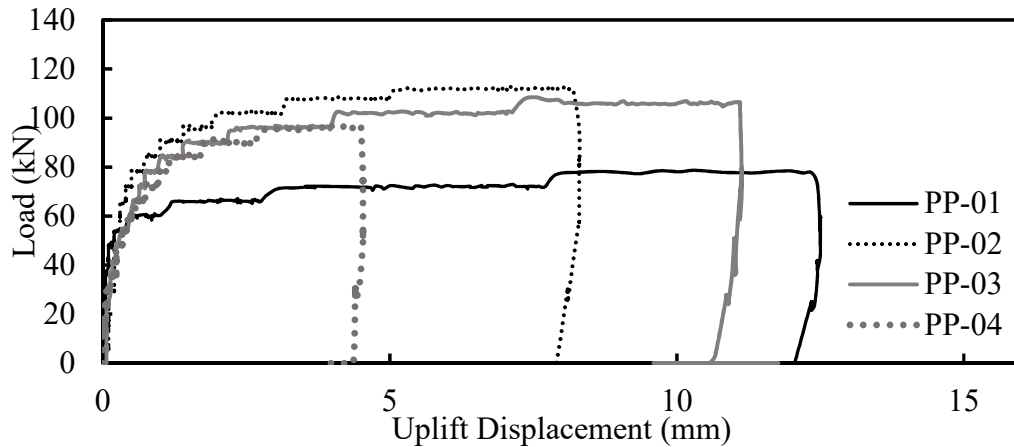
Figure 5-3: Uplift load-displacement curve for plain piles (PP-01,02,03,04).
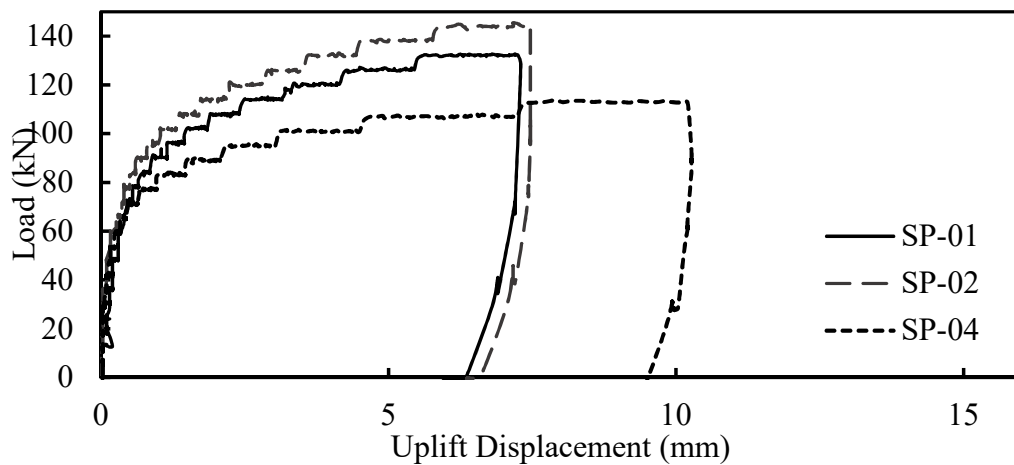
Figure 5-4: Uplift load-displacement curve for single plate piles (SP-01,02,04).

The single plate piles modified with nodes were tested two weeks after installation. The load-displacement curve for these piles are shown in Figure 5-5. The average uplift capacity for the node piles was 76.5 kN, which was significantly lower than both the plain piles and single plate piles without nodes. The nodes did not anchor the pile into the soil, rather they produced significant disturbance in the clay adjacent to the pile, which reduced the strength of soil. The effect of the nodes will be explored further in subsection 5.5 of this chapter. The quality of installation also had some effect on the pile

performance, as only pile SN-03 had an ideal installation while other piles had some notable issues as explained in Chapter three.

The double plate piles DP-01 and DP-02 were tested and the load displacement curves are shown in Figure 5-6. The average uplift capacity was 78 kN, which was significantly lower than the single plate piles. This reduction in uplift capacity may be attributed to the severe disturbance of the soil surrounding the pile caused by the problematic installation of these piles, which included re-lifting and re-driving the piles.
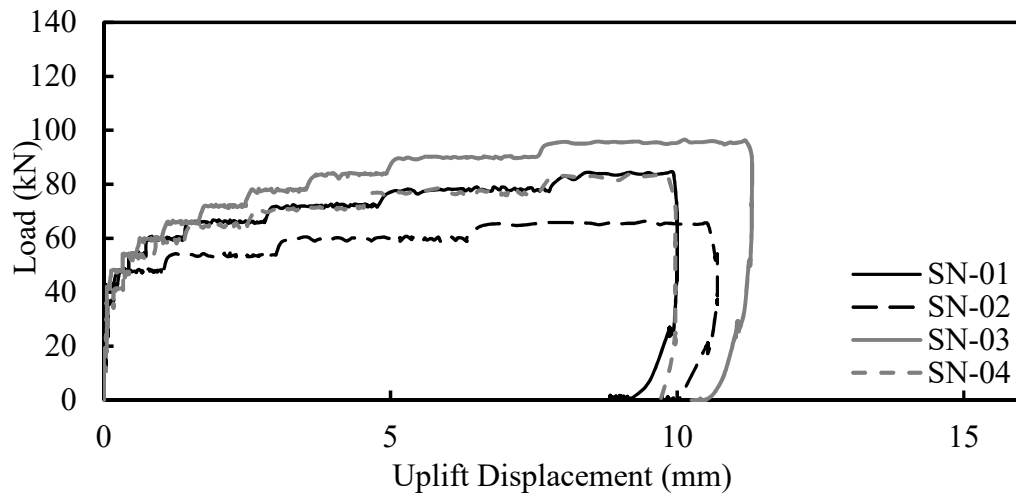
Figure 5-5: Uplift load-displacement curve for single plate piles with nodes (SN-01,02,03,04).
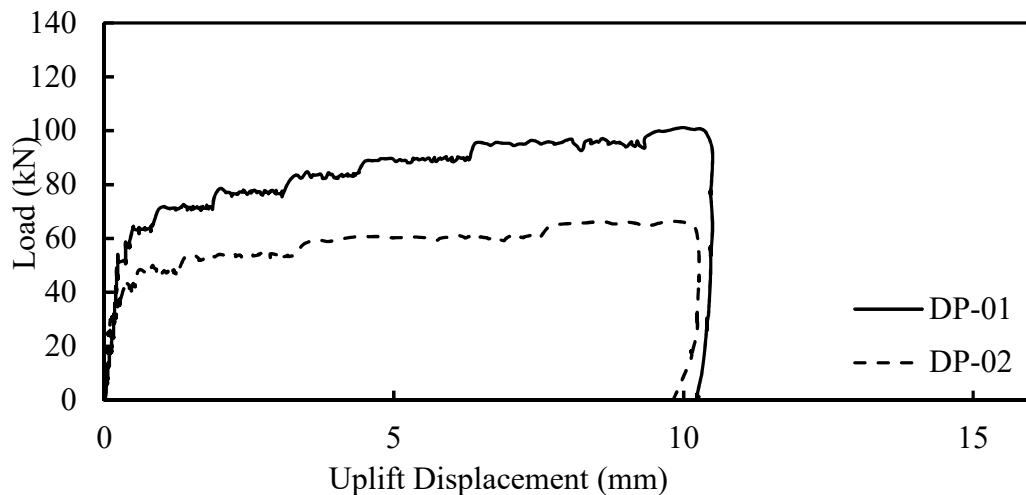
Figure 5-6: Uplift load-displacement curve for double plate piles (DP-01,02).

The drilled shafts were subjected to uplift loading following the completion of all lateral load tests, and their load-displacement curves are shown in Figure 5-7. The load tests were terminated at approximately 3 mm of displacement due to the high uplift capacity of the pile, which exceeded the safe limit of certain components of the load resisting frame. The remainder of the curve up to 10 mm was extrapolated assuming the rate of change of the slope is consistent with the original curve. The average estimated uplift capacity of the drilled shafts was 330 kN. The drilled shafts were expected to have higher uplift capacity due to the additional weight of their concrete shaft and the significantly larger surface area in contact with the supporting soil.
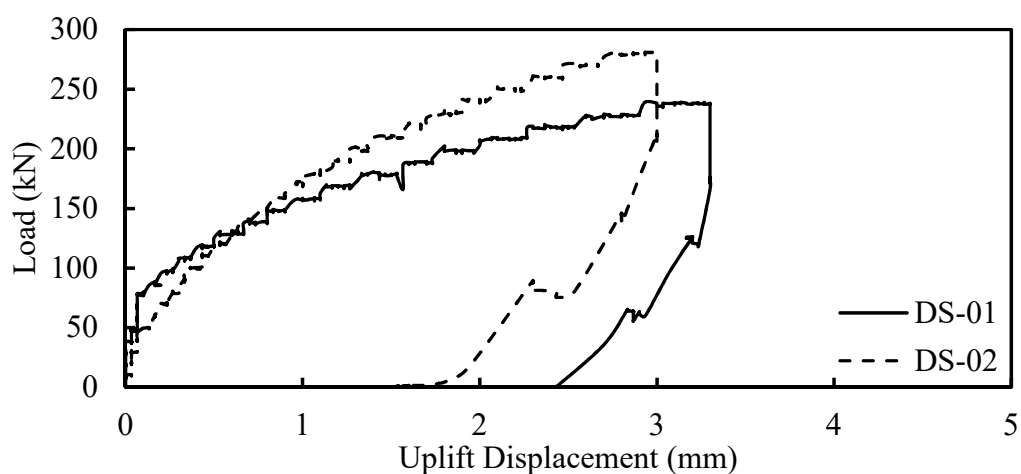
Figure 5-7: Uplift load-displacement curve for drilled shafts (DS-01,02).

The ultimate capacity of all tested piles is compiled in Table 5-1. For each pile, the ultimate capacity is accompanied with the installation quality rating (from 1 – 3) as discussed in Table 3-6 in chapter 3. Three indicates the installation went smoothly with little to no issues during driving, two indicates there were some minor issues during installation which may affect the performance of the pile, one indicates an overall poor installation which will significantly affect the performance of the pile. Table 5-1 shows that the installation quality of the pile has a direct effect on the ultimate uplift capacity of the piles. Piles with an installation quality rating of three generally have the highest uplift capacities and the opposite is true for most piles with a rating of one. The main exception is the drilled shafts; however, the installation quality rating was one for DS-02 due to the

misplacement in the position of steel reinforcement, which would affect lateral capacity and not uplift capacity.

Table 5-1: Summary of pile load test results accompanied with installation quality.

Pile I.D.	Uplift Capacity (kN)	Installation Quality (1-3)
PP-01	72	3
PP-02	112	3
PP-03	102	3
PP-04	100	3
SP-01	132	3
SP-02	144	3
SP-04	108	3
SN-01	78	1
SN-02	60	1
SN-03	90	3
SN-04	78	2
DP-01	96	2
DP-02	60	1
DS-01	300	3
DS-02	360	1

5.4 Calculating Uplift Resistance

The ultimate uplift capacity of the piles was estimated using the alpha method considering only the side resistance of the pile which is calculated using Equation 5-1:

$$Q_u = Q_s = \sum f_s P_p L_p = \sum \alpha S_u P_p L_p \qquad (5\text{-}1)$$

where f_s is the unit shaft resistance of the soil layer, α is the adhesion factor, P_p is the perimeter of the pile, and L_p is the length of the pile in the soil layer. The adhesion factor can be estimated from Equation 5-2 (Canadian Geotechnical Society, 2006):

$$\alpha = 0.21 + \frac{0.26 p_a}{S_u} \leq 1 \qquad (5\text{-}2)$$

This was done for both the minimum and maximum undrained shear strength values measured in the field and laboratory. The alpha method was deemed as appropriate for determining the pile capacity given the nature of soil, i.e., cohesive soil, and the rate of loading (undrained conditions). The effective perimeter (the perimeter of the pile in contact with soil) of the pile sections was taken as the outside perimeter of the H section (square) which calculated an uplift capacity closer to the measured capacity than the values obtained using the actual perimeter of the pile. Table 5-2 presents the calculated uplift capacity of the single plate piles as well as the undrained shear strength and α values used in the calculation. The minimum undrained shear strength estimate correlated well with SP-01 (134.6 kN estimated vs. 132 measured) and the maximum correlated well with SP-02 (151.5 kN estimated vs. 144 kN measured).

Table 5-2: Single plate pile axial uplift resistance calculated using alpha method.

Layer (m)	Layer Thickness (m)	S_u (kPa) Min	S_u (kPa) Max	α Min	α Max	P_P (m)	Load Resistance (kN) Min	Load Resistance (kN) Max	f_s (kPa) Min	f_s (kPa) Max
0 - 0.9	0.9	90	115	0.50	0.44	1.26	50.9	56.9	44.9	50.15
0.9 - 0.95	0.05	60	70	0.64	0.58	1.26	2.4	2.6	38.6	40.7
0.95 - 2	1.05	60	70	0.64	0.58	0.732	29.7	31.3	38.6	40.7
2 - 3.5	1.5	100	140	0.47	0.40	0.732	51.6	60.8	47	55.4
						Total:	134.6	151.5		

The load transfer mechanism for a single plate pile subject to uplift loading is shown in Figure 5-8. SP-01 was selected for the comparison because it had the most functioning strain gauges at the time of testing and therefore could give the most accurate data for the load transfer mechanism. The strain gauges for the other single plate piles provided either very limited or noisy data and therefore were not considered. The force transferred from the pile to the supporting soil was calculated by taking the difference between the axial force in the pile at the top and bottom of each soil layer. For the first two layers (the plated section of the pile, of which 0.9 m is in the first soil layer and 0.05 m is in the second layer), the load transfer was approximated as linear following the center of data points from the strain gauges. A best estimate line matching the data points was selected for the remainder of the pile. The unit shaft resistance values were then calculated for each layer and are summarized in Table 5-3. These values were then compared to the

load distributed from the pile to the soil layer as estimated from the alpha method as shown in Table 5-4.
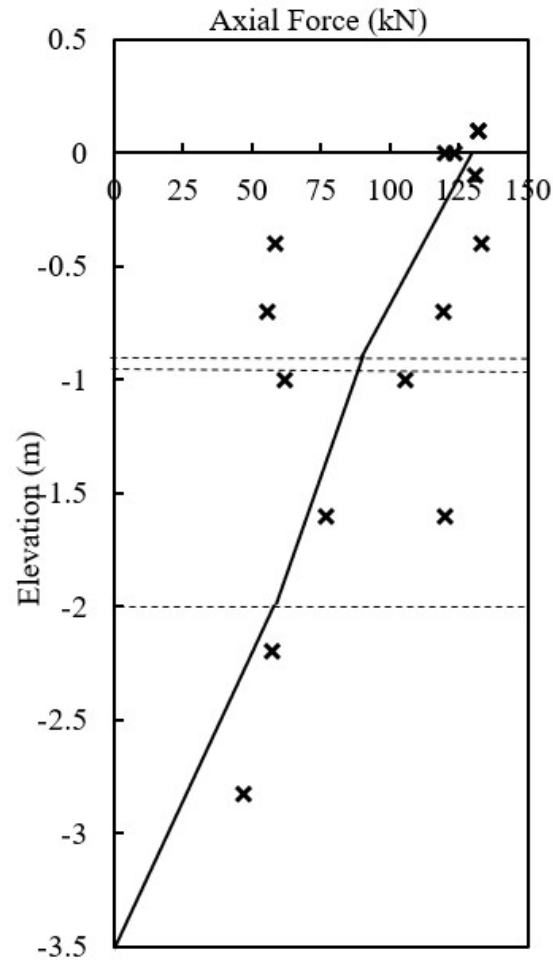
Figure 5-8: Approximation of load transfer mechanism for SP-01.

The calculated unit shaft resistance along the plated section is higher than the measured resistance, while the calculated shaft resistance on the lower part of the pile is less than the observed results. The good match between the calculated and measured ultimate capacity and load transfer mechanism of the pile indicate that the soil was not overly disturbed during installation, and that alpha method is suitable for estimating the ultimate uplift capacity of a single plate pile in clay.

Table 5-3: Back-calculated unit shaft resistance from single plate pile uplift load test.

Layer (m)	Axial Load (kN)		P_p (m)	Layer Thickness (m)	f_s (kPa)
	Start	End			
0 - 0.9	132	90	1.26	0.9	37.0
0.9 - 0.95	90	87.5	1.26	0.05	39.7
0.95 - 2	87.5	60	0.732	1.05	35.8
2 - 3.5	60	0	0.732	1.5	54.6

Table 5-4: Comparison of measured unit shaft resistance along single plate pile to calculated values.

Layer (m)	Unit Shaft Resistance (kPa)		%Diff of Measured
	Measured	Alpha	
0 - 0.9	37.0	44.9	21
0.9 - 0.95	39.7	38.6	-3
0.95 - 2	35.8	38.6	8
2 - 3.5	54.6	47	-14

5.5   Assessment of Node Modification

The load test results clearly demonstrated that installing nodes along the pile flange had a negative effect on the uplift capacity of the piles installed in clay. The load distribution along the shaft for the single plate pile with and without nodes, which is shown in Figure 5-9, were compared to identify whether the cause of the lower uplift capacity is due to the nodes or the poor installation since the node piles faced issues during driving. It is observed that the slope of the curve (unit shaft resistance) is almost identical up to two meters. However, for the last 1.5 m of the node pile, the slope is much more vertical than the pile without nodes. This indicates that the axial load transferred to the soil in this region is lower.

The unit shaft resistance of both piles is calculated and compared in Table 5-5 which confirms that the node attachments are directly responsible for lowering the pile's uplift

capacity. The transferred load and corresponding side resistance are very similar between both piles up to approximately two meters, at which point, the transferred load and corresponding shaft resistance is less than half for the rest of the pile.
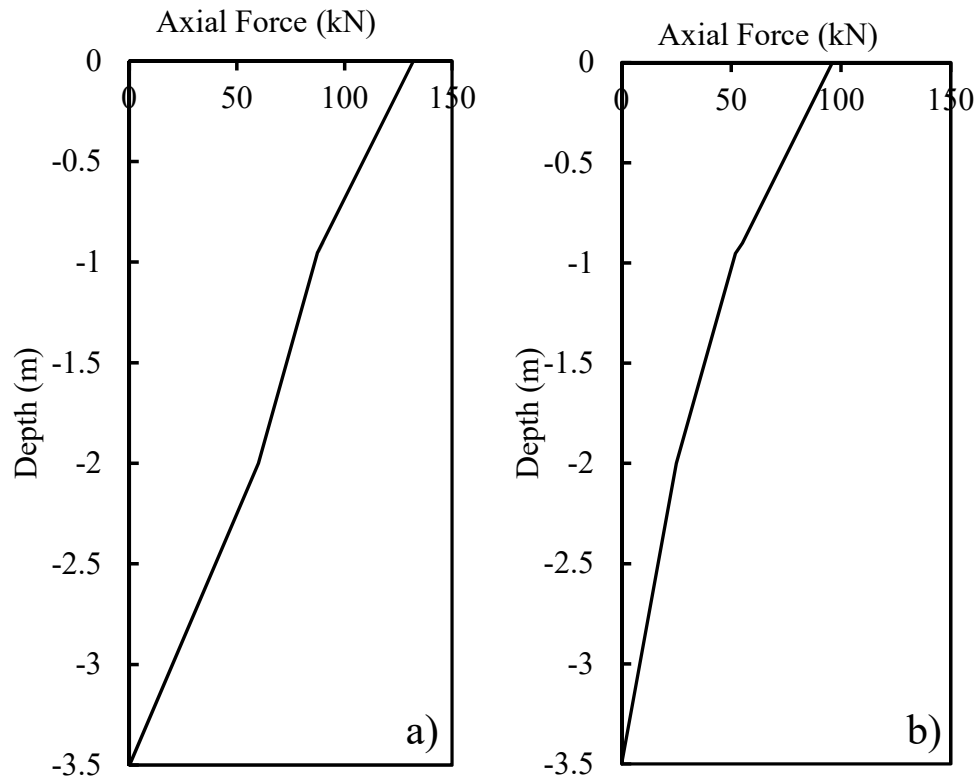
Figure 5-9: Axial load distribution of single plate pile a) without and b) with nodes.

This reduction of shaft resistance is attributed to the significant disturbance of the clay adjacent to the pile caused by the nodes during the driving process. Disturbed clays however may regain some strength over time and therefore the node modification may be practical after sufficient time has passed to allow the disturbed clay to regain its strength (Lommler, 2012). This concept may prove successful for piles installed in sand. When sand is disturbed, it does not remold like clay and therefore will not suffer strength loss like clay. However, the node modification must be tested for piles installed in sand to verify the effect of nodes on uplift capacity.

Table 5-5: Calculated transferred load and unit shaft resistance for a single plate pile with and without nodes.

Layer (m)	Pile Without Nodes		Pile With Nodes	
	Transferred Load (kN)	Unit Shaft Resistance (kPa)	Transferred Load (kN)	Unit Shaft Resistance (kPa)
0 - 0.9	42	37	41	36.2
0.9 - 0.95	2.5	39.7	3	47.6
0.95 - 2	27.5	35.8	27	35.1
2 - 3.5	60	54.6	25	22.8

5.6   Comparison of Pile Uplift Capacity to Adfreeze Loads

The adfreeze loads imposed on piles vary greatly and are dependent on pile type, pile material, soil type, water content, and frost depth. As an example, the performance of piles subject to adfreeze was evaluated for a similar soil type with adfreeze loads measured within the region of the test site. A case study in Southwestern Ontario involved measuring the ultimate adfreeze bond stress of steel piles installed in fine-grained silty soils (USCS classification CL) which is the same classification as the soil at the testing site. The measured adfreeze stress ranged from 30 – 80 kPa with a frost penetration depth of 1.2 m (Levasseur et al., 2015). The comparison of adfreeze force to the pile's uplift resistance will be made at the maximum value of 80 kPa. The adfreeze force for concrete was selected as 65 kPa (Canadian Geotechnical Society, 2006). The net axial uplift load for each pile type is summarized in Table 5-6. The adfreeze force includes the stress acting along the perimeter of the pile up to a depth of 1.2 m, taking into account both the plated and non-plated section of the pile. The dead load includes the weight of the sound wall panel and the post above the ground surface (minus 1.35 m which was already considered during the test) assuming a maximum wall height of 5.0 m and a pile spacing of 3.053 m (10 ft). The ice accretion load was neglected since its presence is not reliable and therefore may not contribute force to counteract adfreeze. Note that all the loads presented are unfactored. The net uplift loads from Table 5-6 are compared to the capacity of each tested pile and the results are presented in Table 5-7.

Table 5-6: Net axial uplift load for each pile type.

Pile Type	Adfreeze Force (kN)	Dead Load (kN)	Net Uplift (kN)
Drilled Shaft	174.3	4.6	169.7
Plain Post	70.3	4.6	65.7
Single Plate Pile	114.8	4.6	110.2
Double Plate Pile	137.7	4.6	133.1

With the current dimensions, the plate piles lack the required uplift capacity to resist adfreeze forces. A major contributing factor for this is the enlarged pile surface area from the plate attachment existing entirely in the frost zone. This increases the pile-soil contact area resulting in a higher uplift force. The results of the uplift tests suggest that the novel piles with their current dimensions are better suited for soils that are not frost susceptible or in regions that experience minimal to no freeze-thaw cycles. For areas with high adfreeze forces, the pile embedded depth should be increased to provide the required uplift capacity. For this specific soil profile, the total length of the pile would have to be approximately 8 m to reach a safety factor of 2.5 for uplift resistance considering the minimum value of S_u for each soil layer.

Table 5-7: Comparison of uplift resistance to uplift loading.

Pile I.D.	Uplift Capacity (kN)	Uplift Load (kN)	F.S.	Average F.S. Per Pile Type
PP-01	72	65.7	1.1	
PP-02	112	65.7	1.7	1.5
PP-03	102	65.7	1.6	
PP-04	100	65.7	1.5	
SP-01	132	110.2	1.2	
SP-02	144	110.2	1.3	1.2
SP-04	108	110.2	1.0	
SN-01	78	110.2	0.7	
SN-02	60	110.2	0.5	0.7
SN-03	90	110.2	0.8	
SN-04	78	110.2	0.7	
DP-01	96	133.1	0.7	0.6
DP-02	60	133.1	0.5	
DS-01	300	169.7	1.8	1.9
DS-02	360	169.7	2.1	

5.7   Summary

A total of 16 piles were subjected to axial tension load tests to evaluate their performance under uplift loading. Adfreeze bond stresses may produce uplift forces that are significant enough to jack the piles out of the ground. The addition of nodes and their effect on uplift capacity was also evaluated which included a comparison of the load distribution between piles with and without nodes. The uplift resistance of the piles was compared by type and also evaluated based on adfreeze forces back-calculated in the same region for steel piles in fine-grained silty soils. The key findings and design recommendations are as follows:

- The plate piles with the tested dimensions did not offer the required capacity to resist uplift forces caused by adfreeze bond stresses. One major reason for this is that the addition of the plate, which exists entirely in the frost zone, increases the pile's surface area in contact with adfreeze bond and thus significantly increases uplift forces. The results of the uplift tests suggest that the novel piles with their current dimensions are better suited for soils that are not frost susceptible or in regions that experience minimal to no freeze-thaw cycles. For this soil profile, the pile length can be increased to 8 m to provide a safety factor of 2.5 against adfreeze loading, assuming the minimum measured S_u for each soil layer.

- The alpha method is suitable for estimating the uplift capacity of the novel piles. The estimated tension capacity of the piles assuming the minimum and maximum undrained shear strengths measured in the field and laboratory was 134.6 kN and 151.5 kN, respectively. This matches the ultimate capacities of SP-01 and SP-02 of 132 kN and 144 kN. Furthermore, the distribution of shaft resistance from the calculations is consistent with the load transfer mechanism measured by the strain gauges.

- Adding nodes to the novel piles resulted in a reduced uplift capacity. A comparison of the load distribution along the pile shaft for a single plate pile with and without nodes demonstrated that the nodes significantly disturbed the cohesive soils during installation, which lowered the uplift capacity of the pile.

The section of the pile without nodes showed very similar load transfer values for both piles, whereas the portion of the pile with nodes reduced the load transfer to less than half of the pile without nodes. It is therefore not recommended to use nodes in cohesive soils. While it is speculated that the nodes would be better suited for piles in cohesionless soils, this needs to be confirmed with field testing.

Chapter 6

6   Summary and Conclusions

6.1   Summary

The main objective of this research program is to investigate the suitability of simple modifications to steel H-piles for sound wall applications. Pile foundations supporting sound walls are typically subjected to lateral forces from wind and uplift forces from adfreeze bond stresses in regions where seasonal freeze and thaw occur. The first modification studied is the addition of one or two steel plates welded to the pile flange for a portion of the pile immediately below the ground surface, which was expected to increase the lateral capacity of the pile. The second modification is the addition of small anchors (or nodes) which are welded to the pile flange near the bottom of the pile, with the goal of increasing the pile's uplift capacity.

A full-scale pile load testing program was designed and executed on sixteen piles, which included four unmodified (plain) H-piles, four single plate piles without nodes, four single plate piles with nodes, two double plate piles, and two drilled shafts. The plain piles were tested to characterize the effect of the plate on H-piles. The drilled shafts were sized according to currently used design dimensions for sound wall applications. All sixteen piles were subjected to axial tensions load tests and loaded until failure. Eight piles (SP-03, SP-04, SN-03, SN-04, PP-01, PP-02, DS-01, and DS-02) were subjected to monotonic lateral load testing and the remaining eight piles (SP-01, SP-02, SN-01, SN-02, PP-03, PP-04, DP-01, and DP-02) were subjected to cyclic lateral load testing. Most piles were instrumented with strain gauges to measure the load transfer mechanism during testing.

The results of the field tests were used to develop a numerical model for single plate piles under monotonic lateral loading using LPILE. The model was calibrated with single plate pile test data and was validated against the plain pile test results and the preliminary tests performed by Atlantic Industries Limited (AIL). The calibrated model was then used to perform a parametric study considering the effect of varying plate dimensions on the

pile's capacity in a range of practical soil conditions. A second numerical model was developed for single plate piles subjected to cyclic lateral loading using the computer program GSNAP. The model was used to estimate the performance of a single plate pile when subjected to larger loads and a higher number of cycles.

6.2 Conclusions

6.2.1 Pile Installation

The main observations made during the installation of the piles are as follows:

- Vibratory driving is suitable for cohesive soil profiles but may experience driving problems if cobbles or boulders are present. Pre-drilling the soil with a diameter less than the pile can address this issue but will sacrifice the overall efficiency of the installation.

- Installing novel piles with vibratory driving proved to be 3.0 – 4.4 times faster than installing drilled shafts. This can lead to significant time and cost savings, especially for large projects requiring many piles.

- The installation of the drilled shafts produced large amounts of soil waste which would ordinarily need to be collected and removed. Using steel piles foregoes this requirement thereby saving additional costs.

- Using vibratory driving is preferable if restriction on noise levels is a requirement. However, observers in an adjacent building approximately 75 m away from the installation mentioned the installation could be readily heard.

6.2.2 Monotonic and Cyclic Lateral Load Testing

The main findings from the lateral load testing program and numerical modelling are as follow:

- The addition of the plate increased the lateral capacity of the piles by approximately 22%. The drilled shafts lateral capacity was approximately twice the magnitude of the single plate piles.

- The single plate piles had a safety factor of 2.2 against the design lateral wind force, which took into account the maximum design pile spacing and wall height and a wind pressure with a 25-year return period.

- With the current dimensions, the top 12B or 4.75W of the pile primarily contributes to the lateral load resistance of the pile, where B is equals the width of the pile flange and W equals the width of the plate. The pile experiences negligible movement below this point.

- The installation quality of the pile had a direct effect on its performance when subjected to monotonic and cyclic lateral loads. Piles with an unideal installation typically suffered from reduced lateral capacities and a higher degree of shakedown.

- LPILE proved to be a suitable tool for estimating the performance of single plate piles subject to lateral loading. It is recommended to use the relationship from Salgado (2008) for estimating the k soil modulus parameter and the relationships from Liang (2002) for estimating ε_{50}.

- The plated section of the novel pile can be modelled as a purely elastic rectangular section in LPILE with user inputted area, moment of inertia, and width equivalent to the pile.

- The plate width generally has a greater influence on a pile's lateral capacity compared to plate length, especially in cohesive soils. For cohesionless soils, the different in increase/decrease between plate width and length equalizes as the soil density increases.

- Modified H-piles may be an effective solutions where lateral capacity governs the design. A smaller pile section may be selected and fitted with a plate to satisfy lateral force requirements.

- The lateral stiffness of all tested piles stabilized within 100 cycles of low-magnitude lateral load. The ratio of k_L/k_{Lo} was approximately 9% lower for single

plate piles compared to unmodified H-piles at the 100th cycle indicating the novel piles experience a minor increase in degradation over unmodified piles.

- The benefit of adding a second plate to a pile for improving cyclic performance was not conclusively observed due to installation problems of the double plate piles which directly affected the results.

- The limited parametric study using GSNAP indicated that the maximum deflection of a single plate pile will not exceed 10 mm regardless of how many cycles of the design load is applied to the pile. However, the pile was estimated to have excessive deflection after only a few cycles at two times the design load indicating the foundation maybe exceed response tolerances if subjected to repeated extreme loads.

6.2.3   Monotonic Axial Tension Load Testing

The main findings from the axial tension load testing program are as follows:

- The novel piles with their current dimensions are better suited for soils that are not frost susceptible or in regions that experience minimal to no freeze-thaw cycles. This is partly due to the enlarged surface area of the pile within the frost-susceptible zone leading to an increase in adfreeze force. For this soil profile, the pile length can be increased to approximately 8.0 m to provide a safety factor of 2.5 against adfreeze loading, assuming the minimum measured S_u for each soil layer.

- The alpha method is suitable for estimating the uplift capacity of the novel piles. The distribution of skin friction from the calculations is consistent with the load transfer mechanism measured by the strain gauges.

- Adding nodes to the pile decreases the ultimate axial tension capacity for piles installed in cohesive soil. An analysis of the load transfer mechanism reveals that the section of the pile with nodes had a reduced skin friction. This reduction in

capacity is linked to the significant disturbance of the soil caused by the nodes during installation.

6.3   Recommendations for Future Research Work

The field testing provided a valuable assessment of the novel pile concept. However, suggestions for additional testing have been provided to more fully evaluate the performance of the piles for sound wall applications:

• Test a variety of plate and pile dimensions to validate the results of the parametric study, which was based on a singular plate and pile dimension.

• Test the piles in cohesionless material to better characterize their performance in other soil types. The node concept is expected to perform better in sand than in clay.

• Re-test the double plate pile concept under cyclic lateral load conditions ensuring an ideal installation is achieved to provide an accurate assessment of its performance.

References

Abd Elaziz, A. Y. (2012). *Performance of hollow bar micropiles under axial and lateral loads in cohesive soils*. The University of Western Ontario, London, ON.

Abdelghany, Y. (2008). *Monotonic and cyclic behavior of helical screw piles under axial and lateral loading*. The University of Western Ontario, London, ON.

Allotey, N., & El Naggar, M. H. (2008). Generalized dynamic Winkler model for nonlinear soil–structure interaction analysis. *Canadian Geotechnical Journal*, *45*(4), 560–573. https://doi.org/10.1139/T07-106

ASTM D3689. (2013). Standard Test Methods for Deep Foundations Under Static Axial Tensile Load. In *Annual Book of ASTM Standards*. West Conshohocken, PA.

ASTM D3966. (2013). Standard Test Methods for Deep Foundations Under Lateral Load. In *Annual Book of ASTM Standards*. West Conshohocken, PA.

Basack, S. (2010). Response of vertical pile group subjected to horizontal cyclic load in soft clay. *Latin American Journal of Solids and Structures*, *7*(2), 91–103. https://doi.org/10.1590/S1679-78252010000200001

Basack, S., & Dey, S. (2011). Pile Subjected to Lateral Cyclic Loading in sand. *Proceedings of Indian Geotechnical Conference*, (Paper No. N343). Kochi.

Basack, S., & Nimbalkar, S. (2018). Measured and Predicted Response of Pile Groups in Soft Clay Subjected to Cyclic Lateral Loading. *International Journal of Geomechanics*, *18*(7), 1–20. https://doi.org/10.1061/(asce)gm.1943-5622.0001188

Bicocchi, N. (2011). *Structural and Geotechnical Interpretation of Strain Gauge Data from Laterally Loaded Reinforced Concrete Piles*. University of Southampton.

Borel, S., Bustamante, M., & Rocher-Lacoste, F. (2006). The comparative bearing capacity of vibratory and impact driven piles. *Proceedings of the Internat. Conf. on*

Vibratory Pile Driving and Deep Soil Compaction TRANSVIB 2006, 277–284. Paris.

Briaud, J.-L., Coyle, H. M., & Tucker, L. M. (1988). *Axial response of three vibratory and three impact driven H-piles in sand*. Transportation Research Record (1277).

Budhu, M. (2011). *Soil Mechanics and Foundations*. Hoboken: John Wiley & Sons, Inc.

Canadian Geotechnical Society. (2006). *Canadian foundation engineering manual*. Richmond, B.C.

Crory, F. E., & Reed, R. E. (1965). *Frost thrust measurements on piles*. CRREL, technical report 145.

CSA Group. (2014). *CAN/CSA-S6-06 Canadian highway bridge design code* (11th ed.). Toronto: CSA Group.

Das, B. (1999). *Shallow foundations: bearing capacity and settlement* (Eleventh E). Boca Raton: CRC Press.

Drbe, O. F. H. (2013). *Investigation of hollow bar micropiles in cohesive soil*. The Univeristy of Western Ontario, London, ON.

Drbe, O. F. H., & El Naggar, H. (2015). *Axial monotonic and cyclic compression behaviour of hollow-bar micropiles*. *54*(2), 426–441. https://doi.org/10.1139/cgj-2014-0052

El Naggar, M. H., & Heidari, M. (2018). Geo-structural nonlinear analysis of piles for performance based design. *Proceedings of the 3rd World Congress on Civil, Structural, and Environmental Engineering*, (April), 1–16. https://doi.org/10.11159/icgre18.1

El Sharnouby, M. M. (2012). *Axial monotonic and cyclic performance of fibre-reinforced polymer (FRP) – steel fibre–reinforced helical pulldown micropiles (FRP-RHPM)*. The University of Western Ontario, London, ON.

Ensoft Inc. (2019). *LPILE v2019 user's manual: a program for the analysis of deep*

foundations under lateral loading.

Fellenius, B. H. (2001). From strain measurements to load in an instrumented pile. *Geotech. News*, *19*(1), 35–38.

Fellenius, B. H. (2015). *Basics of foundation design*. Vero Beach, FL: Pile Buck International, Inc.

FHWA. (1989). The pressuremeter test for highway applications. In *FHWA Publication No. FHWA-IP-89-008*. Department of Transportation, Federal Highway Administration, Washington D.C.

Fleming, K., Weltman, A., Randolph, M., & Elson, K. (2009). *Piling engineering* (Third). New York: Taylor & Francis Group.

Google. (n.d.). 22312 Wonderland Rd. N, Ilderton, ON. Retrieved April 21, 2018, from https://www.google.ca/maps/place/22312+Wonderland+Rd+N,+Ilderton,+ON+N0 M+2A0/@43.0747853,- 81.3367239,315m/data=!3m1!1e3!4m5!3m4!1s0x882eef5441b6fe99:0x661d30012b 3c8786!8m2!3d43.0750518!4d-81.3359139

Haiderali, A. E., Nakashima, M., & Madabhushi, S. P. G. (2015). Cyclic lateral loading of monopiles for offshore wind turbines. *Proceedings of the 3rd International Symposium on Frontiers in Offshore Geotechnics, ISFOG 2015*. Oslo, Norway.

Hardy, R. M. (1953). Prevention of frost heaving by injection of spent sulphite liquor. *3rd Internat. Conf. Soil Mech., v. 2*, 103–106. Zurich.

Heidari, M., El Naggar, H., Jahanandish, M., & Ghahramani, A. (2014). Generalized cyclic p-y curve modeling for analysis of laterally loaded piles. *Soil Dynamics and Earthquake Engineering*, *63*, 138–149. https://doi.org/10.1016/j.soildyn.2014.04.001

I.R. (2015). *Comparison of impact versus vibratory driven piles : with a focus on soil - structure interaction*. 14007-01-Rev2. Deep Foundation Institute.

Jeyapolan, J. K. (1983). *Axial capacity of vibro-driven piles*. Draft report submitted to the US Army Engineer Waterways Experiment Station, Vicksburg, MS.

Johnson, J.B. and Buska, J. S. (1988). *Measurement of frost heave forces on H-piles and pipe piles (CRREL-88-21)*. Alaska Department of Transportation and Public Facilities, Fairbanks.

Khan, M. K. (2005). *Tapered cast-in-place concrete piles*. The University of Western Ontario, London, ON.

Lammertz, P. (2008). *Ermittlung der tragfähigkeit vibrierter stahlrohrpfähle in nichtbinigem boden*. Duisburg and Essen.

Levasseur, P., Maher M L J, & Dittrich, J. P. (2015). A case study of frost action on lightly loaded piles at Ontario solar farms. *GEOQuébec*.

Liang, R. Y. (2002). *Drilled shaft foundations for noise barrier walls and slope stabilization*. No. FHWA/OH-2002/038. University of Akron. Dept. of Civil Engineering, 2002.

Livneh, B. (2006). *The axial performance of square shaft helical piles*. The University of Western Ontario, London, ON.

Lommler, J. C. (2012). *Geotechnical problem solving*. New York: John Wiley & Sons.

Long, J. H., & Vanneste, G. (1994). Effects of cyclic lateral loads on piles in sand. *Journal of Geotechnical Engineering*, *120*(1), 225–244. https://doi.org/10.1061/(asce)0733-9410(1994)120:1(225)

Lyazgin, A. L., Bayasan, R. M., Chisnik, S. A., Cheverev, V. G., & Pustovoit, G. P. (2003). Stabilization of pile foundations subjected to frost heave and in thawing permafrost. *Proceedings of the 8th International Conference on Permafrost, Zurich, Switzerland*, 21–25. Zurich.

Mazurkiewicz, B. K. (1975). Influence of vibration of piles on their bearing capacity.

Proc. 1st Baltic Conference on Soil Mech. and Found. Eng, *3*, 143–153. Gdansk, Poland.

Mosher, R. L. (1987). *Comparison of axial capacity of vibratory-driven piles to impact-driven piles*. Report ITL-87-7. U.S. Army Engineer Waterways Experiment Station, Vicksburg.

Nusairat, J., Liang, R. Y., Engel, R., Hanneman, D., Abu-Hejleh, N., & Yang, K. (2004). *Drilled shaft design for sound barrier walls , signs , and signals. rep no. CDOT-DTD-R-2004-8*. Arkansas.

Peck, R. B., Hanson, W. E., & Thornburn, T. H. (1974). *Foundation engineering* (2nd ed.). New York: John Wiley.

Péwé, T. L., & Paige, R. A. (1963). Frost heaving of piles with an example from Fairbanks, Alaska. *Geological Survey Bulletin 1111-I*, 333–369.

Pihlainen, J. A. (1951). *Building foundations on permafrost, Mackenzie Valley, N.W.T.* Ottawa, ON.

Poulos, H. G. (1982). Single pile response to cyclic lateral load. *Journal of Geotechnical and Geoenvironmental Engineering*, *108*(GT3), 355–375.

Poulos, H. G., & Davis, E. H. (1980). *Pile foundation analysis and design*. New York: John Wiley & Sons, Inc.

Reese, L., & Van Impe, W. (2011). *Single piles and pile groups under lateral loading* (Second). London, UK: Taylor & Francis Group.

Rocher-Lacoste, F., Borel, S., Gianeselli, L., & Po, S. (2004). Comparative behaviour and performance of impact and vibratory driven piles in stiff clay. *Proc. Cyclic Behaviour of Soils and Liquefaction, Balkema*, 533–540.

Salgado, R. (2008). *The engineering of foundations*. New York: McGraw-Hill.

Sivrikaya, O., & Toğrol, E. (2002). Relations between SPT-N and qu. *5th Intern.*

Congress on Advances Civil Engineering, 943–952. Istanbul, Turkey.

Sivrikaya, O., & Toğrol, E. (2006). Determination of undrained strength of fine-grained soils by means of SPT and its application in Turkey. *Engineering Geology*. https://doi.org/10.1016/j.enggeo.2006.05.002

Skempton, A. W. (1986). Standard penetration test procedures and the effects in sands of overburden pressure, relative density, particle size, ageing and overconsolidation. *Géotechnique*, *86*(1), 52–69.

Stroud, M, A. (1974). The standard penetration test in insensitive clays and soft rocks. *European Symposium on Penetration Testing*, *2*(2), 367–375. Stockholm, Sweden.

Terzaghi, K., & Peck, R. B. (1967). *Soil mechanics in engineering practise*. New York: John Wiley.

Tomlinson, M., & Woodward, J. (2008). *Pile design and construction practise* (5th ed.). New York: Taylor & Francis Group.
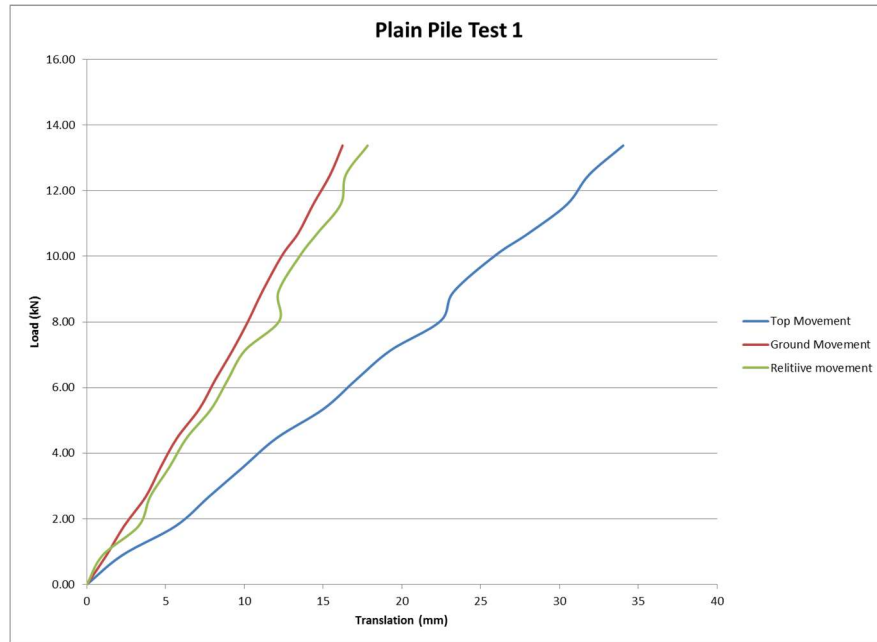
Appendix A

Figure A-1: Preliminary test load-displacement curve of Plain Pile 1.
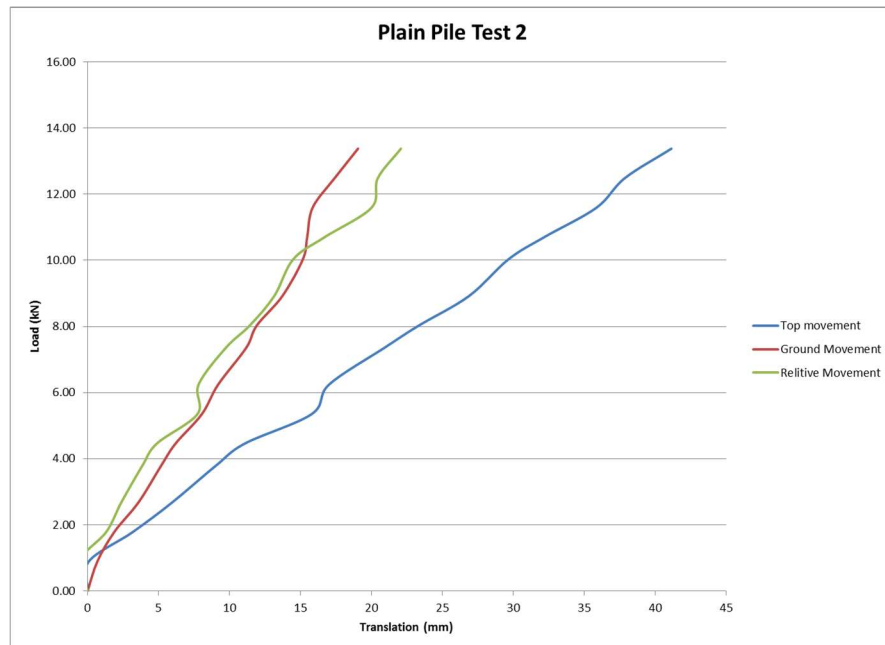

Figure A-2: Preliminary test load-displacement curve of Plain Pile 2.
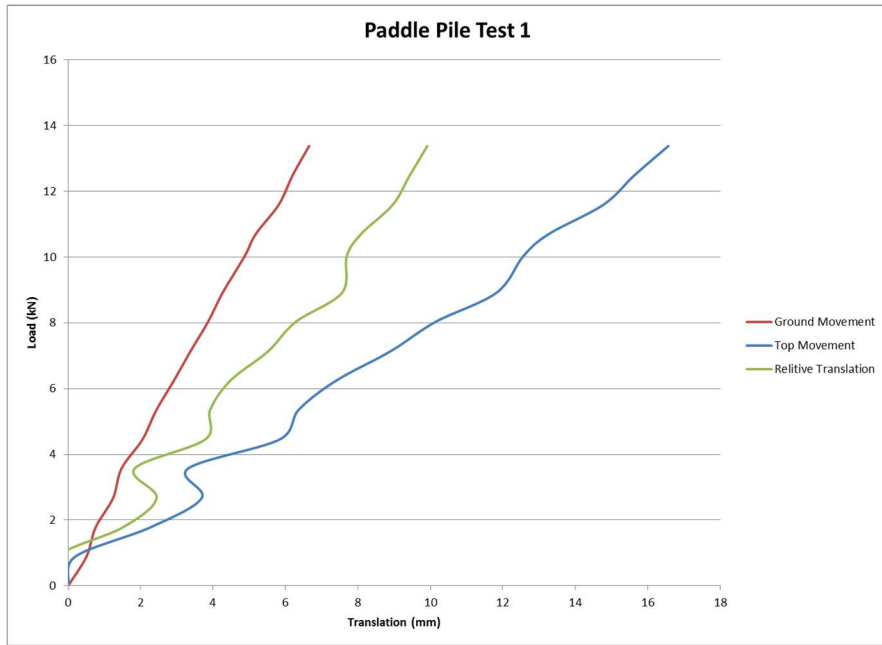
Figure A-3: Preliminary test load-displacement curve of Paddle Pile 1.
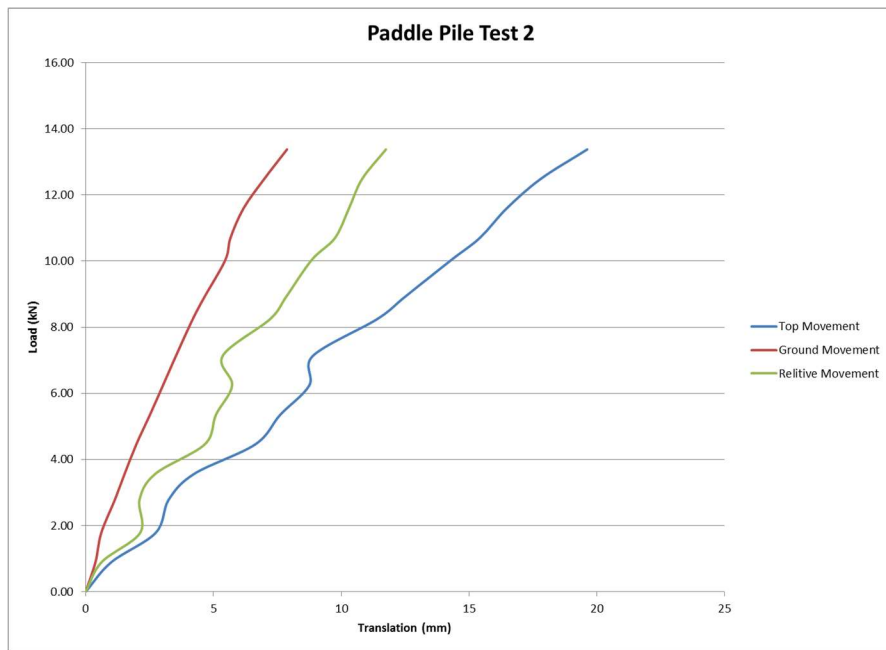
Figure A-4: Preliminary test load-displacement curve of Paddle Pile 2.

Appendix B

Project: Borholes Samples			B.H. No. : I		Sheet: 1/1
Owner: Western University			Start Date: 17/07/2012		End Date:17/07/2012
Location: Western Environmental Site			Casing Depth: 9.00 m		E: ---
Rig Type: CME 55 Mount Drill		Western	G.W. Depth (m): 6.41 m		N: ---
Drilling Method: Rotary Drilling		UNIVERSITY · CANADA	Weather : Sunny		B.H. Elev: ---

Depth. (m)	Thick. (m)	Description	Legend	SPT Counts			N Value	w %	LL %	PL %
				15cm	15cm	15cm	0 10 20 30 40 50			
		200 mm to 300 mm Top Soil								
		Firm to Stiff, brown becoming gray at a depth of 3.8 m, lean CLAY with coarse sand and some gravel.		2	6	12		---	---	
1.00				5	5	6		23.3	30.6	16.5
2.00	4.00			5	6	11		12.28	28.32	16.12
3.00				5	7	11		13.07	25.72	15.68
				5	7	11		13.86	24.92	15.87
4.00										
	1.00	Firm to Stiff, light gray becoming dark gray at a depth of 6.5m, lean CLAY with fine sand and some gravel.		5	5	7		13.00	17.53	12.76
5.00				5	6	7		12.99	24.05	14.27
	1.00	Soft, light gray becoming dark gray at a depth of 6.5m, lean CLAY with fine sand and some gravel.								
6.00				1	2	2		23.78	37.46	21.09
	0.50	Firm, light gray becoming dark gray at a depth of 6.5m, lean CLAY with fine sand and some gravel.		2	3	7		14.79	29.65	15.91
7.00		Very Stiff, dark gray, lean clay with seams fine sand.								
	1.50			2	8	12		16.55	23.65	12.37
8.00				13	16	22		11.92	18.62	13.10
	0.75	Very Stiff to hard, dark gray, lean clay with seams fine sand.								
				11	19	26		13.06	21.30	12.43
9.00	0.25	Hard, gray CLAY								
		END OF BORING								

Figure B-1: Borehole log 1 from Drbe and El Naggar (2015).

Project: Borholes Samples	B.H. No. : II	Sheet: 1/1
Owner: Western University	Start Date: 17/07/2012	End Date: 17/07/2012
Location: Western Environmental Site	Casing Depth: 9.00 m	E: ---
Rig Type: CME 55 Mount Drill	G.W. Depth (m): 6.41 m	N: ---
Drilling Method: Rotary Drilling	Weather : Sunny	B.H. Elev: ---

Depth. (m)	Thick. (m)	Description	Legend	SPT Counts 15cm	15cm	15cm	N Value 0 10 20 30 40 50	w %	LL %	PL %
		200 mm to 300 mm Top Soil								
1.00		Firm to Stiff, brown becoming gray at a depth of 3.8 m, lean CLAY/SILT with coarse sand and some gravel .		1	6	10		---	---	---
	4.00			3	4	5		21.0	29.6	18.8
2.00				7	8	10		11.7	26.8	16.0
3.00				2	7	5		13.5	25.0	16.1
				3	7	10		14.9	23.7	16.1
4.00										
		Firm to stiff, light gray becoming dark gray at a depth of 6.5m, lean CLAY/SILT with fine sand and some gravel.		4	6	7		10.5	20.4	13.0
5.00	2.75			3	3	6		13.9	23.2	14.9
6.00				1	2	3		24.2	37.4	19.6
				1	2	2		13.6	22.2	13.3
7.00	0.50	Medium Dense to Dense, SAND, trace to some silty clay.		7	10	17		17.3	24.3	12.6
8.00	1.00	Hard, dark gray, lean CLAY/SILT with seams fine sand.		15	27	23		18.1	20.2	12.3
	0.50	Dense, SAND, trace to some silty clay.		15	27	22		11.7	21.2	14.4
9.00	0.25	Hard, gray CLAY								
		END OF BORING								

Figure B-2: Borehole log 2 from Drbe and El Naggar (2015).
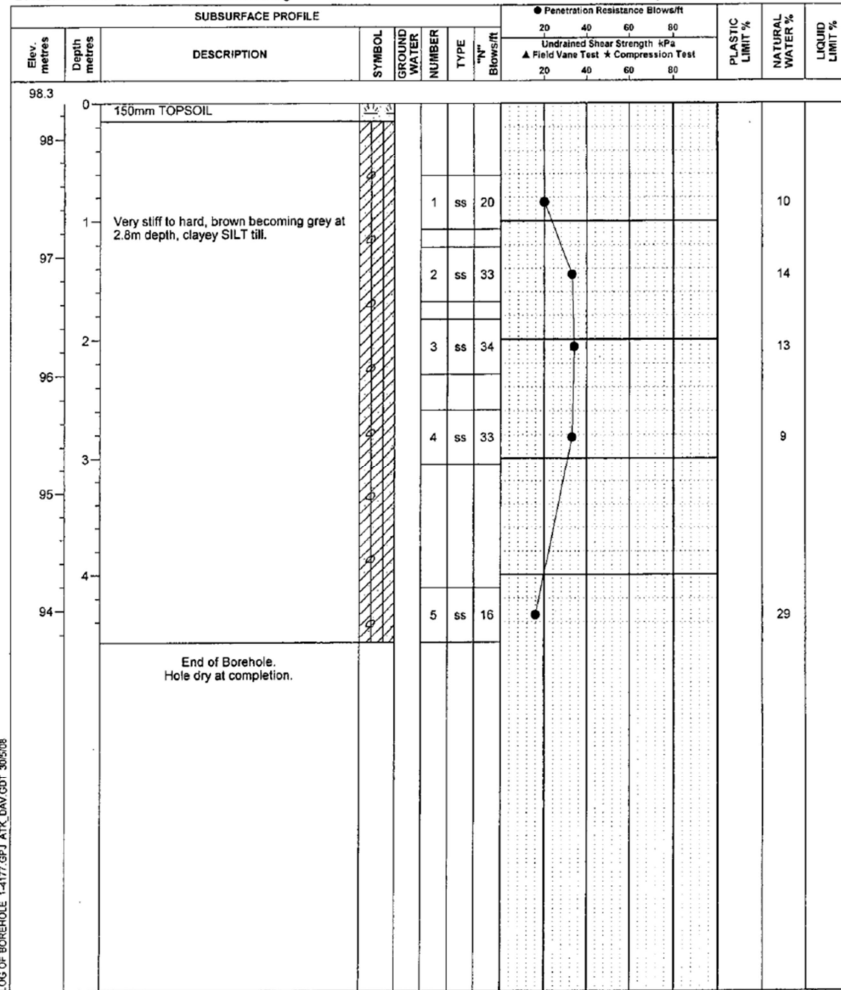
Figure B-3: Borehole log no. 3 from Atkinson Davies in 2008 (Drbe, 2013).
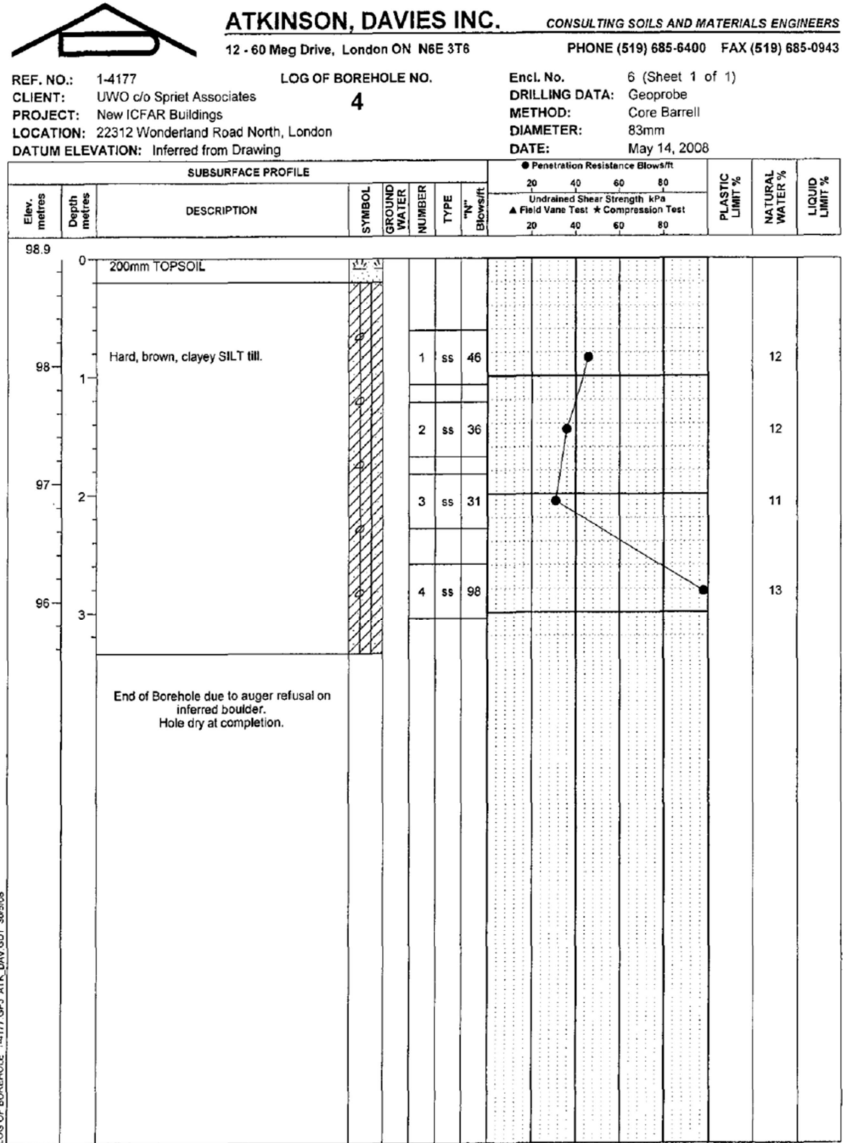
Figure B-4: Borehole log no. 4 from Atkinson Davies in 2008 (Drbe, 2013)

Curriculum Vitae

Name: Daniel Mroz

Post-Secondary Education and Degrees:
Red River College of Applied Arts, Science and Technology
Winnipeg, Manitoba, Canada
2009 – 2012 (Diploma in Structural Engineering Technology)

The University of Manitoba
Winnipeg, Manitoba, Canada
2012 – 2017 (B.Sc in Civil Engineering)

The University of Western Ontario
London, Ontario, Canada
2017 – 2019 (M.Sc in Civil Engineering)

Honours and Awards:
Beach Rocke Engineering Award, 2010

U of M Faculty of Engineering Dean's Honour List, 2013 - 2017

NSERC Undergraduate Student Research Award, 2016

Dr. Allen Lansdown Award, 2017

William E. and Ruth Lardner Award, 2018

Related Work Experience:
Material Testing Technician
TBT Engineering
2010

Geotechnical Technician
TREK Geotechnical
2011 – 2014

Undergraduate Student Researcher (Geotechnical)
The University of Manitoba – Department of Civil Engineering
2015 – 2016

Teaching Assistant
The University of Western Ontario
2017 – 2019